BIOSYSMO

Deliverable D3.5

Report on optimized microbial consortia for enhanced phytoremediation for each combination of target contaminants and matrices

Deliverable information	
Responsible Partner:	UMLP
Work Package	3
Author(s):	UMLP
Contributing Partner(s):	CIIMAR, UBU, JSI
Dissemination Level:	PU - Public
Type:	R – Document, report
Due Date:	31/08/2025
Submission Date:	29/08/2025
Version:	1.0

Project Profile

Programme	Horizon Europe
Call	HORIZON-CL6-2021-ZEROPOLLUTION-01
Topic	HORIZON-CL6-2021-ZEROPOLLUTION-01-10
Number	101060211
Acronym	BIOSYSMO
Title	BIOremediation systems exploiting SYnergieS for improved removal of Mixed pOllutants
Start Date	1 September 2022
Duration	48 months

Document History

Version	Date	Author	Remarks
0.0	09/04/2025	M. Chalot - H. Castillo Gonzalez (UMLP)	First draft distributed to the consortium
0.1	06/07/2025	M. Chalot - H. Castillo Gonzalez (UMLP) M. Pereira - R. Mendes – M. Almeida - AP Mucha (CIIMAR) B. Velasco Arroyo - A. Soto Canas (UBU)	Contribution from UMLP, UBU and CIIMAR added Reviewed by M. Chalot
0.2	15/07/2025	M. Chalot - H. Castillo Gonzalez (UMLP) M. Pereira - R. Mendes – M. Almeida - AP Mucha (CIIMAR) B. Velasco Arroyo - A. Soto Canas (UBU)	Contribution from UMLP, UBU and CIIMAR added Reviewed by D. Losantos (Leitat)
0.3	20/08/2025	M. Chalot - H. Castillo Gonzalez (UMLP) M. Pereira - R. Mendes – M. Almeida - AP Mucha (CIIMAR) B. Velasco Arroyo - A. Soto Canas (UBU)	Reviewed by M. Chalot
1.0	21/08/2025	M. Chalot - H. Castillo Gonzalez (UMLP) M. Pereira - R. Mendes – M. Almeida - AP Mucha (CIIMAR) B. Velasco Arroyo - A. Soto Canas (UBU)	Final version prepared by M. Chalot

Disclaimer

All the contributors to this deliverable declare that they:

- *Are aware that plagiarism and/or literal utilisation (copy) of materials and texts from other Projects, works and deliverables must be avoided and may be subject to disciplinary actions against the related partners and/or the Project consortium by the EU.*
- *Confirm that all their individual contributions to this deliverable are genuine and their own work or the work of their teams working in the Project, except where is explicitly indicated otherwise.*
- *Have followed the required conventions in referencing the thoughts, ideas and texts made outside the Project.*

Executive Summary

Deliverable *D3.1 – Report on optimized bacterial consortia for enhanced phytoremediation for each combination of target contaminants and matrices* is the first deliverable of WP3.

This document is the final compilation of functional data on relevant microbial strains with remediation capabilities to be used for assembling the biosystems and assisting all future project tasks in WP4. The microbes were isolated from 5 case studies located in France (UMLP), Spain (UBU) and Portugal (CIIMAR), either resulting from activities in T1.3 (UMLP and CIIMAR) as reported in D1.2, or from a wetland experiment treating polluted water from Site 6 (UBU). In polluted soils from sites 2 and 10, microbial strains from Hg-contaminated rhizospheres exhibited markedly higher metal resistance than counterparts from unpolluted environments, with active detoxification mechanisms and efflux pathways underpinning tolerance, highlighting the role of environmental selection in shaping microbial adaptation. The rhizosphere fungus UFC_004 demonstrated robust tolerance to Cd, Pb, and Zn, enhanced plant growth under metal stress, and possessed unique detoxification genes, underscoring its bioremediation potential. In estuarine sediments from site 4 and 5, bacterial strains from Juncus maritimus and Sporobolus maritimus exhibited high resistance to Cu and Zn, moderate resistance to other metals, and diverse plant growth-promoting traits, enabling the construction of effective consortia capable of degrading Kpf and Vfx contaminants. These consortia, dominated by genera such as Alcaligenes, Pseudomonas, and Hydrogenophaga, are being tested alongside their host plants in microcosm and mesocosm experiments. Isolated from wastewater from site 6, bacterial communities adapted to chronic metal exposure showed functional enrichment and sustained PGP traits, supporting the development of microaggregates and optimized consortia for Phragmites australis-assisted phytoremediation. Preliminary molecular analyses indicate that plant adaptive responses involve metal transporters and antioxidant pathways, which are activated over prolonged exposure, emphasizing the integrated potential of microbial-assisted phytoremediation systems for heavy metal and pharmaceutical contaminant removal. These microorganisms and consortia are being further used in the design and enhancement of bioremediation systems in WP4.

Table of Contents

List of Figures

List of Tables

Table of Abbreviations

Abbreviation	Definition
ACC	Aminocyclopropane-1-carboxylate
AcetPEI	Acetylated Polyethylenimine
Bzf	Bezafibrate
CARD	Antibiotic Resistance Genes Database
CAZy	Carbohydrate-Active Enzymes
CFU	colony-forming unit
Chi	Chitosan
CPS	cell-particle suspension
DEG	differentially expressed genes
DFOM	DeFerOxamineMesylate
DFVF	Fungal Virulence Factor Database
GEM	Genome-Scale Metabolic Models
GO	Gene Ontology
GPR	gene-protein-reaction
IAA	Indole acetic acid
Kpf	Ketoprofen
ICP-MS	Inductively Coupled Plasma - Mass Spectrometry
ICP-AES	Inductively coupled plasma-atomic emission spectrometry
KEGG	Kyoto Encyclopedia of Genes and Genomes
KOG	Eukaryotic Orthologous Groups
LC-MS	Liquid Chromatography -Mass Spectrometry
ME	Malt extract
MIC	Minimal Inhibitory Concentration
MS	Murashige and Skoog medium
NaOAc	Sodium Acetate
OD	Optical density
PE	Polyelectrolyes
PEI	Polyethylenimine
PBS	Phosphate buffer solution
PDA	Potato Dextrose Agar
PGP	Plant Growth Promoting
PHI	Pathogen-Host Interaction
Prx	Paroxetine
TCDB	Transporter Classification Database
T_gen	Doubling time
TSA	Tryptic Soy Agar
TSB	Tryptic Soy Broth
Vfx	Venlafaxine
WGS	Whole genome sequencing

1 Introduction

1.1 Concept and links with other WPs and related deliverables

The acceleration of industrialization and modern agricultural practices have resulted in significant amounts of harmful substances being released into ecosystems, leading to community restructuring and the selection of resistant organisms. Heavy metal contamination poses a significant threat to soil quality and plant productivity worldwide, making phytoremediation—using plants to remove contaminants—an important ecological strategy. Microorganisms play a crucial role in these processes by decomposing organic matter, enhancing soil fertility, promoting nutrient cycling, supporting plant health, degrading pollutants, and reducing heavy metal toxicity. When combined with plants, they improve plant resistance to contamination and increase biomass production. Recent research has shifted from focusing on microbial taxonomy to exploring microbial functional traits, as these traits are more directly linked to adaptability and ecosystem responses, and are more sensitive to pollution than community structure alone. Functional traits such as pollutant degradation, tolerance mechanisms, and plant growth promotion provide valuable tools for monitoring environmental changes. Among them, plant growth-promoting microbes (PGPM) are especially important, as they enhance bioremediation through mechanisms like metal–protein complex formation, biotransformation, methylation, demethylation, and the production of ACC deaminase, which lowers plant ethylene levels induced by metal stress. Additionally, PGPM support plant growth by secreting hormones and metabolites, increasing nutrient availability via mineral solubilization, fixing nitrogen, forming biofilms, and protecting against pathogens.

This document is the final compilation of functional data on relevant microbial strains with remediation capabilities to be used for assembling the biosystems and assisting all future project tasks in WP4. The intermediate report (D3.1) described the methodologies used and the results obtained on the functional characterization of relevant pollutant-degrading and metal tolerant microorganisms after 18 months of activities, related to task 3.1 activities. These microbes were isolated from 6 case studies located in France (UMLP), Spain (UBU) and Portugal (CIIMAR), either resulting from activities in T1.3 (UMLP and CIIMAR) as reported in D1.2, or from a wetland experiment treating polluted water from Site 6 (UBU).

The objective of D3.5 is to finalize the functional characterization of microbes and communities isolated from polluted sites (Task 1.3-D1.2) and from a pilot experiment using polluted water from Site 6, and to support the selection of the most appropriate microbes for building a consortia. These microorganisms and consortia are being further used in the design and enhancement of bioremediation systems in WP4.

1.2 Overall strategy

Six sites have been investigated, as depicted in Table 1. The full characterization and soil analysis of these sites are provided in D1.1. Metal contamination was investigated in three rhizospheric soils (sites 1, 2, and 10, France) and in one groundwater-polluted site (site 6, Belgium), where a *Phragmites australis* mesocosm system was established and irrigated with contaminated groundwater from site 6. In parallel, diffuse organic contamination was assessed through the analysis of two rhizo-sediments (sites 4 and 5, Portugal), representing environments impacted by persistent organic pollutants.

Table 1. Sites and groups of microbes investigated in task T3.1

Type of matrix	Site	Partner	Major contaminants	Main group of microbes	Provenance of microbial isolates
Rhizospheric soils	1	UMLP	Zn, Pb and Cd	Bacteria & fungi	Site described in WP1 (D1.2)
	2	UMLP	Hg	Bacteria & fungi	Site described in WP1 (D1.2)
	10	UMLP	Zn, Pb and Cd PAHs	Bacteria & fungi	Site described in WP1 (D1.2)
Estuarine sediments	4	CIIMAR	Prx, Kpf, Bzf, Cd	Bacteria	Site described in WP1 (D1.2)
	5	CIIMAR	Bzf, Prx, Vfx, Cu	Bacteria	Site described in WP1 (D1.2)
Contaminated groundwater from an industrial area	6	UBU	Cu, Ni, Zn	Bacteria ~~& fungi~~	Pot experiment using *Phragmites australis* exposed to polluted water from Site 6. WP3, Task 3.1

1.3 Summarized descriptions of the methodologies

Table 2 provides a summarized description of the methodologies used during RP1 and RP2. As a full description of the methodologies used during RP1 is provided in D3.1, only additional methods developed/used during RP2 are detailed in sections 2.2, 3.2 and 4.2.

Table 2. Summary of methodologies used for measuring functional traits in isolated microbes. Methodologies not developed in D3.1 are indicated in light blue and are fully described in the following sections.

Trait	Summarized methodology	Equipment
Metal tolerance for soil/sediment microbes	Microbial cultures exposed to increasing concentrations of metals in solid and liquid media	TECAN, ICP-MS or ICP-AES. Microplate reader.
Removal capacities of organic + metal pollutants for sediment microbes	• Paroxetine degradation • Bezafibrate degradation • Ketoprofen degradation • Venlafaxine degradation • Copper removal • Cadmium removal Cultures/isolated bacterial strains are exposed to pharmaceuticals and metals. Removal capacities are measured by High-performance Liquid Chromatography (HPLC) with a Diode Array Detector (DAD) and High-performance Liquid Chromatography (HPLC) with a Fluorescence Detector (FLD) for pharmaceuticals; and Atomic Absorption Spectroscopy, with flame atomisation (FAAS) and with electrothermal atomisation (ETAAS).	HPLC-DAD, HPLC-FLD, FAAS, ETAAS
Plant growth promoting traits	• Siderophore production • Nitrogen fixation • Phosphate solubilization • IAA production • Biofilm production • ACC deaminase activity Cultures are exposed to metals and PGP traits are measured by colorimetric method or bacterial growth	TECAN, colorimetric techniques, Microplate reader, Bacterial growth.
Selection of plant microbe assemblages	Model plants / microbe assemblage are co-cultivated in pot experiments while exposed to contaminants. Growth traits are measured.	Greenhouse
Functional characterization	Mapping binary fungal species interactions	Lab equipment for fungus cultivation and tests
DNA sequencing	Full-depth analysis of sequenced DNA from isolated microbes	DNA sequencing facilities
RNA sequencing	Microbial cultures exposed to metals and subsequent transcriptomic analysis	RNA sequencing facilities
Compatibility tests for bacterial strains to	Adapted Disc diffusion method and iACME (Interspecies Aggregation Combinatorics, Microfluidics, Entrapment) selection tools.	Flow cytometry, Electrophoretic and Dynamic Light Scattering device, Microscopy,

develop consortia		Encapsulator, Microplate Reader

2 In-depth characterization of microbes from rhizospheric soils (sites 2 and 10) and consortia assembly

2.1 Introduction

Recently, increasing attention has been given to the pivotal role of plant-associated microbiomes, particularly fungi, in the success of phytomanagement. In polluted soils, the microbial community structure is often disrupted as a consequence of pollutant loads (Su et al., 2023), which can limit plant establishment and growth. These microbial partners are essential for nutrient acquisition, stress mitigation, and pollutant degradation, fundamentally shaping plant health and resilience in contaminated environments (Saha et al., 2021; Ma et al., 2022). Poplar species (*Populus* spp.) are known to engage in a diverse array of microbial partnerships. These associations range from dual mycorrhizal and endophytic relationships to complex rhizosphere interactions, each contributing unique functions that enhance nutrient acquisition, stress tolerance and pollutant degradation. Documented cases include *Serendipita vermifera*, an endophytic fungus, with exceptional metal tolerance and the ability to enhance both root and shoot biomass in poplar. This fungus promotes plant growth by facilitating nutrient uptake and modulating stress responses (Lacercat-Didier et al., 2016). Another notable fungus is *Fusarium pseudograminearum*, which forms a novel ectomycorrhizal (ECM) -like mutualism with poplar roots. This interaction mimics classical ECM colonization, offering benefits such as improved phosphorus acquisition and pathogen resistance (Yang et al., 2025). In addition to fungi, bacteria also play a crucial role in supporting poplar growth under stress conditions. Certain plant growth-promoting rhizobacteria (PGPR), such as *Pseudomonas* and *Bacillus* species, enhance nutrient solubilization, produce phytohormones, and suppress soil-borne pathogens. In addition to fungi, bacteria also play a crucial role in supporting poplar growth under stress conditions. Certain plant growth-promoting rhizobacteria (PGPR), such as *Pseudomonas* and *Bacillus* species, enhance nutrient solubilization, produce phytohormones, and suppress soil-borne pathogens. Some bacterial strains have demonstrated heavy metal tolerance and the ability to degrade organic pollutants, further contributing to the success of phytoremediation strategies (Gamalero and Glick, 2024). The synergistic action between bacterial and fungal communities is increasingly recognized as essential for optimal plant performance in contaminated environments.

Building on poplar's innate ability to establish, and in some cases form novel, fungal associations, we aim to harness similar symbiotic relationships to enhance plant establishment and resilience in heavy metal-contaminated environments. Our primary objective is to obtain functionally complementary fungal partners by integrating strains with diverse functional roles, enzymatic activities, metal tolerance, and symbiotic strategies. The foundation of constructing effective fungal consortia lies in the careful selection and characterization of thefungal candidates. In our case, the strains were isolated from contaminated sites to ensure ecological adaptation and a co-evolutionary history with the host plant and soil environment. Research indicates that native fungi demonstrate higher rhizosphere competence

and colonization stability *in situ*, both essential qualities for long-term phytomanagement success (Middleton & Bever, 2010; Murali et al., 2021; Mohamed et al., 2023).

To address this, fungal consortia synthetically designed to mimic natural microbial diversity while providing targeted functional benefits have emerged as a promising approach to enhance plant performance and soil restoration (Chaudhary et al., 2023; Efremenko et al., 2024). In recent years, significant progress has been made in cultivation-based techniques by modifying culture media and incubation conditions to better mimic natural habitats and support less competitive or slow-growing strains (Clagnan et al., 2024). These efforts are increasingly coupled with metagenomic and metatranscriptomic data to guide the reconstruction of consortia that reflect native ecological complexity and functional diversity (Lin, 2022).

We employed a bottom-up engineering strategy to assemble and characterize synthetic fungal consortia tailored to support poplar growth and phytomanagement in heavy metal-contaminated soils. For this, we integrated well-characterized beneficial strains from native fungal diversity to maximize functional complementarity, resilience, and ecological compatibility. Through this work, we aim to elucidate the potential of fungal consortia as bioinoculants for sustainable phytoremediation and to support activities developed in T4.2. Section 2.3 below is related to site 2 (chlor-alkali site) and Hg tolerance of microorganisms, while section 2.4 is related to site 10 (industrial wasteland) and tolerance to Zn, Pb and Cd.

2.2 Methodologies implemented in RP2

Here we describe only methodologies not detailed in D3.1, especially those concerning genomic and transcriptomic activities carried out in WP3 (T3.1), that complemented the RP1 methodologies.

2.2.1 Production of bacterial consortia

JSI

Bacterial consortia capable of reducing metals were obtained from sampling site 10 using the micro-Lure, Microfluidics, and Entrapment (uLUME) method developed at JSI, as described in D1.2. Briefly, 10 g of soil was incubated with 200 mL of 0.05 M EDTA solution at 180 rpm for 3 hours, then sequentially filtered through 180 µm, 60 µm, and 10 µm meshes, and washed twice to remove EDTA residues by centrifugation at 5000 g for 5 minutes. The resulting cell-particle suspension (CPS) was characterized for colloidal surface properties using a particle analyzer (DelsaNano, Beckman Coulter, UK). Biomass content in the CPS was quantified using flow cytometry combined with fluorescent labeling.

The CPS was incubated with 4 µm-sized vaterite particles loaded with a mixture of 50 mM pyrene and benzo[a]pyrene as the sole carbon source. Incubation was carried out for 24 hours at 180 rpm and 28 C. The resulting vaterite particles with attached bacterial cells represented distinct species combinations, referred to as consortia. These samples were analyzed via flow cytometry and subsequently entrapped in alginate beads with a diameter of 120 µm using a microencapsulator (Buchi B-390). Each separated and alginate-stabilized consortium was cultivated in a microtiter plate using resazurin (0.1 mg/mL) as an indicator of respiratory activity.

Selection of promising uLUME candidates—those exhibiting the highest growth while utilizing PAHs in the loaded vaterite—was based on analysis of growth curves using statistical methods in R.

UMLP

Bacterial suspensions were obtained by inoculating a colony of bacteria from a LB agar plate into 300 ml of LB broth at 30 °C and 150 rpm for 48 hours. The suspensions were then centrifuged at 6,000 g for five minutes and resuspended in sterile phosphate buffer solution (PBS). A colony-forming unit (CFU) count was performed for each bacterial strain to determine the relationship between optical density (OD) at 600 nm and CFU/mL. The bacterial concentration was then adjusted to the required level in CFU/mL using PBS.

Microbial consortium solutions were obtained by mixing the bacterial suspensions. An equal volume of the consortium solution was poured onto the rhizosphere soil in each pot to inoculate the plants. The final concentration in the inoculated pots was 10^6 CFU/g of soil.

2.2.2 Mapping binary fungal species interactions *in vitro* to optimize the production of fungal consortium (UMLP)

The protocol aims to evaluate fungal relationships, not only focusing on interactions (e.g., mutualistic, antagonistic) but also accounting for priority effects. Fungal species will be inoculated in the presence of a background specie to assess how these interactions influence growth dynamics, including inhibition, promotion, or neutrality, as measured by colony size. These interactions provide critical insights into the selection or exclusion of strains, contributing to the long-term functioning and resilience of microbial consortia.

Two different media were used to test the interaction within the consortium. Sabouraud Broth medium was used to prepare the spore solutions. This liquid medium is one of the most common for isolating and growing fungi from the soil. Due to its glucose concentration, fungi may grow rapidly but could exhibit slower sporulation compared to other media that provide more balanced nutrient conditions. In the next step, we used Potato Glucose Agar (PGA) to better control spore production and to map binary fungal species interactions *in vitro*. This medium is rich in glucose, readily available to fungi, allowing them to grow rapidly. The following protocols were used for binary interaction: preparation of spore solutions and homogenization of concentrations (i) and inoculation of suspensions (ii). The growth medium composition and steps are detailed in Annex 7.1.

(i) To prepare the spore solution, 5 mL of Sabouraud Broth was added to the Petri dish containing the fungal spores. The spores were detached, and the resulting spore solution collected and filtered through a cotton filter. The concentration in spores/mL of each fungal species in the consortium was determined using a Malassez cell. To ensure that the solutions were homogeneous, they were diluted to a concentration of 10^6 spores per mL according to Kamal & Barlow (2023), as illustrated in Figure 1.

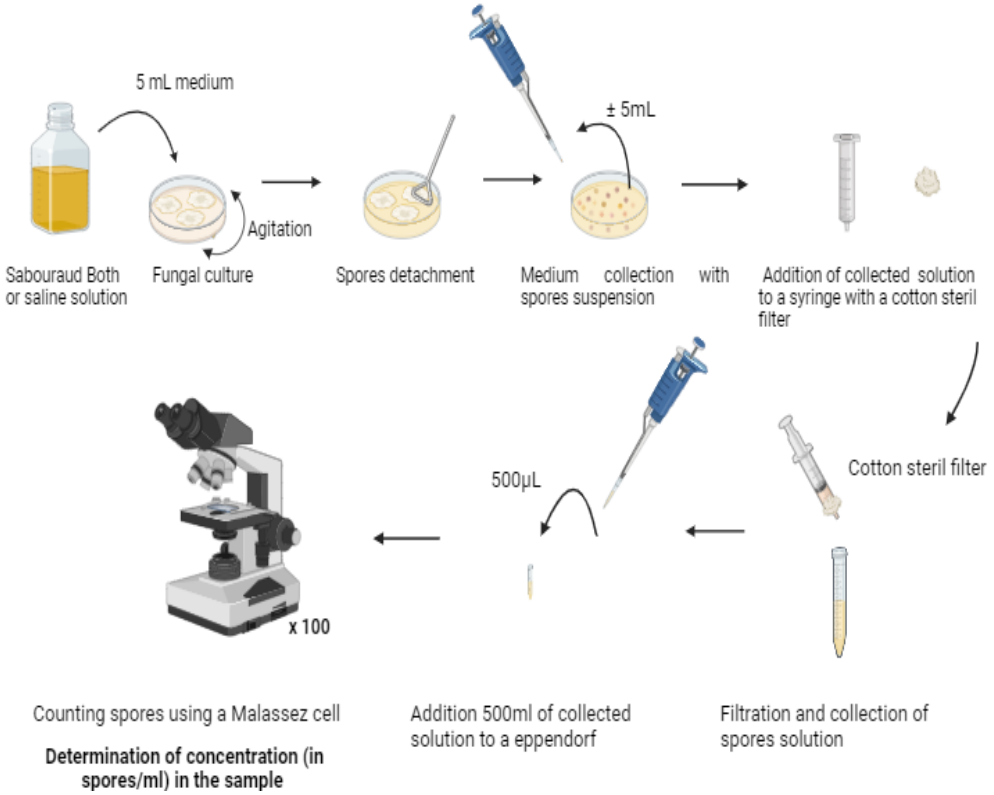

Figure 1. Diagram of the protocol for the preparation of spore solutions and homogenization of concentrations (created in Biorender.com).

(ii) 300 µL of spore solution at a concentration of 10^6 spores/mL was used to inoculate eight Petri dishes containing Potato Dextrose Agar (PDA) medium, using an L-shaped spreader. Three replicates were carried out for each of the eight fungi species, and the control dishes (no fungi). The plates were incubated for 18 hours at 25°C, to allow the spores to germinate. To study binary interactions, fungal discs were added to each of the 27 plates containing the background species as illustrated in Figure 2:

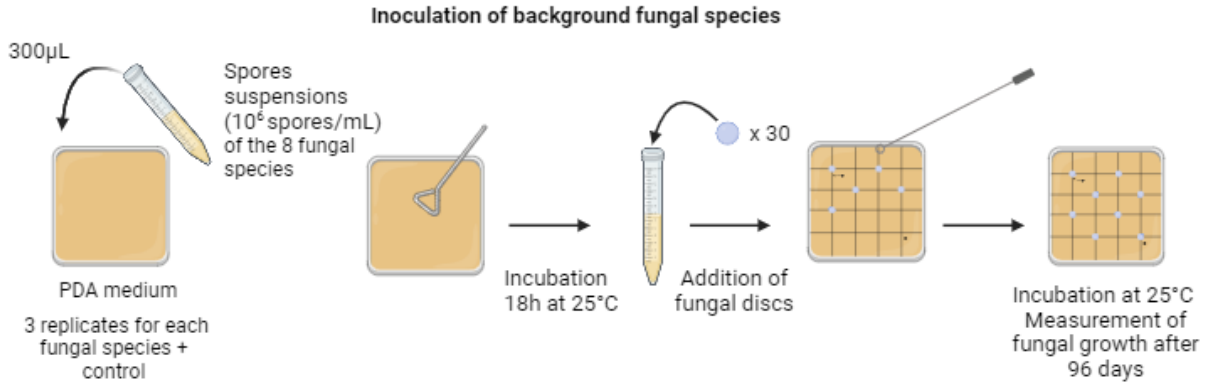

Figure 2. Diagram of the inoculation protocol for eight fungal species and 1 background specie (created in Biorender.com).

Fungal species were inoculated in the presence of a background specie to assess how these interactions influence growth dynamics, including inhibition, promotion, or neutrality as measured by colony size. These interactions provide critical insights into the selection or exclusion of strains, contributing to the long-term functioning and resilience of microbial consortia.

To compare binary interactions and quantify the different responses, multiple top-down pictures were taken with a ruler placed next to them for scale. Then an image scale was created using Image J software based on the ruler. The diameter of growth of the fungi strains was measured and compared using Student's t-tests in Excel.

2.2.3 DNA sequencing (UMLP)

Whole genome sequencing (WGS)

A hybrid sequencing strategy was employed, combining Illumina short reads and Oxford Nanopore Technologies (ONT) long reads. The Illumina sequencing was performed following the standard protocol. Genomic DNA was assessed for quality before fragmentation using ultrasonic shearing. The fragmented DNA was purified, end-repaired, A-tailed, and ligated with sequencing adapters. The library was size selected using agarose gel electrophoresis, followed by PCR amplification. The final library underwent quality control, and qualified libraries were sequenced using the Illumina NovaSeq 6000 platform. Raw sequencing reads were filtered using fastp (version 0.20.0, https://github.com/OpenGene/fastp) to remove low-quality data (Chen, 2023).

For Nanopore sequencing, genomic DNA was randomly fragmented, and large DNA fragments were enriched and purified using magnetic beads. The large DNA fragments were recovered via gel electrophoresis, followed by damage repair. The purified DNA fragments were end-repaired and A-tailed before ligation of sequencing adapters using the SQK-LSK109 ligation kit. The final DNA library was quantified and sequenced using the Oxford Nanopore PromethION platform. Nanopore sequencing reads were filtered using Filtlong (v0.2.1, https://github.com/rrwick/Filtlong) with parameters set to remove reads shorter than 1000 bp and those with an average quality score below 7.

Genome assembly

A genome survey was performed prior to assembly to estimate genome size, heterozygosity, and repeat content. The k-mer frequency distribution was analyzed using GCE (https://github.com/fanagislab/GCE), which allowed for genome characteristic estimation. Preliminary genome assembly was conducted using SPAdes (v3.15.4), which aligned Illumina reads to assembled contigs, evaluated GC content bias, and identified repetitive sequences (Bankevich et al., 2012). To reduce sequencing errors, raw Nanopore reads were corrected using Canu (Koren et al., 2017). The corrected reads were further refined using LoRDEC, which employed short-read Illumina data for additional correction (Salmela and Rivals, 2014). Genome assembly was performed using NextDenovo (v2.5, https://github.com/Nextomics/NextDenovo/) (Hu et al., 2024). The initial assembly results were aligned with corrected Nanopore reads using minimap2 (v2.1) for further refinement (Li, 2018). Final polishing was carried out using NextPolish (v1.4.0, https://github.com/Nextomics/NextPolish) (Hu et al., 2020) for three rounds of Nanopore-based correction, followed by three rounds of short-read correction using Pilon (Walker et al., 2014). The completeness of the final genome assembly was assessed using

BUSCO (v5.2.1, database version 10), which evaluates the presence of conserved single-copy orthologous genes (Simao et al., 2015).

Genome component prediction

Protein-coding genes were predicted using Augustus (v3.3.3, https://github.com/Gaius-Augustus/Augustus). The identification of non-coding RNAs was carried out using tRNAscan-SE for tRNA genes (Lowe and Eddy, 1997), RNAmmer for rRNA genes (Lagesen et al., 2007), and Rfam for small RNA annotation (Griffiths-Jones et al., 2003). Repetitive sequences in the genome were identified using RepeatModeler (v2.0.1), followed by repeat annotation using RepeatMasker (Tarailo-Graovac and Chen, 2009).

Gene function annotation

The assembled genome was annotated by comparing predicted genes against multiple functional databases: NR (Non-Redundant Protein Database) (Altschul et al., 1990), SwissProt (http://www.uniprot.org/), KEGG (Kyoto Encyclopedia of Genes and Genomes, http://www.genome.jp/kegg/), KOG (Eukaryotic Orthologous Groups, https://www.ncbi.nlm.nih.gov/COG/), GO (Gene Ontology, http://www.geneontology.org/), Pfam (Protein Families Database) (Mistry et al., 2013), CARD (Antibiotic Resistance Genes Database, https://card.mcmaster.ca/), CAZy (Carbohydrate-Active Enzymes Database, http://www.cazy.org/), DFVF (Fungal Virulence Factor Database, http://sysbio.unl.edu/DFVF/Download.php), PHI (Pathogen-Host Interaction Database, http://www.phi-base.org/), TCDB (Transporter Classification Database, http://www.tcdb.org/).

The identification of secreted proteins was conducted using SignalP (v4.1), which predicts the presence and location of signal peptides (Petersen et al., 2011). Transmembrane protein domains were identified using TMHMM (v2.0), which analyzed predicted protein sequences to determine transmembrane regions.

Comparative genomics and phylogenetic analysis

The identification of orthologous and paralogous genes across different species was carried out using OrthoFinder (v2.3.5), while homologous gene clustering was performed using BLAST (v2.10.1) (Altschul et al., 1990). Gene family evolution was analyzed based on the clustering results. Phylogenetic relationships among species were inferred using RAxML (v8.2.12), which constructed a maximum-likelihood phylogenetic tree using single-copy orthologous genes with the PROTGAMMAJTT model and 1000 bootstrap replicates. Whole-genome synteny analysis was conducted using NUCMER(v4.0.0beta2) with the --mum parameter, and the results were visualized through Dot-plot graphs to illustrate genomic collinearity.

Creation of genomic-scale metabolic models

Homologous protein sequences were used to build metabolic models without the need for template models. This protocol utilizes protein sequence data and metabolic reactions from the KEGG and the MetaCyc databases. A crucial component of this method is the use of KEGG Orthology (KO) IDs, which are manually annotated gene sets that contain similar metabolic functions and are subsequently associated with numerous metabolic reactions. The process begins by downloading relevant sections

of the KEGG and MetaCyc database to a local directory, parsing this data to generate a comprehensive GEM.

2.2.4 RNA-Seq analysis

Biomass production

The bacterial strains *UFC_B020* and *P31* were pre-cultured overnight in LB broth supplemented with Hg (20 µM for *UFC_B020* and 1 µM for *P31*, corresponding to 10% of the respective minimal inhibitory concentration values) at 30°C under agitation. Fresh cultures were subsequently prepared by inoculating LB broth with a 1:100 dilution of the pre-cultures, followed by incubation at 30°C under agitation. Each strain was grown in triplicate in either LB broth alone or LB broth supplemented with Hg (20 µM for *UFC_B020* and 1 µM for *P31*). Optical density at 600 nm (OD_{600}) was measured at the beginning of incubation and subsequently every hour for a total duration of 10 hours to monitor bacterial growth. Kinetic parameters (growth rate, generation time, and lag phase) were estimated from the experimental growth kinetic data using Sym'previus software (https://symprevius.eu/en/).

RNA extraction and Hg monitoring in bacterial cultures

Each strain was pre-cultured overnight in LB broth supplemented with mercury at 30°C under agitation. Fresh LB broth cultures (without Hg) were subsequently inoculated with a 1:100 dilution of the pre-cultures and incubated at 30°C under agitation (250 rpm) until the OD_{600} reached 0.4-0.5, corresponding to the early exponential phase (LaVoie & Summers 2018). Hg was then added to the medium for further incubation. Two concentrations were tested: 0 µM (control) and either 20 µM for *UFC_B020* or 1 µM for *P31* (representing 10% of their respective mercury MIC values). Two exposure times were evaluated: 30 minutes (t1, approximately one generation cycle, to assess short-term bacterial responses) and 3 hours (t2, encompassing several cell divisions, to evaluate long-term effects). At the end of each exposure period, the OD_{600} of the cultures was measured and cells were harvested by centrifugation for 5 minutes at 4°C and 14,000 g. The cells were washed in PBS, and the resulting bacterial pellets were immediately frozen at -80°C pending RNA extraction. For each experimental condition, additional culture aliquots were collected and pooled for Hg quantification using the AMA 254 analyzer (Altec Ltd., Prague, Czech Republic).

Within the following days, bacterial pellets were slowly thawed on ice and RNA extractions were performed using the RNeasy Mini Kit (Qiagen, Hilden, Germany) according to the manufacturer's instructions, including the optional DNase treatment step. RNA quality and quantity were assessed using a NanoDrop spectrophotometer (ThermoFisher Scientific, Waltham, MA, USA) and by agarose gel electrophoresis. RNA extracts were stored at -80°C until sequencing.

Necromass production as killed control

Each strain was pre-cultured overnight in LB broth supplemented with Hg at 30°C under agitation (same concentration as above). Fresh LB broth cultures (without Hg) were subsequently inoculated with a 1:100 dilution of the pre-cultures and incubated at 30°C under agitation until the OD_{600} reached 0.4-0.5, as previously described. The cultures were further incubated for 24 hours at 30°C under agitation to obtain bacterial necromass. Hg was subsequently added to the medium, and the same protocol described in the previous section was followed for monitoring Hg concentration with necromass

incubation. To verify bacterial death and confirm the absence of viable cells, the necromass solution was plated onto LB agar medium and incubated overnight at 30°C to ensure no growth occurred.

Library preparation and RNA sequencing

Library construction and Illumina sequencing were performed by Novogene (Cambridge, UK). Raw reads were processed using fastp software to remove adapter-containing reads, poly-N-containing reads, and low-quality reads (Chen et al. 2018), and Q20, Q30, and GC content metrics were calculated. Clean reads were subsequently aligned to the genome sequence of *Pseudomonas canadensis* PseudoSSchier:P31 (Mei et al. 2023) using Bowtie2 v2.2.3 (Langmead & Salzberg, 2012). Novel genes were identified using Rockhopper software. Read counts mapped to each gene were quantified using HTSeq v0.6.1, and the expected number of Fragments Per Kilobase of transcript sequence per Million mapped reads (FPKM) for each gene was calculated based on gene length and corresponding read counts (Anders et al. 2014).

Gene expression analysis

K-means clustering was performed on read count data using the iDEP 2.01 web tool (integrated Differential Expression and Pathway analysis, https://bioinformatics.sdstate.edu/idep/) (Ge et al. 2018). The top 400 genes with the lowest standard deviation in expression levels were selected for clustering, and the optimal number of clusters was determined using the elbow method. For each cluster, networks of enriched Gene Ontology (GO) terms related to biological processes (BP) were generated using iDEP 2.01. Fold-change analysis of transcripts and identification of differentially expressed genes (DEGs) were performed using DESeq2 v42.1 through the R package Bioconductor (Love et al. 2014). The criteria for significant differential expression were set as $|\log_2\text{FoldChange}| > 1.5$ and fold change ratio (FDR) < 0.05. Gene Ontology enrichment analysis was implemented using the GOseq R package, which corrects for gene length bias. GO terms with corrected p-values < 0.05 were considered significantly enriched among DEGs. Venn diagrams were generated using the VennDiagram R package, while other visualizations were created with the ggplot2 R package. DEGs were grouped by biological function within cells according to their associated GO terms and primary functions based on literature searches and descriptions from UniProtKB (Bateman et al. 2022).

Statistical analysis

The results were analysed with the R Studio software. As the normal distribution of the data was not confirmed, non-parametric Kruskal-Wallis tests were carried out to compare the different conditions of a given experiment, and if the p-value was inferior to 0.05, a Dunn's test was performed to form the groups according to their significance.

2.3 In-depth characterization of isolated microbes from the chlor-alkali sediment disposal (site 2)

As detailed in D1.1, site 2 is a chlor-alkali site, which received Hg contaminated sediments for more than 50 years. However, the effect of Hg on the rhizospheric microbial communities that likely drive plant productivity is unknown. It is thus important to characterize the microbial communities from the site, as it may help in understanding the revegetation processes of contaminated areas.

During the reporting period 2, we aim to improve our knowledge of the molecular and cellular mechanisms involved in the accumulation and tolerance of Hg by soil microorganisms to better understand their role in the biotransformation and transfer of this contaminant. The work was performed at a Hg-contaminated chlor-alkali site (site 2) where Hg speciation has been fully characterized (D1.1). The Hg-tolerant bacteria and fungi were isolated by culture-dependent approaches, as reported in D1.2. The final aim was to select the most appropriate microbial strains to build a microbial consortium for further activities in WP4.

2.3.1 Hg tolerance of isolated bacteria

The work described here focused on the isolated bacteria *UFC_B020*, which was compared to a control strain P31 isolated from an uncontaminated environment, kindly provided by an external laboratory (Groningen Institute for Evolutionary Life Sciences, University of Groningen). *UFC_B020* appeared to be much more resistant than P31 to Hg, which indicates the environmental selection pressure in a contaminated soil context. There was a significant difference of growth kinetics between the 2 strains: same latency period but smaller generation time for *UFC_B020* (Figure 3).

For transcriptomic analysis, we selected a Hg concentration for each strain equivalent to 10% of the MIC, i.e. 20 µM for *UFC_B020* and 1 µM for *P31* so that strain growth was not affected.

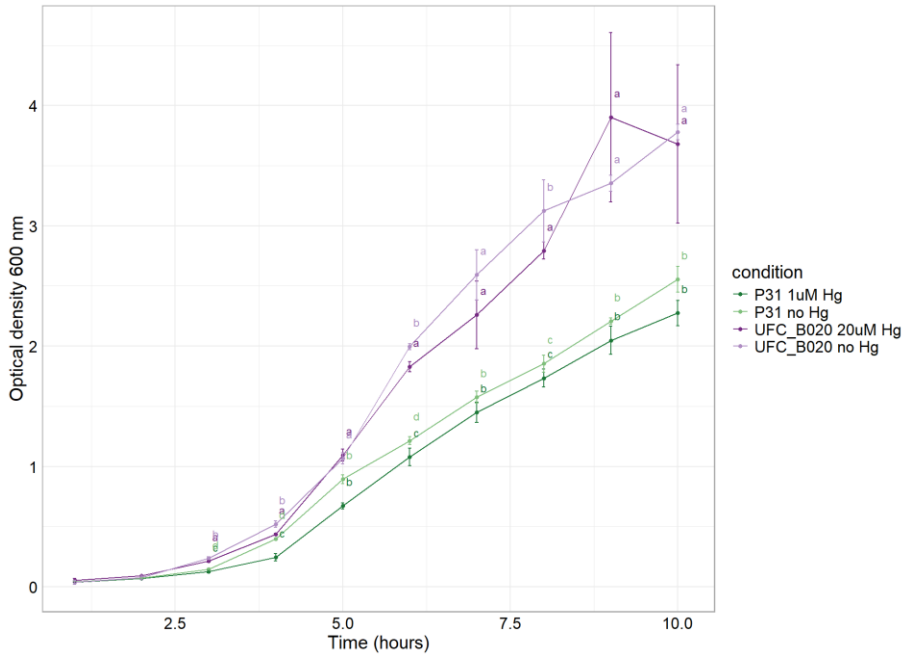

Figure 3. Growth curves of *UFC_B020* and *P31* in absence or presence of Hg. OD_{600nm} of the culture medium was measured over time of incubation at 30°C. Under Hg stress, concentrations correspond to the $MIC_{10\%}$ of each strain (20 µM for *UFC_020* and 1 µM for *P31* respectively). Error bars correspond to the standard deviation calculated from triplicates. Different letters indicate significant differences between conditions according to Kruskal-Wallis test ($p<0.05$).

2.3.2 Removal of Hg from the culture medium by biovolatilisation processes

We observed a significant removal of Hg in the medium by *UFC_B020*, whereas no more removal was observed when using the necromass, which indicates that an active process was involved (Figure 4). A decrease of Hg in the medium with *P31* could be seen, but no significant differences between biomass and necromass after 3h of exposition: in this non-tolerant reference strain, only passive mechanism (e.g. adsorption onto cell walls) occurred.

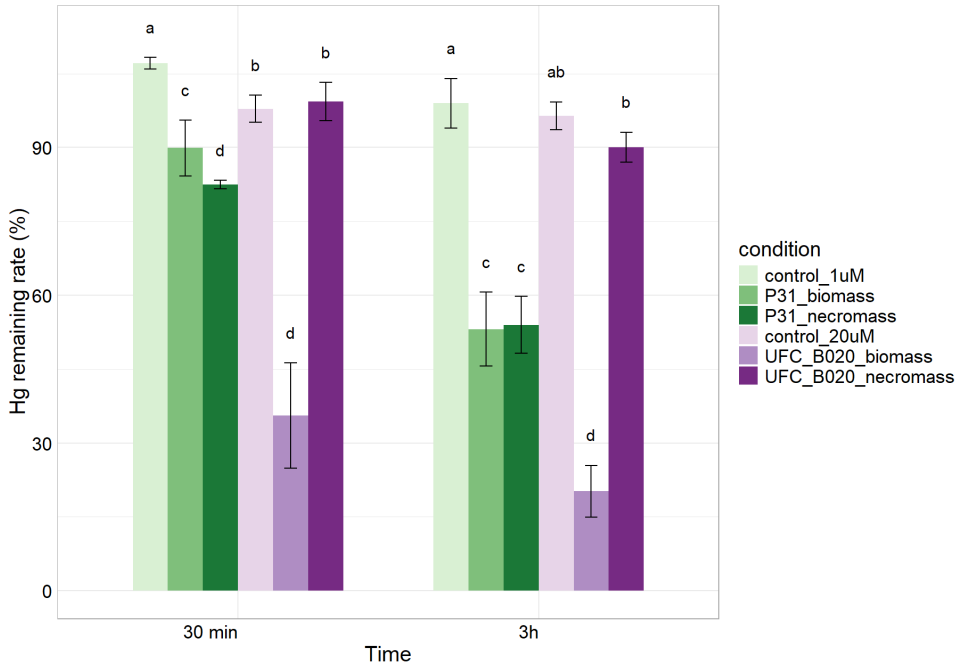

Figure **4**. Barplots representing the Hg remaining rate (%) in the medium after different incubation conditions for 30 min or 3h. Hg concentrations were set to the $MIC_{10\%}$ of each strain (20 µM for *UFC_020* and 1 µM for *P31* respectively) and controls were incubated without bacterial material. Error bars correspond to the standard deviation calculated from triplicates. Different letters indicate significant differences between conditions according to Kruskal-Wallis test ($p<0.05$).

2.3.3 Transcriptomic analysis of *UFC_B020* strains following Hg exposure

Analysis of gene expression patterns through clustering

K-means clustering of the 400 genes with lowest expression variance allow to identify seven functional modules of co-regulated genes (Figure 5A). Key findings include:

- Cluster 1 showed strain-specific Hg response, with strong overexpression in *P31* at 30 minutes, suggesting rapid stress adaptation. *UFC_B020* exhibited similar but less pronounced responses.
- Cluster 3 contained genes overexpressed in both strains under Hg exposure at both time points, indicating core Hg tolerance mechanisms.

- Clusters 2 and 5 demonstrated strain-specific expression patterns independent of Hg treatment, with consistent *P31* overexpression and *UFC_B020* underexpression. Cluster 4 showed the inverse pattern, with characteristic *UFC_B020* overexpression.
- Clusters 6 and 7 exhibited temporal regulation patterns, with expression changes driven primarily by exposure time rather than strain or Hg stress.

Network analysis of enriched biological processes revealed functionally coherent responses (Figure 5B):

- Cluster 1: Nucleotide metabolism (dTMP/dTTP biosynthesis) and protein repair mechanisms, indicating DNA and protein protection against Hg-induced damage.
- Cluster 3: Dense networks of ion transport pathways for inorganic ions, cations, and metals, consistent with cellular detoxification and ion homeostasis.
- Cluster 6: Energy metabolism and catabolism processes, reflecting temporal adaptation independent of mercury exposure.
- Cluster 7: Phosphate homeostasis and protein quality control mechanisms.

These results demonstrate biologically coherent transcriptomic responses with distinct functional modules corresponding to Hg stress adaptation, strain-specific differences, and temporal physiological changes.

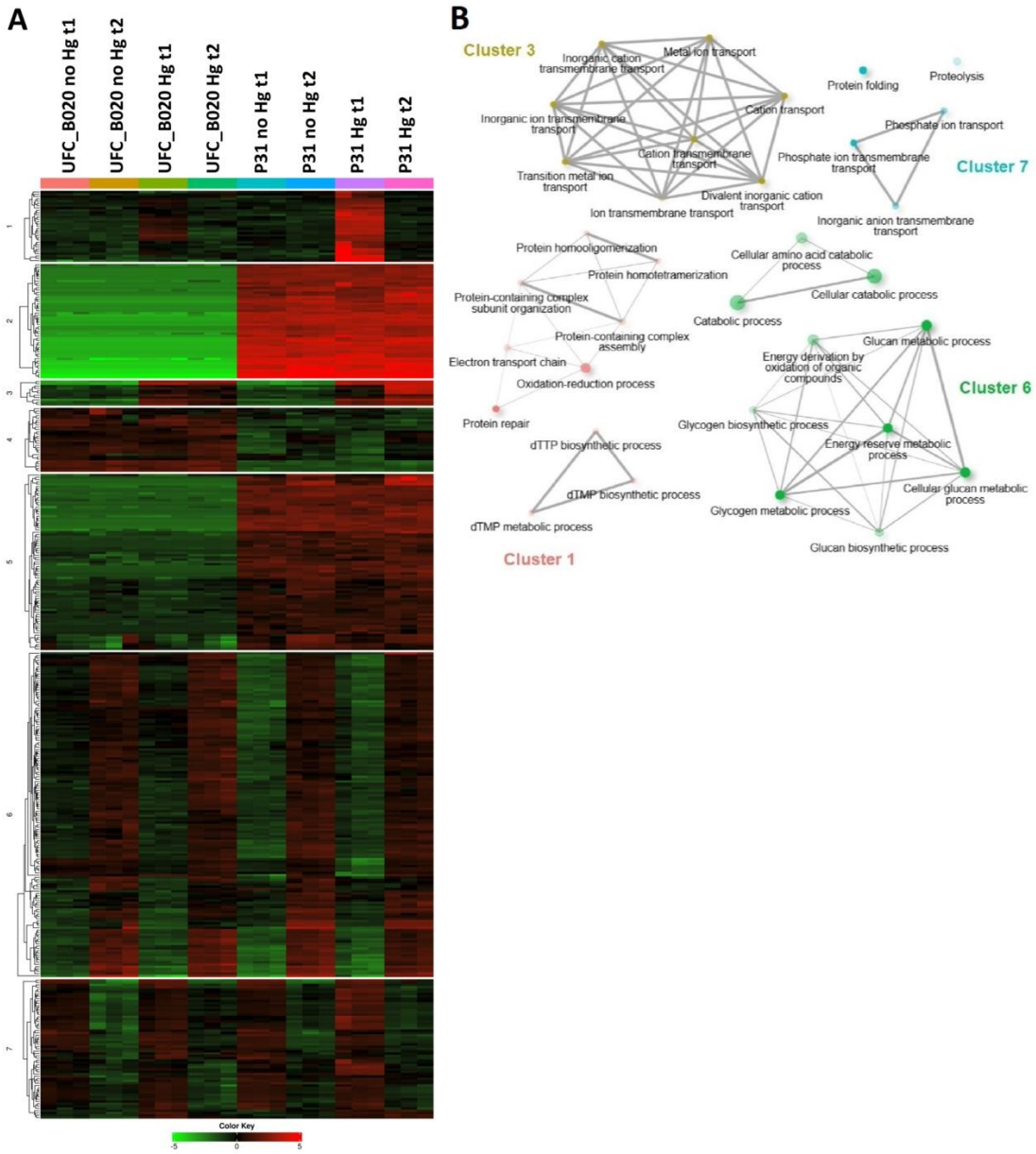

Figure 5. Global expression pattern and GO enrichment across genes clusters. (A) K-means clustering of the top 400 genes with the lowest standard deviation for their expression levels. Genes whose expressions were greater than the mean are coloured red while those below the mean are coloured green. Each column represents a specific condition (with 3 replicates per condition) and the dendrogram on the left shows the distance between genes. (B) Networks of main pathways associated with some clusters of genes, based on GO enrichment for BP subontology.

DEGs analysis

UFC_B020 exhibited 25 up-regulated and 3 down-regulated DEGs at t1 (30 min), decreasing to 16 up-regulated and 5 down-regulated DEGs at t2 (3 hr), while maintaining similar $\log_2$FoldChange values. At t1, metal ion transport (GO:0030001) was the most enriched biological process, with transmembrane transporter activity (GO:0022857) and transporter activity (GO:0005215) as significantly enriched

molecular functions (6A). No GO terms were significantly enriched at t2 due to limited DEGs distributed across various categories. The early response (30 min) indicates active Hg efflux for potential volatilization. The more heterogeneous long-term response reflects effective Hg detoxification, as over two-thirds of initial Hg was removed from the medium after 3 hours, reducing cellular stress and differential pathway expression.

P31 showed 60 up-regulated and 8 down-regulated DEGs at t1, and 49 up-regulated and 3 down-regulated DEGs at t2 (Figure 6B). The prevalence of up-regulated genes suggests Hg response primarily involves activating tolerance mechanisms rather than repressing cellular functions. Compared to *UFC_B020*, *P31* exhibited more DEGs with greater log_2FoldChange amplitudes, particularly for up-regulated genes. No GO terms were significantly enriched at t1, indicating diffuse Hgst ress response mechanisms without clear transcriptional pathways. At t2, organonitrogen compound catabolic process (GO:1901565) was the only enriched pathway, with related DEGs involved in cell wall catabolism and allantoin degradation. This suggests long-term activation of cell division and inhibition of nitrogen molecule degradation as a potential nitrogen source.

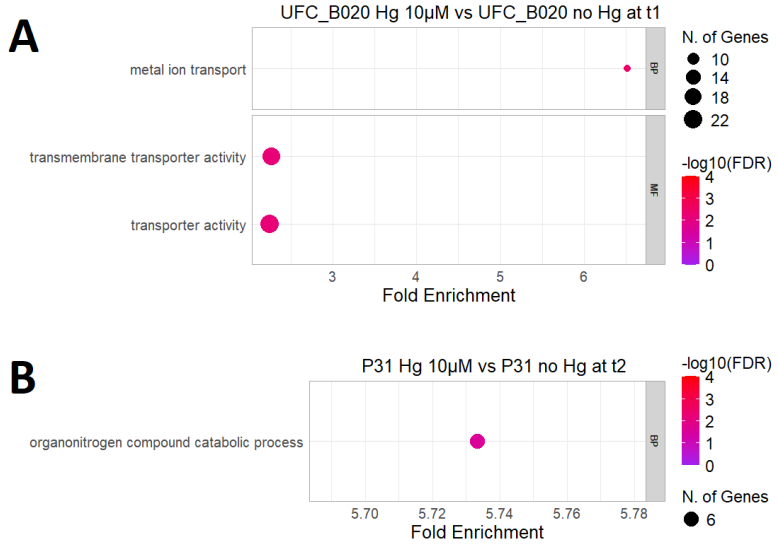

Figure 6. (A) Dot plot showing the significantly enriched GO terms for *UFC_B020* under Hg stress vs no Hg stress at t1. (B) Dot plot showing the significantly enriched GO term for *P31* under Hg stress vs no Hg stress at t2. DEGs for GO enrichment were screened with the following criteria: |log2Foldchange| >1.5 and FDR < 0.05. BP: biological process; MF: molecular function.

Linear regression analysis of DEGs between *UFC_B020* and *P31* under Hg stress showed poor correlation, with R^2 values of 0.139 and 0.098 at t1 and t2, respectively (Figure 7). The strains shared 12 common DEGs at t1 and 9 at t2. Notably, approximately half of *UFC_B020*'s differentially expressed genes were also found in *P31*, while *P31* exhibited a substantially broader and more diverse transcriptional response.

Despite sharing some Hg response mechanisms, the two strains demonstrate distinct adaptive strategies with different response amplitudes and strain-specific gene expression patterns, regardless of exposure duration.

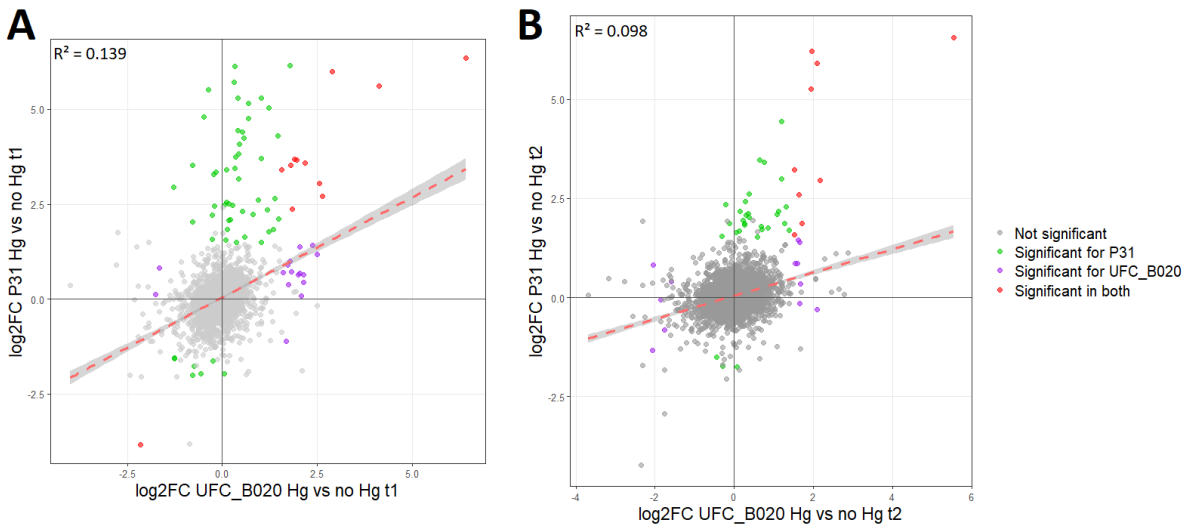

Figure 7. Pairwise scatter plots of the log2 FC values of DEGs for *UFC_B020* and *P31* (A) at t1 and (B) at t2 following Hg exposure. DEGs were obtained by comparing gene expression levels of a given condition under Hg stress to the same condition without Hg exposure. Red spots indicate DEGs present in both strains; purple spots indicate DEGs present only in *UFC_B020*; green spots indicate DEGs present only in *P31*. DEGs were screened with the following criteria: |log2Foldchange| >1.5 and FDR < 0.05. The plots were fitted with a linear regression, corresponding to the red dotted line, and R^2 values are shown on the respective graphs.

2.3.4 Conclusions

This study compared the response to Hg stress of two strains of *UFC_B020*, which was isolated from a Hg-contaminated medium, and *P31*, which was isolated from an unpolluted medium, used as a reference strain. By using multiple experimental approaches, including monitoring Hg transfer processes in the presence of biomass and bacterial necromass, as well as microscopic observations and RNA-Seq, we were able to characterise the processes involved in Hg detoxification at cellular and molecular levels, and assess their effectiveness. Themain conclusions of this work are summarized in Figure 8.

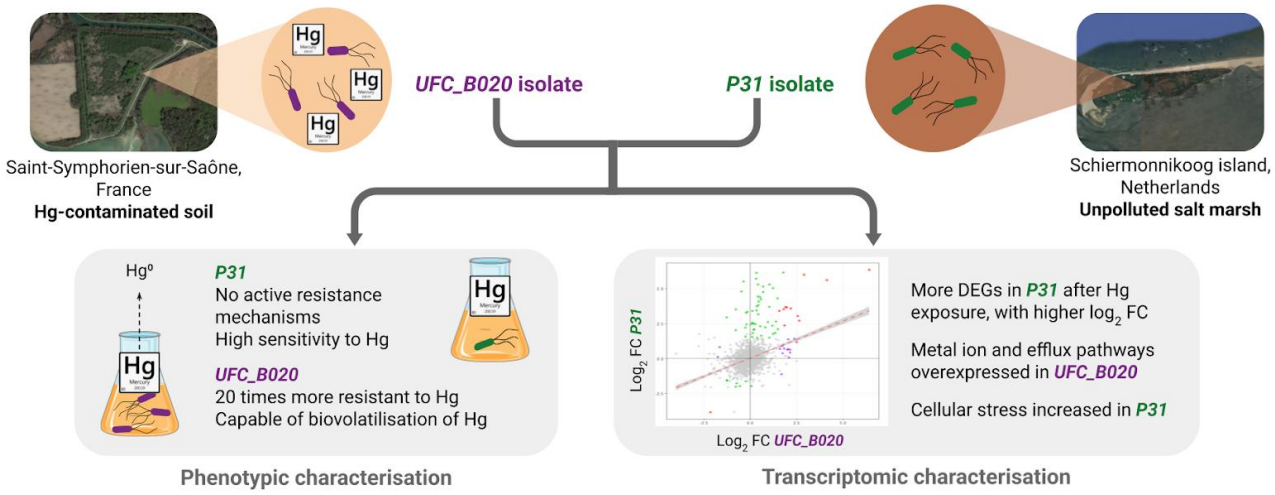

Figure 8. Main findings of phenotypic characterization and transcriptomic approaches for Hg resistance pathways.

The *UFC_B020* strain exhibited a much greater ability to withstand Hg stress than *P31*; the former displayed active resistance mechanisms, such as biovolatilisation, whereas the latter exhibited passive and compensatory mechanisms in response to Hg toxicity (Figure 9.). Despite their high genomic similarity, these results demonstrated how environmental conditions can impact the selection of Hg resistance genes and provided insights into the response to Hg stress in this genus.

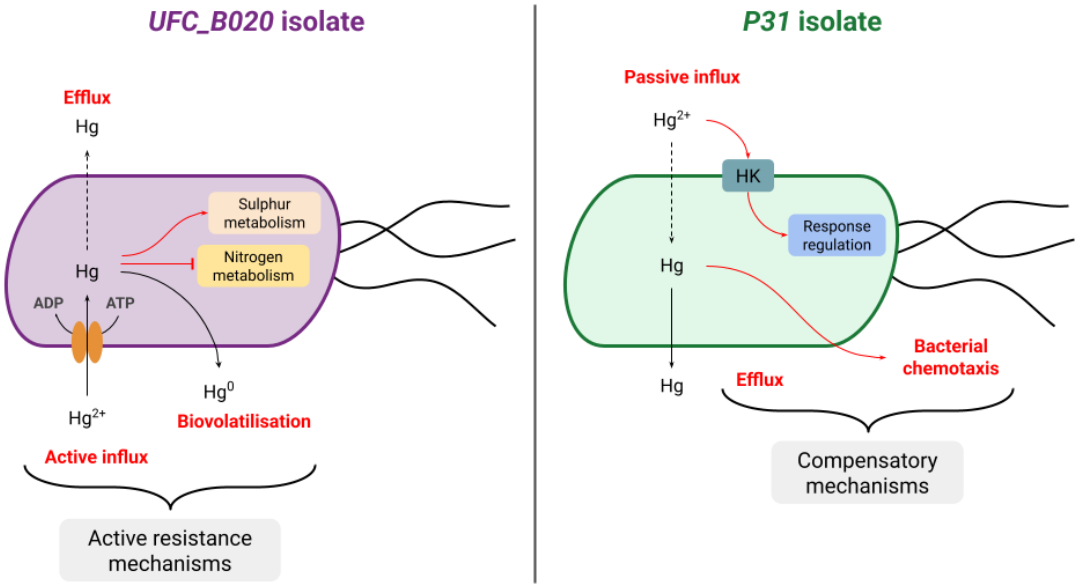

Figure 9. Proposed model depicting the main pathways of responses to Hg stress in *UFC_B020* (left) and *P31* (right). Red arrows denote the effects of Hg on metabolic pathways while black arrows represent Hg transfers. HK: Hexokinase; ATP: Adenosine triphosphate.

2.4 In-depth characterization of isolated microbes from an industrial wasteland (site 10)

The polluted wasteland at Site 10 is located on the edge of the urban center, in the immediate vicinity of the Belfort-Montbéliard Greenway and exhibits high risks for human health as recently demonstrated, due to the presence of As, Pb and Zn in excess (Collot et al. 2023). The microbiome from this highly contaminated soil has been described in D1.2. Briefly, three sampling campaigns were performed (D1.1) for the isolation of 80 fungi and for their initial characterization for metal tolerance and PGP traits (D3.1).

During RP2, we aim to improve our knowledge on some of these fungi isolated from this site, and to determine the potential of the isolated strains to cope with certain metals. The final aim was to select the most appropriate fungal strains to build a fungal consortium for further activities in WP4. In D3.5, we report some general genomic features on 6 fungal strains and further focus on completed work on the fungal isolate *UFC_004* from site 10.

2.4.1 General features of isolated fungal strains

From the initial screening in D3.1, 6 fungal strains from site 10 were retained for further characterization in WP2 and WP3 (D3.1) during RP1. These strains were analyzed in depth by molecular means using WGS approaches, as described in Figure 10.

- 2 of them (*UFC_006 and UFC_007*) matched well with their reference genomes and have been analyzed in WP2.
- 4 of them (*UFC_003, UFC_004, UFC_008 and UFC_009*) have been “de novo” re-sequenced because the retrieved genomes did not match their reference genomes with enough accuracy.

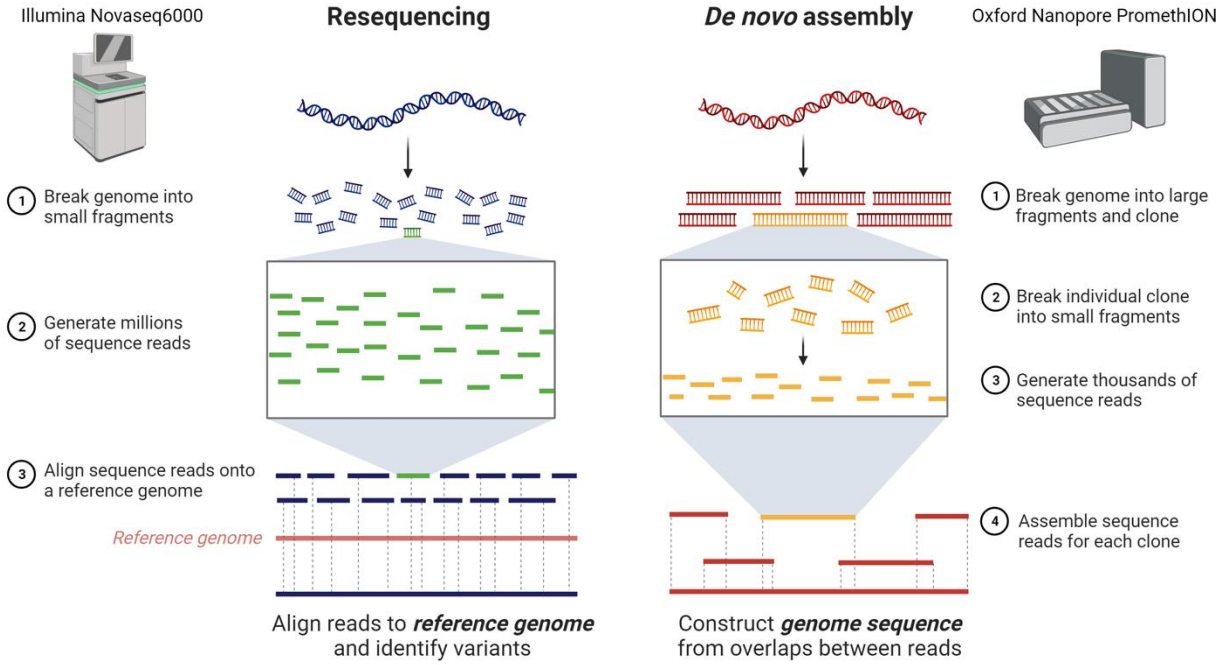

Figure 10. Main steps for fungal genome sequencing.

The initial genomic characterization of the 6 strains is summarized in Table 3.

Table 3. Sequencing features of six fungal strains from site 10.

Strain ID	Family	Sequencing
UFC_003	Cordycipitaceae	***De novo***
UFC_004	Clavicipitaceae	***De novo***
UFC_006	Hypocreaceae	Resequencing
UFC_007	Clavicipitaceae	Resequencing
UFC_008	Myxotrichaceae	***De novo***
UFC_009	Cordycipitaceae	***De novo***

The main features of the 4 *de novo* genomes are provided in Figure 11 .

UFC003

ID	Number of Reads	Number of Bases	Mean Read Length	N50 Read Length
UFC003	586787	6778388944	11551	26331

Kmer	Depth	n_kmer	Genome size	Heterozygous ratio	Repeat sequence content
17	24	893293944	34.2 Mb	0.46%	12.12%

Gap free
Chromosome level

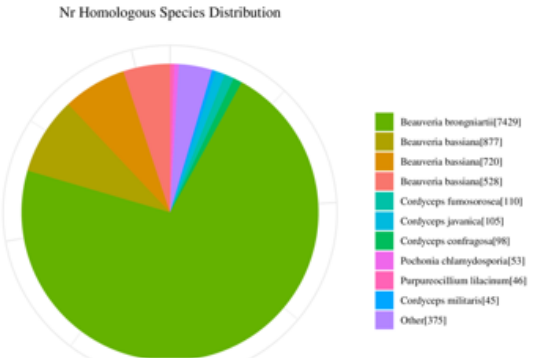

UFC004

ID	Number of Reads	Number of Bases	Mean Read Length	N50 Read Length
UFC004	8150493	24637625899	3022	3727

Kmer	Depth	n_kmer	Genome size	Heterozygous ratio	Repeat sequence content
17	12	893293077	69.2 Mb	0.29%	13.99%

Gap free
Chromosome level

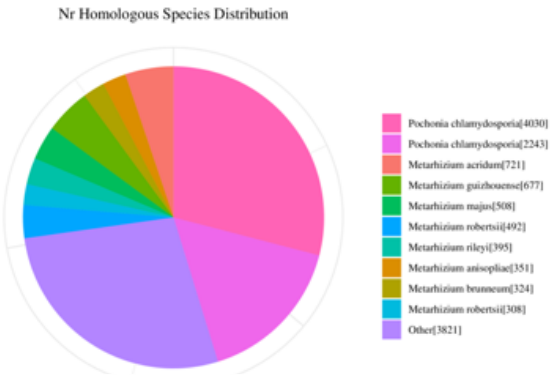

UFC008

ID	Number of Reads	Number of Bases	Mean Read Length	N50 Read Length
UFC008	701823	6043294776	8610	22134

Kmer	Depth	n_kmer	Genome size	Heterozygous ratio	Repeat sequence content
17	18	893291936	48.4 Mb	0.27%	2.87%

Gap free
Chromosome level

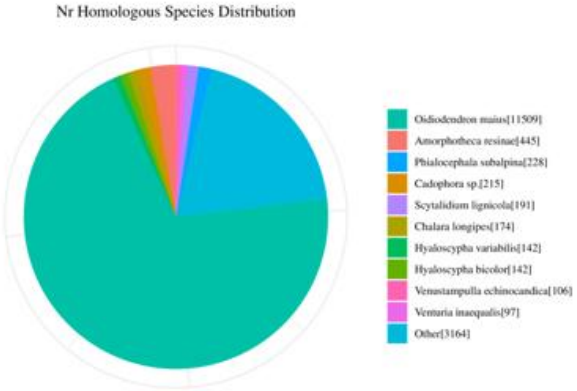

UFC009

ID	Number of Reads	Number of Bases	Mean Read Length	N50 Read Length
UFC009	530641	5784812065	10901	24945

Kmer	Depth	n_kmer	Genome size	Heterozygous ratio	Repeat sequence content
17	22	893293571	39.6 Mb	0.13%	7.40%

Gap free
Chromosome level

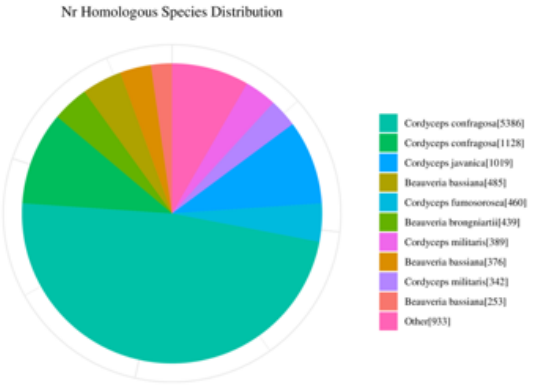

Figure 11. Main features of the 4 *de novo* fungal genomes from fungi isolated from site10.

Based on the *de novo* genome sequencing data, it appears that the 4 genomes were of high quality and matched with some existing genomes. *UFC_004* in particular is very interesting since there is no existing close-matching reference genome andit might be considered as a novel strain. Given this original feature, together with a high tolerance to metals, UMLP and IDENER pursued the full characterization of strain *UFC_004* (see section below), using the strategy summarized in Figure 12. This analysis enables the modelling of the metabolic network of fungi with high remediation potential. It

also provides means for reconstructing strains to enhance their abilities for growth, pollutants consumption and by-product production.

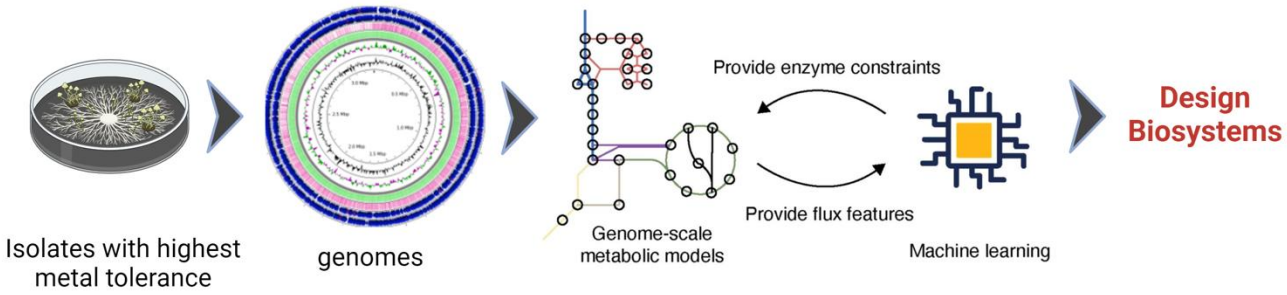

Figure 12. Genome-scale metabolic models of fungal species isolated from heavy metal contaminated sites.

2.4.2 In-depth characterization of *UFC_004*

In this section, we describe one of the major outputs of the BIOSYSMO activities, based on an integrative approach that provided a comprehensive understanding of the functional capabilities of *UFC_004* and its potential role in promoting plant health under heavy metal stress. To achieve these objectives, we employed a multifaceted approach that includes: (1) isolating and culturing *UFC_004* from rhizosphere soil samples (D1.2); (2) performing *de novo* whole genome sequencing using high-throughput sequencing technologies; (3) conducting bioinformatic analyses to assemble and annotate the genome, identifying genes associated with metal tolerance; (4) carrying out a comparative genomic analysis to explore shared and unique genes, gene families, phylogenetic relationships, and synteny with closely related species; and (5) constructing a genome-scale metabolic model to predict the metabolic capabilities and interactions of the fungus.

To date, no genomic resources are available for species within the *UFC_004* genus. The comprehensive genomic analysis of *UFC_004* provided valuable data on genes involved in heavy metal tolerance and plant-fungal interactions. Furthermore, constructing a genome-scale metabolic network is invaluable for translating genomic information into functional insights, particularly in understanding how *UFC_004* metabolizes and responds to environmental stressors, including heavy metals. which are crucial for the organism's detoxification mechanisms and overall stress tolerance.

Genome assembly and characteristics analysis

The *UFC_004* genome assembly contained ~ 54.6 Mbp. The final assembly results (Table 4) showed that the genome assembly consisted of 28 contigs with an N50 of 4,411,586 bp. The maximum length of the assembled contig was 6,264,885 bp. The total contig length was 54,637,677 bp. The average GC content of the resulting *UFC_004* genome was 49.10% . BUSCO v5.2.1 software was used to assess the integrity of the genome assembly and annotation completeness. The results showed that 98.7% (748 BUSCOs) were complete genes based on the BUSCO assessment, while 0.1% (1 BUSCOs) were fragmented and 1.2% (9 BUSCOs) were missing.

Table 4. Genome characteristics of *UFC_004*.

Parameters	number
Contigs	28
Genome size (bp)	54637677
Largest contig (bp)	6264885
N50 (bp)	4411586
L50	6
GC (%)	49.1
Complete BUSCOs (%)	98.7
Complete and single-copy BUSCOs (%)	97.6
Complete and duplicated BUSCOs (%)	1.1
Fragmented BUSCOs (%)	0.1
Missing BUSCOs (%)	1.2
Gene number	14509
Gene total length (bp)	27947132
Gene average length (bp)	1926.19
Percent of genome size (%)	51.15
rRNA	64
tRNA	190
sRNA	32
GO annotation	7786
KEGG annotation	13598
KOG annotation	6950
Pfam annotation	10477
Swissprot annotation	8479
NR annotation	13886
Total annotated	13902

Gene annotation

In the GO analysis, 7,786 coding genes were annotated in *UFC_004* and classified into cellular component, molecular function, and biological process (Figure 13). Among these categories, seven functional entries had more than 4,000 annotated genes. These genes were enriched in cell (5,858), cell part (5,846), cellular process (4,957), metabolic process (4,894), organelle (4,687), catalytic activity (4,406) and binding (4,059).

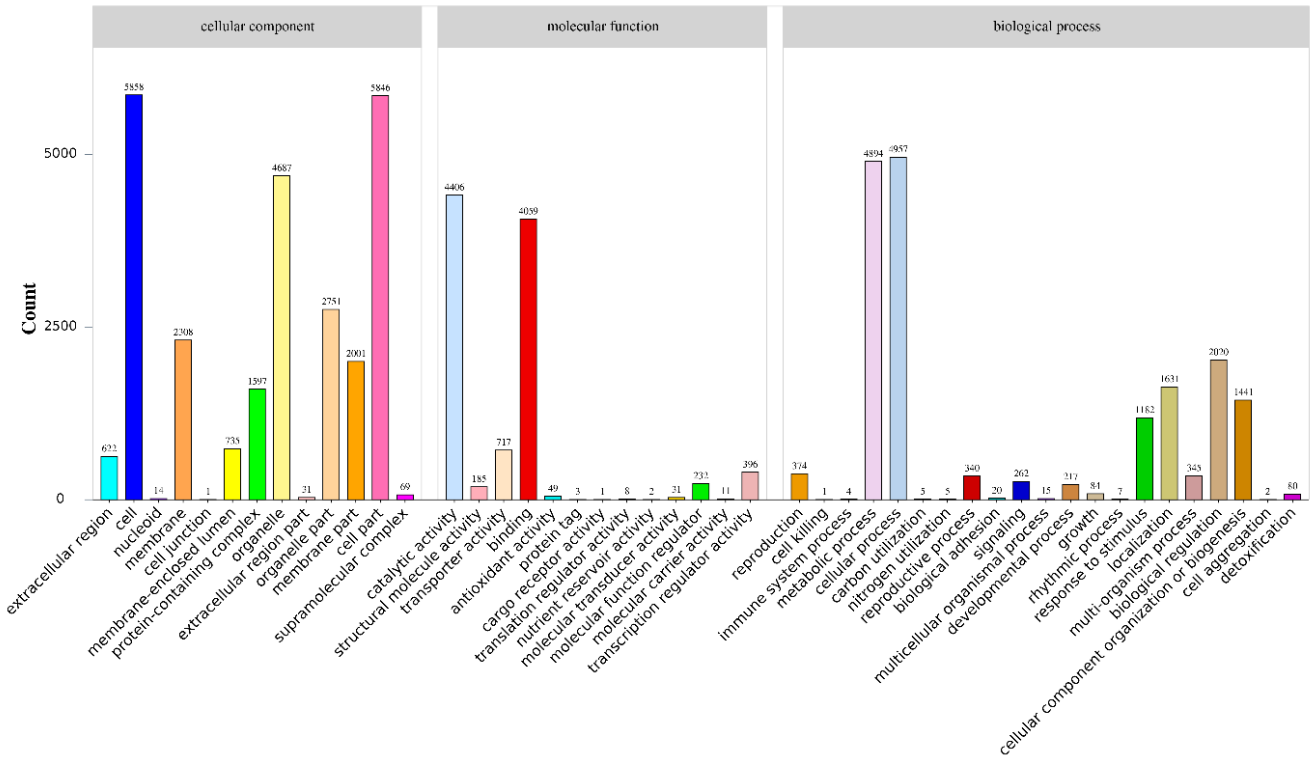

Figure 13. GO functional classification of *UFC_004*. The horizontal axis represents the GO functional classification, the left vertical axis represents the number of genes annotated in this category.

Proteomic analysis of metal resistance-associated proteins

The proteomic analysis identified in *UFC_004* several proteins potentially associated with metal resistance mechanisms, normalized to account for overrepresentation (Figure 14). Key proteins such as *YCF1, vacuolar metal resistance ABC transporters*, and *metal resistance proteins* play a role in divalent metals (As, Hg, Cd, Se) detoxification through sequestration or efflux mechanisms. Additionally, the presence of ArsH and ArsB proteins highlights potential resistance to arsenic (As) , while PcaA suggests possible tolerance to cobalt (Co) and Niquel (Ni). To maintain clarity, only proteins with a relatively high identity score with the metal interaction proteins from fungi are represented in Figure 14. .

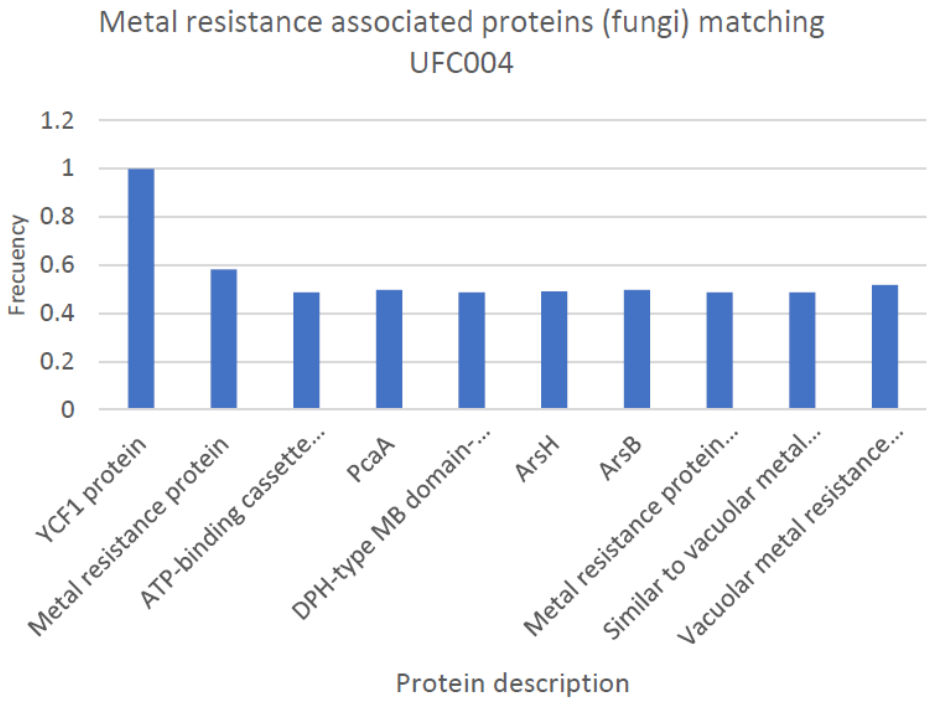

Figure 14. Bars plot representing the frequency of metal resistance proteins detected in *UFC_004* proteome. Data is normalized.

To broaden the scope of metal resistance gene discovery in the *UFC_004* genome, we conducted a comparative analysis against curated bacterial metal resistance protein datasets. This approach was based on the extensive functional characterization of prokaryotic detoxification systems, particularly those involving arsenic resistance and ABC-type efflux systems, which are often conserved across domains (Ben Fekih et al., 2018; Chang et al., 2018). Identifying homologs of these well-annotated bacterial proteins in *UFC_004* allowed us to enable a most robust functional annotation, while also offering insight into potential horizontal gene transfer events or functionally convergent adaptations. Moreover, bacterial datasets offer a comprehensive reference for resistance-associated domains that may be underrepresented in fungal-specific annotations.

The alignment results revealed a profile focused primarily on As resistance (

Table 5), supported by multiple matches to Arsenic resistance protein ArsH. ArsH is a well-characterized system for detoxifying As through oxidative transformation and its repeated identification underscores As resistance as a key trait for *UFC_004* (Chang et al., 2018).

Table 5. Top-scoring protein matches between the predicted proteome of fungal isolate *UFC_004* and the curated reference dataset of metal resistance proteins from bacteria. Table includes the gene ID from the *UFC_004* genome, the matched sequence identifier and description from the reference database, the gene name, alignment statistics (identity, coverage, and e-value), and the metal(s) associated with the matched protein based on the reference dataset employed.

Gene (from *UFC_004*)	Sequence ID (from reference dataset)	Description of matched protein (from reference dataset)	Id of matched protein	Identity (%)	e-value	coverage (%)	Metal(s) associated
g9432.t1	sp|P74312|ARREH_SYNY3	NADPH-dependent quinone reductase ArsH	P74312	65	2.87E-88	94	As
g10608.t1	sp|P32875|LIPA_YEAST	Lipoyl synthase, mitochondrial	P32875	64	4.16E-162	81	Not direct relation
g12453.t1	sp|P74312|ARREH_SYNY3	NADPH-dependent quinone reductase ArsH	P74312	63	1.50E-86	94	As
g9432.t1	tr|E8PS81|E8PS81_YERPE	Arsenic resistance protein ArsH	E8PS81	57	9.11E-88	96	As
g584.t1	sp|P40035|PIC2_YEAST	Mitochondrial phosphate carrier protein 2	P40035	56	3.88E-111	95	As and Cd
g4779.t1	sp|P25297|PHO84_YEAST	Inorganic phosphate transporter PHO84	P25297	56	0	91	Mn and Co
g12453.t1	tr|E8PS81|E8PS81_YERPE	Arsenic resistance protein ArsH	E8PS81	56	2.53E-85	96	As
g3019.t1	tr|Q8NTP4|Q8NTP4_CORGL	Arsenite efflux pump ACR3 and related permeases	Q8NTP4	51	1.11E-111	97	As

Construction of the genome-scale metabolic model (GEMs) of M. suchlasporia UFC_004

The genome-scale metabolic model was constructed directly from the amino acid FASTA sequence derived from the *de novo* sequencing of the microorganism. Model reconstruction was carried out using the RAVEN toolbox, which applies a homology-based alignment strategy to identify gene-protein-reaction (GPR) associations by comparing the input sequences against curated databases such as KEGG and MetaCyc. This approach allows us to move beyond basic protein annotation, enabling a more in-depth exploration of functional metabolic pathways and mechanisms that may be encoded within the genome. One of the key advantages of this strategy is its ability to extract GPR associations

directly from the amino acid sequences, allowing us to link genes to enzymatic functions and their corresponding reactions. As a result, this facilitates a more comprehensive understanding of the organism's metabolic capabilities. During model construction, 2,390 reactions were identified from the MetaCyc database and 880 reactions from KEGG. These reactions encompass core metabolic functions, including central carbon metabolism (e.g., glycolysis, the TCA cycle), amino acid and nucleotide biosynthesis.

A significant aspect of the model is its prediction of GPR associations related to metal interactions, particularly for arsenic, cadmium, and zinc. Using a curated collection of metal interaction proteins, several genes were identified that likely contribute to the microorganism's ability to tolerate and metabolically respond to metal stress, with potential implications for bioremediation. The *UFC_004* GEM contained annotated genes that shared a high degree of similarity with metal interaction genes such as ArsH and Lip (Figure 15), that are involved in internal detoxification and oxidative stress management, enhancing the cell's defense mechanism under toxic metal exposure.

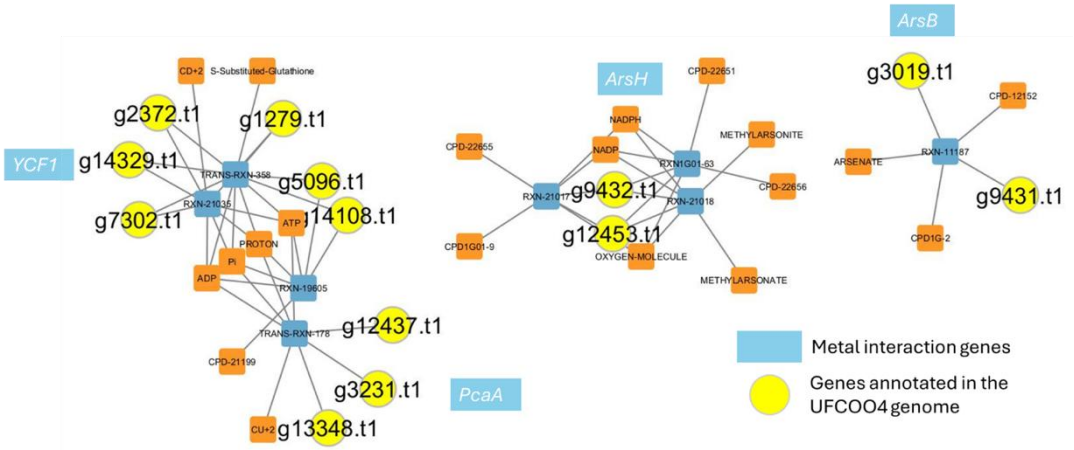

Figure 15. Metal interaction mechanisms identified within the *UFC_004* genome. Yellow circles represent genes annotated within the genome, blue squares indicate associated reactions, and orange squares denote metabolites. The network layout was generated using Cytoscape's Prefuse Force Directed algorithm that arranges nodes based on their stability parameters. Gene annotated in the *UFC_004* GEM were aligned with known metal interaction proteins from a curated dataset. The names of closely related reference proteins are indicated next to the corresponding genes.

2.4.3 Conclusions

This work provides a detailed exploration of the genomic and metabolic attributes of fungi isolated from site 10. Our results reveal that *UFC_004* exhibits considerable tolerance to Cd, Pb, and Zn, with MIC_{50} values of 4.43 ± 1.17 mM, 5.31 ± 0.77 mM, and 38.36 ± 11.01 mM, respectively (D1.2). These findings highlight its capacity to withstand metal stress, positioning it as a promising candidate for bioremediation in contaminated environments. Additionally, inoculation of *Salix aquatica grandis* trees with *UFC_004* resulted in a 64% increase in dry biomass, demonstrating its ability to enhance plant growth under challenging conditions, as detailed in D3.1. This suggests potential applications for improving agricultural productivity in metal-polluted soils (D3.1). In the present work, the genome of *UFC_004*, assembled *de novo* to approximately 54.6 Mbp across 28 contigs with an N50 of 4,411,586 bp, offers

a robust foundation for understanding its functional capabilities. Annotation identified 14,509 protein-coding genes, many of which are linked to metal resistance, pathogenicity, and diverse metabolic processes. Notably, genes encoding ATP-dependent transporters, redox enzymes, and metal-chelating proteins were prevalent, providing mechanistic insights into its ability to detoxify heavy metals. Phylogenetic analysis positioned *UFC_004* closely to *P. chlamydosporia*, yet it harbors unique gene families that reflect specialized adaptations. *P. chlamydosporia* is quite a versatile and well-studied fungus with several traits of interest relevant to phytomanagement, particularly in the context of plant growth promotion and biocontrol. While it is not traditionally known as a contaminant-detoxifying organism, its indirect roles in enhancing plant resilience could still be highly relevant, especially if similar traits were observed in your isolate (UFC_004).

The GEM of *UFC_004*, encompassing 3,270 reactions and 3,682 metabolites, further elucidated its metabolic versatility, particularly in pathways related to metal detoxification, such as those involving As and Cd.

2.5 Optimization of plant and microbial resources

In the following sections, we describe the results obtained by UMLP on the optimization of microbial inoculum from sites 2 and 10, taking advantage of the physiological and molecular traits obtained from the individual strains, as described in sections 2.3 and 2.4, as well as in D3.1 and D1.2. In addition, strains that were not listed in D3.1 have been isolated and characterized from site 1. For these additional strains, we followed the same procedure as that described in D1.2 for selecting the most appropriate isolates, based on metal tolerance and PGP traits.

The assembly of a microbial consortium can be carried out using top-down and bottom-up approaches. For this study, the latter approach was selected. It begins with individual components - in this case, fungi isolated from polluted sites - and aims to assemble them into a functional consortium by studying their interactions and collaborations. The consortium is created by selecting fungal strains based on compatibility and potential synergies. Once assembled, it can then be tested on plants to assess its positive or negative effects.

2.5.1 Functional traits of fungal strains in consortium A.

In **Error! Reference source not found.**, we provide functional traits of strains presented in D2.1 (*UFC_003, UFC_006, UFC_009* and *UFC_016*), and five additional strains not included in D3.1 (highlighted in red). All nine fungal strains exhibited multiple PGP traits, including phosphate solubilisation, production of IAA (Indole acetic acid) and siderophores. Most strains showed low to moderate apparent IAA poor production, as indicated by pale to moderately pink coloration in the Salkowski assay. *UFC_058* was a notable exception, displaying a distinctly more intense pink colour compared to the other strains, suggesting higher relative IAA production. In nitrogen-deficient medium, most strains exhibited limited growth, with the exception of *UFC_009 sp.* and *UFC_096,* which showed moderate growth under these conditions. Both *UFC_003* and *UFC_009* showed mycelium formation on lignin as sole carbon source and produced comparatively high levels of siderophore and EPS (Extracellular Polymeric Substances) compared to the other fungi. Siderophore production results for *UFC_053* were inconclusive due to delayed colony development. In the case of *UFC_096*, red

secondary metabolites interacted with the blue chromogenic siderophore assay medium, resulting in a purple colouration that shifted to orange after three additional days of incubation.

Table 6. Plant growth promoting traits of the fungi consortium. – inconclusive; + = low; ++ = moderate; +++ = high. ✓ = Presence of the trait. In red : additional strains not included in D3.1.

Strains	*UFC_003*	*UFC_006*	*UFC_009*	*UFC_019*	*UFC_053*	*UFC_058*	*UFC_096*	*UFC_016*	*UFC_050*
Phosphate solubilisation	✓	✓	✓	✓	✓	✓	✓	✓	✓
IAA production	+	+	+	+	+	+++	+	++	+
Siderophore production	+++	++	+++	+	-	+	+	++	++

2.5.2 Optimization of microbial consortia assembling

Optimization of fungal strains from sites 1 and 10

For assembling fungal isolates to build a PGP consortium, the individual strains should:

1. exhibit a soil health-promoting activity
2. exhibit pollution-alleviating capabilities
3. exhibit plant growth promoting capacities
4. represent a wide fungal diversity
5. exhibit compatibility and interactions among them
6. produce spores for easy handling

The criteria 1-4 were fully evaluated in the scope of T3.1 activities, during RP1, and fully described in D3.1. To summarize, some of the isolated microbes from sites 1 and 10 showed very high capacities to tolerate metal stress, which is due to the considerably high concentrations of metals at the isolation area (D1.2). This is linked to the elevated production of siderophores, which allows microbes to scavenge metals. The usefulness of isolated microbes and their PGP traits were further demonstrated by confrontation with plants in simple growth systems, using the model tree willow. Some of the isolated strains showed significant and high performance in terms of growth improvement. The best performing strains were thereafter selected for use in WP4.

For criteria 5-6, in a first series of tests, we evaluated the interactions between two candidate fungal strains isolated from site 10. We tested these interactions by inoculating species A first and then pinning species B and all other strains on top, and then the reverse was conducted, i.e., species B inoculated first, followed by species A and all others. Interactions can be positive (synergistic), negative (antagonistic), or neutral. By evaluating the effects from both directions, we can better understand how each strain influences the growth and behavior of the other. However, the order of species introduction into the environment affects the final composition and function of the community. Thus, the first isolate to establish may influence the success or failure of subsequent ones, as early colonizers can alter environmental conditions, nutrient availability, or microbial dynamics that affect later arrivals. A representative set of obtained data is presented in Table 7.

Table 7. Comparison of the growth effects of each fungus according to background species compared with the control using Student's t test (p-value < 0.05). An 'x' indicates no growth; '↘' indicates reduced growth; '⇗' indicates increased growth; '0' indicates no effect on growth; 'ND' indicates no available data.

Background species	Fungal strains tested					
	UFC_036	*UFC_025*	*UFC_027*	*UFC_089*	*UFC_009*	*UFC_058*
UFC_036	---	⇗	↘	↘	⇗	0
UFC_025	↘	---	↘	↘	↘	⇗
UFC_027	↘	nd	---	x	↘	⇗
UFC_089	↘	nd	↘	---		↘
UFC_009	↘	nd	↘	↘	---	↘
UFC_058	↘	x	↘	x	x	---

These binary interaction studies of the fungal species consortium led to the conclusion that most of the fungi tested can co-exist. However, some fungal strains showed a highly competitive behavior, e.g. *UFC_036* inhibited the growth of most of the other fungi and *UFC_089* suppressed the growth of *UFC_027 and UFC_058*. *UFC_036* is used as biocontrol agent in many other studies and able to produce many secondary metabolites against other fungi. Although of interest, this type of fungus is therefore not suitable for consortia assembling. We therefore selected additional isolates from our initial collection (D1.2).

On a general note, the absence of standardized protocols for the study of fungal interactions has constituted a limitation to this research and there was a need to improve the protocol. In a second series of tests, we therefore optimized the protocol for improving spore production by each isolate, varying parameters linked to growth (medium, incubation time, initial spore concentration, spore solution, growth period) and inoculation methods onto the agar plates (pinning method andback ground inoculation method), as described in Table 8.

Table 8. Conditions tested for optimization of spore production and inoculation method on agar plates by varying 7 parameters.

Parameter	Condition 1	Condition 2	Condition 3
Medium	Glucose PGA	Czapek – Dox	Czapek – Dox + 0.5% yeast extract
Incubation time	18 h	20 h	22 h
Spore concentration	10^5	10^6	10^7
Spore solution	Saline Solution	Saline Solution + Tween	Nutritional Broth
Pinning method	Pipetting	Filter Paper Disc	Hole
Back-ground inoculation	L-shaped spreader	Glass beads	--
Evaluation	72 h	96 h	120 h

After testing these various combinations with some fungal isolates, we proposed an optimized protocol (Figure 16), which allowed us to improve the inoculation of agar plates and obtain more reliable results. This protocol is now routinely used in our laboratory.

Figure 16. *Optimized protocol for confrontation tests*.

The final result of the confrontation tests led us to consider the assembly of 2 consortia: consortium A is made of fast-growing isolates, that are fully compatible. Consortium B is made of isolates with lower growth rates, but with a higher diversity. Strains from consortium B were not compatible with strains from consortia A as their growth was partially or totally inhibited by strains A. Also, PGP traits have been demonstrated in all strains by literature search.

Table 9. Optimized fungal consortia A and B from site 10

Class	Consortium A	Consortium B
Sordariomycetes	*UFC_003*	*UFC_020*
	UFC_006	*UFC_035*
	UFC_009	*UFC_038*
	UFC_019	
	UFC_053	
	UFC_058	
Eurotiomycetes	*UFC_096*	*UFC_116*
	UFC_016	*UFC_013*
	UFC_050	
Leotiomycetes		*UFC_008*
		UFC_113
Dothideomycetes		*UFC_017*

Consortium A has been shipped to partner UPM for testing with poplar. Consortium B is being tested during RP2 and will continue to be evaluated during RP3.

Optimization of fungal and bacterial strains from site 2

As explained in the previous section, the formation of microbial consortia was based on the association of strains exhibiting PGP traits and demonstrated tolerance to Hg. The isolation, identification and characterisation of the different species from Site 2 contaminated with Hg were fully evaluated during RP1 and fully described in D3.1.

All fungal and/or bacterial strains were then inoculated in pairs on Petri dishes to ensure that there were no antagonistic effects. The compatibility of the strains was assessed quantitatively by observing the contact zone between the two strains. These confrontation tests led to the combination of three bacterial strains to form a bacterial consortium, two fungal strains to form a fungal consortium, and a mixture of these strains to form a mixed consortium (with the exception of *UFC_B029*, which demonstrated antagonistic effects on the fungal strains). The composition of these consortia is shown in Table 10.

Table 10. Optimized microbial consortia from site 2

Condition	Composition of microbial consortia
Bacterial consortium	*UFC_B029* *UFC_B030* *UFC_B037*
Fungal consortium	*UFC_019* *UFC_022*
Mixed consortium	*UFC_019* *UFC_022* *UFC_B030* *UFC_B037*
Control consortium	Autoclaved microbial cultures

2.6 Conclusions and linked activities with WP4

At sites 2 and 10, UMLP went deeper into the characterization of some of the isolated strains during RP1.

- We compared two strains of *Pseudomonas sp.*, isolated from contrasting environments, in terms of their Hg resistance mechanisms: the first strain (*UFC_B020*) was isolated from the rhizosphere of Hg-contaminated soil and the second (*P31*) from an unpolluted environment, obtained from an external laboratory. *UFC_B020* exhibited 20-fold higher mercury resistance than the second strain and displayed significant biovolatilisation capacity. Comparative analysis of the responses of bacterial biomass and necromass to mercury exposure revealed that the strain from an unpolluted environment lacks active detoxification mechanisms and relies primarily on passive resistance. Transcriptomic analysis further elucidated the molecular basis of these phenotypic differences: the mercury-resistant strain rapidly upregulated genes involved in metal detoxification and efflux pathways. In contrast, the transcriptional response of the second strain indicated increased cellular stress and compensatory mechanisms, including thiol metabolism, DNA repair, and oxidative stress response. These results confirm that environmental Hg contamination exerts

selective pressure, favoring the maintenance and expression of resistance genes within microbial populations. This comparative study sheds new light on the molecular mechanisms underlying mercury tolerance in *UFC_B020* and highlights the potential of naturally selected strains for bioremediation applications.

- We presented the first comprehensive genomic and metabolic analysis of *UFC_004*, a rhizosphere-resident fungus isolated from an industrial wasteland. The strain exhibited robust heavy metal tolerance with MIC_{50} values of 4.43 mM for Cd, 5.31 mM for Pb, and 38.36 mM for Zn, and notably enhanced *Salix aquatica grandis* plant biomass by 64% under metal stress conditions. A high-quality genome assembly (~54.6 Mbp, 98.7% complete BUSCOs) revealed 14,509 protein-coding genes, including numerous candidates implicated in metal detoxification such as ArsH and YCF1. To understand the mechanisms associated with these genes, a genome-scale metabolic model was reconstructed with a network of 3,270 reactions and 3,682 metabolites, revealing distinct arsenic detoxification pathways that differentiate *UFC_004* from closely related species. Comparative genomic analyses further positioned *M. suchlasporia* within the Clavicipitaceae family and highlighted unique adaptive features, likely contributing to its resilience in heavy metal-rich environments. Overall, these findings not only elucidate the molecular mechanisms underpinning heavy metal tolerance in *M. suchlasporia UFC_004* but also underscore its potential utility in bioremediation and sustainable agriculture.
- We optimized consortia obtained from sites 2 and 10 using binary interaction tests, that led to the production of microbial inocula that are currently being tested in WP4. The results were reported by UMLP in D4.2. Further on-going experiments by UMP using the UMLP consortia will be reported in the next period.

3 Optimization of microbes and microbial consortia from estuarine sediments (sites 4 and 5)

3.1 Introduction

Estuaries are highly productive ecosystems that have a crucial role in biogeochemical cycles and unique physical-chemical conditions that support a large diversity and a multitude of ecosystem services. However, they are subjected to high anthropogenic pressures, and they are considered sinks of organic and inorganic contaminants, which can affect their ecological functions. Contamination of estuarine ecosystems by different contaminants, including metals and pharmaceuticals, has been widely reported (Cunha et al., 2024, Fernandes et al., 2021). The development of bioaugmented phytoremediation strategies as nature-based solutions for the recovery of estuarine environments exposed to mixed contamination arises as a sustainable alternative, as saltmarsh plants and their associated microbial communities can have an important role in the removal of organic and inorganic contaminants from estuarine sediments. One of the main challenges for the effective implementation of these strategies is the selection of a combination of salt marsh plants and microbial consortia that can be efficient in the removal of mixed contaminants. For this, in BIOSYSMO, the microbial communities associated with salt marsh plants and sediments are being explored for their diversity and function, and relevant bacterial strains are being isolated, characterised for their bioremediation potential, and combined in optimised consortia for enhanced phytoremediation.

The two estuaries selected as case studies in BIOSYSMO are the Douro estuary (site 4), an urban estuary receiving diffuse pollution, and the Lima River estuary (site 5), an urbanised-industrialised estuarine environment affected by different anthropogenic activities. Contamination by metals and pharmaceuticals has already been reported for both estuaries (D1.1), so these were the contaminants selected for the isolation of bacterial strains in task 1.3 (D1.2), using estuarine sediments and rhizosediments associated with the plants *Sporobolus maritimus* and *Juncus maritimus*. The isolated bacteria, described in D1.2, started to be tested in D3.1 for their capacity to degrade several pharmaceuticals, though the pharmaceuticals Ketoprofen or Venlafaxine were selected to be further explored in WP4. In addition, bacterial isolated strains were characterised in terms of metal tolerance, both by the trace metal resistance assay (Cu, Cd, Cr, Pb, Zn) and the minimum inhibitory concentration assay (Cu and Cd). Finally, bacterial isolated strains were characterized by their plant growth promoting (PGP) traits, including phosphate solubilization and siderophore production. These two last characterisations were a laboratory work that started to be developed in D3.1 and are presented in full in this document. From site 4, one consortium was already established and tested for its potential Ketoprofen degradation and Cd removal abilities. Isolates from site 5 were used as a source to select optimal strain combinations for contaminant degradation through the interspecies Aggregation, Combinatorics, Microfluidics and Entrapment (iACME) methodology, performed collaboratively by CIIMAR and JSI. This approach systematically reduced the number of candidate species, resulting in twelve promising consortia that are currently being tested for their Venlafaxine degradation and Cu removal abilities, minimum inhibitory concentration assay (Cu) and biofilm production (PGP trait).

3.2 Methodologies

3.2.1. Degradation of pharmaceuticals

Ketoprofen (Kpf) degradation

Nine bacterial strains, previously isolated from the enriched culture obtained in D3.1 using Kpf and Cd as selectors, were tested individually to assess their potential to degrade Kpf (1mg/L) in Mineral Salts Minimal (MM) Medium with 1 % NaCl. The selected strains were supplemented with 500 mg/L of NAOAc. All cultures were incubated in the dark and at room temperature (21°C) under static conditions, for 4 weeks. Bacterial cultures were transferred to new sterilised flasks once a week, to avoid oxygen depletion, and fed with 500 mg/L of NaOAc twice a week. The pharmaceutical removal efficiency for each isolated strain was assessed by analysing MM media by High-performance Liquid Chromatography with a Diode-Array Detector (HPLC-DAD). Abiotic degradation controls were used with just MM media supplemented with the pharmaceutical.

Venlafaxine (Vfx) degradation

Twenty bacterial strains, previously isolated from the enriched culture obtained in D3.1 using Vfx and Cu as selectors, were tested individually to assess their potential to degrade Vfx (1mg/L) in MM Medium with 1 % NaCl. The selected strains were supplemented with 500 mg/L of NAOAc. All cultures were incubated in the dark and at room temperature (21°C), under static conditions, for 4 weeks. Bacterial cultures were transferred to new sterilised flasks once a week, to avoid oxygen depletion, and fed with 500 mg/L of NAOAc twice a week. The pharmaceutical removal efficiency for each isolated strain was assessed by analysing MM media by High-performance Liquid Chromatography with a Fluorescence Detector (HPLC-FLD). Abiotic degradation controls were used with just MM media supplemented with the pharmaceutical.

Characterisation of Metal Tolerance

To characterise the metal tolerance of the different isolated strains obtained, two methodologies were applied– Trace Metal (TM's) Resistance Assays and Minimum Inhibitory Concentration (MIC) Assays. For both, all strains were activated from cryopreservation in PCA (Plate Count Agar) or MM agar media to ensure proper growth and purity. The metal tolerance traits were assessed for strains obtained either from the enriched cultures selected using metals (Cd or Cu) or selected using both metals and pharmaceuticals (Cd and Kpf or Cu and Vfx).

Trace Metal Resistance (TM's) Assays

The TMs resistance assays were only performed for bacterial strains isolated previously in PCA, media in which this assay is performed, and were performed using an adapted Disk Diffusion method described in detail in the deliverable D3.1.

Minimum Inhibitory Concentration (MIC) Assays

To test the susceptibility of the isolated strains to TMs, the MICs were determined in a microdilution assay in a 96-well microplate. The method for this is described in (Sütterlin et al., 2018; Cheng-Han Liu et al., 2023; Ćirković et al., 2023) and detailed in deliverable D3.1.

3.2.1 Characterisation of PGP traits in rhizosediment bacteria

Plant Growth-Promoting (PGP) traits were assessed in the isolated strains to identify the most effective candidates for use in combination with salt-marsh plants for contaminant removal. The traits analysed, and described below, included siderophore production, phosphate solubilization, ACC deaminase activity, biofilm formation, and nitrogen fixation.

Siderophore production

Siderophore production was detected in deferrated PCA (Balado et al.,2015; Lankford, 1994), following the methodology detailed in deliverable D3.1.

Phosphate solubilization

Phosphate-solubilizing bacteria were identified using the phosphate growth medium from Ejikeme & Uzoma (2013) and methodology described in detail in the previous deliverable D3.1.

ACC Deaminase production

ACC (1-aminocyclopropane-1-carboxylate) deaminase production was identified using a sterile minimal DF (Dworkin and Foster) salts media: 4.0 g L^{-1} KH_2PO_4, 6.0 g L^{-1} Na_2HPO_4, 0.2 g L^{-1} $MgSO_4 \cdot 7H_2O$, 2.0g $C_6H_{12}O_6$, 2.0 g L^{-1} $C_6H_{12}O_7$, 2.0 g L^{-1} $C_6H_8O_7$,15 g L^{-1} Agar,1 mg L^{-1} $FeSO_4 \cdot 7H_2O$, 10 mg L^{-1} H_3BO_3,11.19 mg L^{-1} $MnSO_4 \cdot H_2O$, 124.6 mg L^{-1} $ZnSO_4 \cdot 7H_2O$, 78.22 mg L^{-1} $CuSO_4 \cdot 5H_2O$, 10 mg L^{-1} MoO_3. The $(NH_4)_2SO_4$ was replaced from the original media with 3 mM ACC as the sole nitrogen source (Dworkin & Foster, 1958; Penrose & Glick, 2003). Before the test, 30 µmol · $plate^{-1}$ of 3.0 mM ACC solution was spread on sterile minimal DF media and allowed to dry fully. Each bacterial strain was cultivated in the prepared media and incubated at 28 °C. Growth was assessed after 72 hours and after one week. Positive results (bacteria grown on the plates) indicated the bacteria produced ACC deaminase and negative results (the bacteria did not grow on the plate) indicated they did not produce ACC deaminase. The test was conducted in triplicate.

Biofilm production

Biofilm production was assessed according to (Paredes-Páliz et al., 2016). Between 10-15 colonies were inoculated in 2.5 mL of the corresponding origin media, and incubated for 48-72 hours at 28°C under orbital agitation at 100 rpm. The culture's optical density (OD) was measured at λ = 600 nm (OD600) and adjusted to 1.0 using sterile medium. After that, the normalised bacterial suspensions were inoculated in triplicate (60 µL per well) into 96-well microtiter plates. A control row of wells containing 60 µL of sterile PCB or MM medium was also used. The 96-well microtiter plates were incubated for 4 days at 28 °C, under static conditions. After incubation, the bacterial suspensions were removed by inverting the plates, followed by washing the wells 5 times with deionized water (100 µL) each time, to eliminate non-adherent cells. Biofilms were then stained with a 0.01% crystal violet solution (100 µL) and incubated for 20 minutes. After that, excess crystal violet was rinsed off by washing the wells 3 times with deionised water (100 µL). The remaining dye was solubilised using 100 µL of a solution of 96% ethanol and glacial acetic acid (65%/35% v/v, respectively). The absorbance at λ = 570 nm was measured using a microplate spectrophotometer reader to measure biofilm formation in comparison with the control row.

Nitrogen Fixation

Bacterial strains were tested in screening assays to evaluate their ability to fix nitrogen, as performed in (Ferreira et al., 2021). Nitrogen Free Glucose Mineral Media (NFGMM) was prepared: 10 g L^{-1} $C_6H_{12}O_6$,10g L^{-1} $C_4H_6O_5$, 1 g L^{-1} K_2HPO_4, 0.1 g L^{-1} $CaCl_2$, 0.2 g L^{-1} $MgSO_4 \cdot 7H_2O$, 0.01 g L^{-1} $SO_4 \cdot 7H_2O$, 0.01 g L^{-1} $Na_2MoO_4 \cdot 2H_2O$, 0.01 g L^{-1} $MnSO_4 \cdot 5H_2O$, 25 g L^{-1} NaCl, 15 g L^{-1} agar, 0.0025 g L^{-1} $C_27H_{28}Br_2O_5S$. Each bacterial strain was cultivated in the prepared media. In each plate the strain was tested in half of plate with a single colony circle, and in the other half with a zig-zag streak and incubated at 28°C. Bacterial growth was evaluated after 72 hours and one week of incubation. Tests were performed in triplicate.Results were interpreted as follows: Positive = Bacteria grow on the plates and media colour changes from green to blue; Negative = Bacteria either do not grow or grow on the plates and media colour does not change from green to blue (it might change to orange/yellow).

Conventional selection of bacteria to develop consortia (site 4)

Following the evaluation of bacterial Ketoprofen (Kpf) degradation potential, cadmium (Cd) tolerance, and the presence of plant growth-promoting (PGP) traits, nine bacterial strains were selected for compatibility testing. This step aimed to ensure that a bacterial consortium could be assembled without antagonistic interactions which could lead to biological instability and reduce pollutant degradation. The selected strains were *PCDK2, PCDK5, PCDK9, PCDK15, PCDK16, MCDK2, MCDK4 and MCDK9.*

The strains were tested through a direct co-culture assay, where each strain was exposed to the supernatant of every other strain to assess potential antagonistic interactions. All bacterial strains were grown in 5 mL of Nutrient Broth medium and incubated in a shaker (28°C, dark) for 5-7 days. The OD_{625nm} of the bacterial suspensions was adjusted to 0.1 in saline solution (0.85 % v/v). Then. 30 µL of this suspension were spread onto PCA using a sterilised cotton swab to ensure even distribution. Simultaneously, 1 mL of each liquid culture was centrifuged at 10,000 rpm for 7 minutes, and its supernatant transferred to sterile Eppendorf tubes. Sterile diffusion disks were placed in the centre of each inoculated plate, and 15 µL of supernatants from each different strain was pipetted onto each disk. Plates were incubated at 28°C in the dark for 3-4 days. Zones of inhibition (halos) around the diffusion disks were visually assessed.

iACME (interspecies Aggregation Combinatorics Microfluidics Entrapment) selection of bacteria to develop consortia (site 5)

Biomass cultivation and construction of C57 mock consortium

The 57 isolated strains from an enriched culture with Vfx and Cu (previously identified as described in D3.1) were put to grow (initially coming from plates) in 25mL of Minimal Mineral-salts medium (MM) (see composition in D1.2) with the respective contaminants of origin (either Vfx 1mg/L, Cu 1mg/L or both) in the presence of light at 180 rpm. The strains were grown for 2 weeks, feeding NaOAc 500mg/L twice a week. Growth of individual strains was assessed via flow cytometry method, where absolute number of cells was determined. Mock consortium of all strains (hereinafter C57) was made by mixing all isolates at an equal cell ratio. The obtained C57 suspension was used as a starting material for all downstream aggregation and optimization studies. Before experiments, it was characterized by colloidal properties (size, surface charge, electrophoretic mobility) using Dynamic Light Scattering (DLS) and Electrophoretic Light Scattering (ELS) methods as described elsewhere (Rybki et al,. 2019).

Selection of polyelectrolyte and optimization of aggregation protocol

To promote aggregation of the bacterial cells, a difference in the net surface charge is required. Modification of bacterial surface charge from negative to positive implies the application of polyelectrolytes (PE's). Since it is known that most cationic PE's have toxic effects for bacteria (Boulange-Petermann, 2005), thorough selection of appropriate PE is needed. For this purpose, the toxic effect of three different PE's: Polyethyleneimine (PEI), Acetylated version of Polyethyleneimine with reduced number of amino-groups (acetPEI) and Chitosan (Chi), has been estimated for C57. The PE toxicity test was made in 96-well microplates as follows: 90µL of MM media supplemented with Cu (1 mg/L), Vfx (1 mg/L), resazurin (0.5 mg/L) and NaOAc (500 mg/L) was distributed in wells; Six different concentrations for each PE (1.25, 0.625, 0.315, 0.165, 0.075 and 0.035 mg/L) were added (90uL) by using two-fold dilutions with ultra-pure water . Each concentration was tested in triplicates. Growth and respiration (Absorbance at 450 nm and 600 nm, and Fluorescence at ex: 560nm / em: 590nm respectively) were measured over 48h every 30 min using a microplate reader (SynergyH4, BioTek). The obtained growth curves were analysed using R software with "growthcurver" package (Sprouffske et al., 2016) attached, and the doubling time (t_gen) was graphed and compared for the different concentrations of PE.

Following the toxicity assessment, the C57 mock consortium was subjected to different surface modification protocols with varying parameters including PE concentration (2.5 and 12.5 mg/L), exposure time (5 and 30 min), and ionic strength of the solution (0.154 and $1.54x10^{-4}$ mol/L). Detailed procedures of PE's deposition are described in Annex II of D1.2 and in (Rybki et al., 2019). These experiments aimed to identify optimal surface modification conditions while minimizing toxicity effects.

Based on the cell's surface modification protocol results, the most effective coating procedure was selected and applied to half of the C57 consortium suspension, resulting in positively charged bacterial cells. This positively charged fraction was then mixed with the remaining negatively charged half of the C57 for the optimization of the aggregation protocol. The protocol was performed using 1:5 dilutions with 12.5 mg/L of acetPEI, and an incubation time of 30 minutes (following the protocols described in Annex II of D.1.2.) The resulting aggregates were characterized for size distribution and visualized using fluorescently labeled microscopy methods.

Microfluidics Entrapment

Following aggregate formation, stabilization and isolation of individual aggregates was necessary, as each aggregate represents a unique combination of the 57 bacterial isolates and requires separate testing. The aggregate suspension concentration was precisely determined using fluorescent labeling and flow cytometry (Accuri C6plus, FL1 488 and FL4 640 nm lasers). These quantitative data, combined with size distribution results from DLS measurements, enabled calculation of aggregate hydrodynamic volumes.

Using a custom R script based on Poisson distribution function, these parameters were used to calculate the probability of entrapping exactly one aggregate within a single alginate bead. The aggregate suspension was then diluted to achieve optimal conditions for single-aggregate entrapment, targeting a ratio where one bead contained an aggregate while nine remained empty per 10 µL aliquot.

Encapsulation was performed using a Encapsultortor-390B (B'U'CHI (B'U'CHI supplierer) following procedures described in Annex II of D1.2. The final number of aggregate-containing beads per 10 µL aliquot was quantified using light microscopy (Zeiss AxioObserver Z1).

Aggregates cultivation and Consortia Candidate Selection

Following optimization of the alginate bead entrapment ratio, the encapsulated aggregates were subjected to growth performance testing to identify the most promising consortium candidates. The cultivation experiment was conducted in 384-well microplates using a SynergyH4 microplate reader (BioTek), with 10 µL of alginate beads inoculated per well in 40 µL of MM media containing various selective conditions.

Six different selective conditions were tested: (1) Vfx (1 mg/L); (2) Vfx (1 mg/L) + Cu (1 mg/L); (3) Cu (1 mg/L); (4) Vfx (1 mg/L) + NaOAc (500 mg/L); (5) Vfx (1 mg/L) + Cu (1 mg/L) + NaOAc (500 mg/L); and (6) Cu (1 mg/L) + NaOAc (500 mg/L). Two identical plates were prepared, one cultivated under aerobic conditions and another under anaerobic conditions using a Baker Ruskinn BugBox glove chamber (atmosphere: 85% CO_2, 10% N_2, 5% H_2). Both cultivations were conducted over 110 hours.

Growth monitoring was performed by measuring absorbance (450 and 600 nm) to assess biomass accumulation and fluorescence (excitation 560 nm, emission 590 nm) to evaluate respiratory activity. Technical details of the measurement procedures are described in Annex II of D1.2. For the aerobic plate, continuous kinetic measurements were taken every 30 minutes, while the anaerobic plate was measured discontinuously at 0, 38, 62, 68, 86, 92, and 110 hours. Plates were shaken for 30 seconds prior to each measurement to ensure proper mixing.

Growth curve analysis was performed using custom R scripts using the growthcurver, dplyr, FactoMineR, and factoextra libraries. Curves were constructed using the logistic growth equation describing population size N_t at time t :

$$N_t = \frac{K}{1 + (\frac{K - N_0}{N_0})e^{-rt}}$$

The growthcurver package determined optimal values for carrying capacity (K), intrinsic growth rate (r), and initial population size (N_0) for each growth curve.

Three key parameters were used to evaluate consortium candidate performance: area under the curve (auc_l), doubling time (t_gen), and time to midpoint of maximum growth capacity (t_mid). The detailed analytical procedures and candidate selection criteria are described in D4.1. Based on this analysis, the most promising candidates were selected from different performance clusters for further optimization studies.

Characterisation of iACME Consortia Candidates

DNA extraction was performed on consortia candidates grown in aerobic conditions, according to a modified protocol from the iHelix extraction kit, candidates grown in anaerobic conditions will be analysed for DNA composition in a later date when the biomass is enough for the process. For all candidates, PCR amplification, library prep and sequencing was done accordingly: The sequencing of

the 16S rRNA gene weas performed based on the PCR amplification of the 16S rRNA gene fragment using the 16S Barcoding Kit 1-24 (#SQK-16S024, Oxford Nanopore Technologies) and LongAmp® Taq 2X Master Mix (#M0287, NEB) according to the manufacturer's instructions (Nanopore Protocol - 16S Barcoding Kit 1-24, Version: 16S_9086_v1_revL_14Aug2019; Oxford Nanopore Technologies); Amplified DNA was purified using the AMPure XP Reagent for PCR Purification (Beckamn Coulter) and sequencing library was prepared according to the manufacturer's instructions (Nanopore Protocol - 16S Barcoding Kit 1-24, Version: 16S_9086_v1_revL_14Aug2019; Oxford Nanopore Technologies); Sequencing was performed using the MinION sequencing device (Oxford Nanopore Technologies) according to manufacturer's instructions (; Nanopore Protocol - 16S Barcoding Kit 1-24, Version: 16S_9086_v1_revL_14Aug2019; Oxford Nanopore Technologies). The sequenced results were blasted against isolated bacterial strains previously identified, using thepreviously described protocol.

3.3 Results on the microbes and microbial consortia from the Douro Estuary (Site 4)

The presence of pharmaceuticals in aquatic ecosystems, particularly in estuarine environments, has emerged as a growing concern due to their potential ecological impact and implications for aquatic health (Fernandes et al., 2021). Among pharmaceutical compounds that have been studied in the scope of BIOSYSMO for D3.1, Ketoprofen was chosen as a case study pharmaceutical for site 4 due to its widespread occurrence and persistence in estuarine habitats, alongside Cd, to better understand the effects of mixed contamination. Based on previous works regarding the application of autochthonous bacteria for biodegrading pharmaceuticals in water (Duarte et al., 2019), CIIMAR tested the pharmaceutical biodegradation as well as metal resistance abilities and the presence of plant growth-promoting traits of microorganisms isolated from rhizosediments (from the plant *Juncus maritimus*) of the Douro River estuary. Based on the characteristics of isolated microorganisms, nine strains were selected based on their balanced abilities to be tested for compatibility and their Kpf degradation potential. The compatibility tests allowed for the construction of a microbial consortium of four compatible strains further tested in microcosm experiments under WP4 (T4.3).

3.3.1 Trace metal resistance to Cu, Cd, Pb, Zn and Cr

Trace metal resistance was assessed for strains isolated in PCA media and isolated from the enriched culture in which both Kpf and Cd, or just Cd, were used as selectors. Results are shown in Table 12. Most strains presented tolerance to Cu and Zn, both essential metals, whereas for the other metals ten strains were resistant to Cd, fourteen to Cr and five to Pb.

Table 11. Trace Metal resistance of tested bacterial strains isolated from site 4. 1 means resistant; 0 means susceptible.

Bacterial Strain	Trace Metals (resistant=1; susceptible=0)				
	Cd (0.23 mg/L)	**Cu (0.13 mg/L)**	**Cr (0.10 mg/L)**	**Pb (0.41 mg/L)**	**Zn (0.13 mg/L)**
PCD1	0	1	0	0	0
PCD2	0	1	0	0	0
PCD3	0	1	0	0	1
PCD4	0	1	1	0	0
PCD5	1	1	0	1	1
PCD6	1	1	1	0	1
PCD7	1	1	1	0	0
PCD8	0	1	0	0	0
PCD9	0	1	1	1	1
PCD10	0	1	0	0	1
PCD11	0	1	1	0	1
PCDK1	1	1	1	0	1
PCDK2	0	1	0	0	1
PCDK3	0	1	0	0	0
PCDK4	0	1	0	0	1
PCDK5	1	1	1	0	1
PCDK6	0	1	0	0	1
PCDK7	1	1	1	0	1
PCDK8	1	1	1	0	1
PCDK9	1	1	0	0	1
PCDK10	0	1	1	1	1
PCDK11	0	1	1	0	1
PCDK12	1	0	1	1	1
PCDK13	0	1	1	1	1
PCDK14	0	0	1	0	0
PCDK15	1	1	0	0	1
PCDK16	0	1	0	0	1

3.3.2 Minimum inhibitory Concentration for Cd

Similar to trace metal resistance, the minimum inhibitory concentration (MIC) for Cd was assessed for strains isolated in PCA or MM media and isolated from the enriched culture in which both Kpf and Cd, or just Cd, were used as selectors. The MIC is presented as an interval due to the exponential concentrations tested; the p-value for each growth OD measured was calculatedto distinguish between

positive control growth and determine the inhibitory concentration (Table 12). MIC concentration for Cd ranged between the intervals of 0-1 mg/L and higher values such as 32-64mg/L.

Table 12. Minimum Inhibitory Concentration (MIC) for Cd of tested bacterial strains isolated from site 4; n.a = non aplicable

Bacterial Strain	MIC (mg/L)		p value	
PCD1	0	1	n.a.	0.049
PCD2	2	4	0.513	0.049
PCD3	0	1	n.a.	0.049
PCD4	32	64	0.513	0.049
PCD5	4	8	0.049	0.049
PCD6	8	16	0.275	0.049
PCD7	4	8	0.127	0.049
PCD8	8	16	0.050	0.050
PCD9	4	8	0.275	0.050
PCD10	0	1	n.a	0.050
PCD11	0	1	n.a	0.046
PCDK1	4	8	0.513	0.049
PCDK2	2	4	0.513	0.049
PCDK3	4	8	0.127	0.049
PCDK4	8	16	0.275	0.049
PCDK5	16	32	0.827	0.049
PCDK6	1	2	0.127	0.049
PCDK7	0	1	n.a	0.049
PCDK8	1	2	0.049	0.049
PCDK9	16	32	0.513	0.049
PCDK10	8	16	0.127	0.049
PCDK11	8	16	0.049	0.049
PCDK12	8	16	0.827	0.049
PCDK13	8	16	0.049	0.049
PCDK14	8	16	0.127	0.049
PCDK15	16	32	0.827	0.049
PCDK16	2	4	0.658	0.050
MCDK1	0	1	n.a	0.050
MCDK2	16	32	0.513	0.050
MCDK3	0	1	n.a	0.050
MCDK4	32	64	0.275	0.050
MCDK5	0	1	n.a	0.050
MCDK6	0	1	n.a	0.050
MCDK7	0	1	n.a	0.050
MCDK8	0	1	n.a	0.050
MCDK9	16	32	0.513	0.046
MCDK10	0	1	n.a	0.046

3.3.3 PGP traits characterisation

PGP traits characterisation of bacterial strains isolated in PCA or MM media and isolated from the enriched culture in which both Kpf and Cd were used as selectors is still ongoing, but preliminary tests are shown in **Error! Reference source not found.**. The PGP traits were not accessed yet for all the strains but most of the strains presented at least one PGP trait, with one strain (PCDK2) presenting three PGP traits.

Table 13. PGP traits of tested bacterial strains isolated from site 4. 1 means positive; 0 means negative.; "-": means it is not measured the parameter yet

Bacterial Strain	PGP'S (positive=1; negative=0)				
	Nitrogen fixation	**Phosphate solubilization**	**Biofilm production**	**Siderophores production**	**ACC Deaminase activity**
PCDK1	-	-	1	-	-
PCDK2	-	1	1	-	1
PCDK3	-	-	0	-	1
PCDK4	-	-	0	-	-
PCDK5	-	-	1	-	1
PCDK6	-	-	0	-	1
PCDK7	-	-	0	-	1
PCDK8	-	-	0	-	1
PCDK9	-	1	0	-	1
PCDK10	-	-	0	-	-
PCDK11	-	-	1	-	-
PCDK12	-	-	0	-	-
PCDK13	-	-	0	-	1
PCDK14	-	-	1	-	-
PCDK15	-	-	0	-	-
PCDK16	-	-	0	-	-
MCDK1	-	-	0	-	-
MCDK2	-	-	0	-	-
MCDK3	-	1	0	-	-
MCDK4	-	-	1	-	1
MCDK5	-	-	0	-	-
MCDK6	-	-	1	-	1
MCDK7	-	-	0	-	1
MCDK8	-	-	1	-	1
MCDK9	-	-	0	-	-
MCDK10	-	-	0	-	-

3.3.4 Kpf degradation abilities by isolated bacteria

Based on the results obtained in the previous sections, regarding metal resistance (able to tolerate Cd at higher levels and 2 different trace metals) and/or PGP traits (at least 2 traits), nine bacterial strains Kpf biodegradation potential. Kpf removal percentages are demonstrated in Table 14.

Table 14. Kpf removal percentages of the tested bacterial strains isolated from site 4

Bacterial Strain	Kpf Removal from Solution (%)
PCDK2	81
PCDK5	86
PCDK9	88
PCDK15	86
PCDK16	81
MCDK2	79
MCDK3	70
MCDK4	48
MCDK9	37

3.3.5 Conventional selection of bacteria to develop consortia (site 4)

Compatibility test results

Overall, all strains tested were compatible against each other, with the exception of PCDK5 vs PCDK9, (i.e when the supernatant collected after the PCDK5 strain was added to a plate seeded with PCDK9). From the compatibility results, Kpf degradation, metal resistance tests, and PGP traits, four bacterial strains were selected to construct a consortium in equal proportions (PCDK2, PCDK9, MCDK2 and MCDK3) to be tested for Kpf degradation potential and further tested in microbe-assisted phytoremediation microcosms.

Kpf degradation abilities of the selected consortium

The consortium selected consisted of the following four strains: PCDK2 MCDK2; PCDK9; and MCDK3, which had high Kpf removal percentages (70-88%), and positive compatibility between them. The strains were mixed in the same proportion, measured by OD and CFU count. The consortium was named ACFG. The Kpf removal percentages by the microbial consortium are shown in Table 15.

Table 15. Kpf removal from solution by the assembled consortium (*ACFG*) with strains isolated from site 4 and in abiotic control (on Day 14). Abiotic indicates a solution where no microbial strains were added.

Treatment	Kpf Removal from Solution (%)
Day 14 Abiotic	10
Day 14 ACFG	84

3.4 Results on the microbes and microbial consortia from the Lima Estuary (Site 5)

Lima River estuary (site 5) is an example of an urbanised-industrialised estuarine environment affected by different anthropogenic activities. This environment presents different potential pollution sources, in particular metals, such as Cu, but also pharmaceuticals (Cunha et al., 2024; Fraga-Santiago et al., 2022), like Venlafaxine (Vfx), chosen to be explored further for the case study of the estuary of the Lima River. Bacterial strains isolated from enriched cultures (obtained from rhizosediments in the Lima estuary, from the *Sporobolus maritimus* plant) as previously described in D3.1, were tested in laboratory assays to evaluate their potential to degrade pharmaceuticals, metal resistance abilities and the presence of plant growth-promoting traits. Apart from the individual characterisation of some of the bacterial strains isolated, all 57 strains were subjected to iACME selection tools in partnership with JSI, in order to develop compatible and efficient consortia to be further tested and, in the future, applied in microbe-plant biosystems.

3.4.1 Vfx degradation abilities by isolated bacteria

Twenty bacterial strains isolated from the enriched culture in which both Vfx and Cu were used as selectors were explored for their biodegradation abilities of Vfx, results being presented in Table 16. The isolated strains were able to degrade Vfx from solution between 10 to 48%, and one of the strains (PCV8) wasn't

Table 16. Vfx removal percentages of the tested bacterial strains isolated from site **5**

Bacterial Strain	Vfx Removal from Solution (%)
PCV1	17
PCV2	30
PCV3	20
PCV4	27
PCV5	13
PCV6	15
PCV7	15
PCV8	0
PCV9	11
PCV10	48
PCV11	30
PCV12	13
MCV1	13
MCV2	10
MCV3	21
MCV4	13
MCV5	31
MCV6	17
MCV7	28
MCV8	21

3.4.2 Trace metal resistance to Cu, Cd, Pb, Zn, Cr

Trace metal resistance was assessed for strains isolated in PCA media and isolated from the enriched culture in which both Vfx and Cu, or just Cu, were used as selectors (Table 17). Most strains presented tolerance to Cu and Zn, both essential metals, whereas for the other metals eleven strains were resistant to Cd, six to Cr and three to Pb.

Table 17. Trace Metal resistance of tested bacterial strains isolated from site 5. 1 means resistant; 0 means susceptible.

Bacterial Strain	Trace Metals (resistant=1; susceptible=0)				
	Cd (0.23 mg/L)	**Cu (0.13mg/L)**	**Cr (0.10mg/L)**	**Pb (0.41mg/L)**	**Zn (0.13mg/L)**
PC1	0	1	0	0	1
PC2	1	1	0	0	1
PC3	1	1	1	0	1
PC4	0	1	1	0	1
PC5	0	1	0	0	0
PC6	0	1	0	0	0
PC7	0	1	0	0	1
PC8	0	1	0	0	1
PC9	0	1	0	0	1
PC10	0	1	0	0	1
PC11	0	1	1	1	1
PC12	0	1	0	0	1
PC13	0	1	0	0	1
PC14	1	1	0	0	0
PC15	1	1	0	0	1
PCV1	1	1	0	0	1
PCV2	1	1	0	1	1
PCV3	0	1	1	0	1
PCV4	0	1	0	0	1
PCV5	0	1	1	0	1
PCV6	1	1	0	0	1
PCV7	0	1	0	0	1
PCV8	1	1	0	0	1
PCV9	0	0	0	0	1
PCV10	1	1	0	0	1
PCV11	1	1	1	1	1
PCV12	1	0	0	0	1

3.4.3 Minimum inhibitory Concentration for Cu

Similar to trace metal resistance, and to what was done for site 4, the minimum inhibitory concentration (MIC) for Cu was assessed for strains isolated in PCA or MM media and isolated from the enriched culture in which both Vfx and Cu, or just Cu, were used as selectors. The MIC is presented as an interval due to the exponential concentrations tested; the p-value for each growth OD measured was calculated to distinguish between positive control growth and determine the inhibitory concentration (Table 18).

MIC concentration for Cu ranged between the intervals of 1-2 mg/L and higher values such as 64-128 mg/L.

Table 18. Minimum Inhibitory Concentration (MIC) for Cu of tested bacterial strains isolated from site 5

Bacterial Strain	MIC (mg/L)		p value	
PC1	4	8	0.275	0.049
PC2	8	16	0.513	0.049
PC3	32	64	0.275	0.049
PC4	2	4	0.275	0.049
PC5	8	16	0.050	0.049
PC6	1	2	0.050	0.049
PC7	2	4	0.127	0.049
PC8	16	32	0.127	0.049
PC9	2	4	0.127	0.049
PC10	1	2	0.827	0.049
PC11	4	8	0.127	0.049
PC12	16	32	0.513	0.049
PC13	64	128	0.050	0.049
PC14	8	16	0.513	0.049
PC15	16	32	0.049	0.049
PCV1	32	64	0.658	0.046
PCV2	32	64	0.513	0.046
PCV3	16	32	0.827	0.049
PCV4	4	8	0.275	0.049
PCV5	4	8	0.513	0.049
PCV6	32	64	0.049	0.049
PCV7	2	4	0.127	0.049
PCV8	64	128	0.513	0.049
PCV9	64	128	0.513	0.049
PCV10	64	128	0.127	0.049
PCV11	64	128	0.268	0.049
PCV12	32	64	0.046	0.049
MCV1	1	2	0.077	0.046
MCV2	16	32	0.507	0.046
MCV3	16	32	0.500	0.043
MCV4	16	32	0.046	0.046
MCV5	0	1	n.a	0.046
MCV6	0	1	n.a	0.046
MCV7	2	4	0.268	0.046
MCV8	2	4	0.121	0.046

3.4.4 PGP traits characterisation

PGP traits characterisation was conducted on bacterial strains isolated in PCA or MM media and isolated from the enriched culture in which both Vfx and Cu, or just Cu, were used as selectors. Results are presented in Table 19. All strains presented at least one PGP trait, with one strain (PCV3) presenting all the PGP traits.

Table 19. PGP traits of tested bacterial strains isolated from site 5. 1 means positive; 0 means negative.

Bacterial Strain	PGP'S (positive=1; negative=0)				
	Nitrogen fixation	Phosphate solubilization	Biofilm production	Siderophores production	ACC Deaminase activity
PC1	1	0	1	0	0
PC2	0	0	1	0	1
PC3	0	0	0	1	0
PC4	0	0	1	0	1
PC5	1	0	1	1	0
PC6	1	0	1	1	1
PC7	0	0	1	0	1
PC8	0	0	1	0	1
PC9	1	0	1	0	1
PC10	0	0	1	1	1
PC11	0	0	1	1	1
PC12	0	0	0	0	1
PC13	0	1	1	1	0
PC14	0	0	1	0	1
PC15	0	0	0	1	0
MC1	0	0	1	1	0
MC2	0	0	0	1	0
MC3	0	0	1	0	0
MC4	1	0	1	0	1
MC5	0	0	0	1	1
MC6	0	0	1	0	1
PCV1	1	0	1	1	1
PCV2	1	0	1	1	1
PCV3	1	1	1	1	1
PCV4	1	0	1	1	0
PCV5	1	0	1	0	1
PCV6	0	0	1	1	0
PCV7	1	1	1	1	1
PCV8	1	0	1	1	1
PCV9	1	0	1	1	0
PCV10	0	0	1	1	0
PCV11	1	0	1	1	1
PCV12	0	1	1	1	1
MCV1	1	0	1	0	0
MCV2	1	0	1	0	1
MCV3	1	0	1	0	0
MCV4	1	0	1	0	0
MCV5	1	0	1	0	1
MCV6	1	0	1	0	0
MCV7	1	0	1	0	1
MCV8	0	0	0	0	0

3.4.5 iACME selection of bacteria to develop consortia (site 5)

Biomass cultivation and construction of C57 mock consortium

The mock consortium assembled with the 57 strains isolated from the Lima estuary was characterised by dynamic and electrophoretic light scattering (DLS and ELS) to help develop an aggregation protocol. Results revealed a uniform, stable colloidal suspension with low polydispersity (PI 0.888) and a strong negative surface charge. The mean hydrodynamic diameter of particles in the consortium was 2439.6 ± 292.7 nm (Figure 17). These properties indicate relatively uniform morphological characteristics among the bacterial isolates contributing to the suspension. This morphological uniformity was confirmed by forward scatter histograms (FSC) during biomass growth normalization (data not shown), where only 4 to 6 bacterial strains exhibited distinct light scattering patterns compared to the majority of strains.

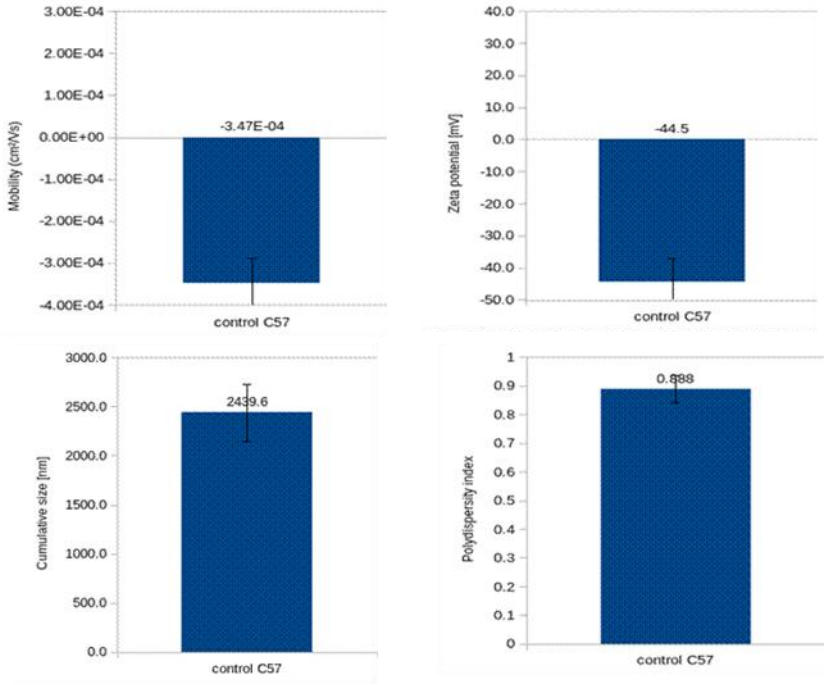

Figure 17. Electrophoretic mobility, zeta potential, size and polydispersity index of constructed mock consortium C57.

Selection of polyelectrolyte and optimization of the aggregation protocol

Assessment of PE toxicity was conducted by measuring changes in doubling time (t_gen) of the C57 consortium relative to unexposed controls. PE concentrations ranging from 0.035 to 1.25 mg/L were tested.

Chitosan exhibited the highest toxicity across all tested concentrations, with an average doubling time increase of 8 hours compared to non-exposed controls. PEI demonstrated a concentration-dependent toxic effect: no toxicity was observed at concentrations up to 0.625 mg/L, but concentrations ≥1.25 mg/L resulted in toxicity levels comparable to chitosan. In contrast, acetPEI showed the most favorable toxicity profile, displaying only minor increases in doubling time at all tested concentrations without the

severe growth inhibition observed with PEI and chitosan at higher concentrations. Based on these results, PEI and acetPEI were selected for subsequent surface modification protocol optimization, as they demonstrated acceptably low toxicity levels within the working concentration range required for effective bacterial surface charge modification (results in Figure 18).

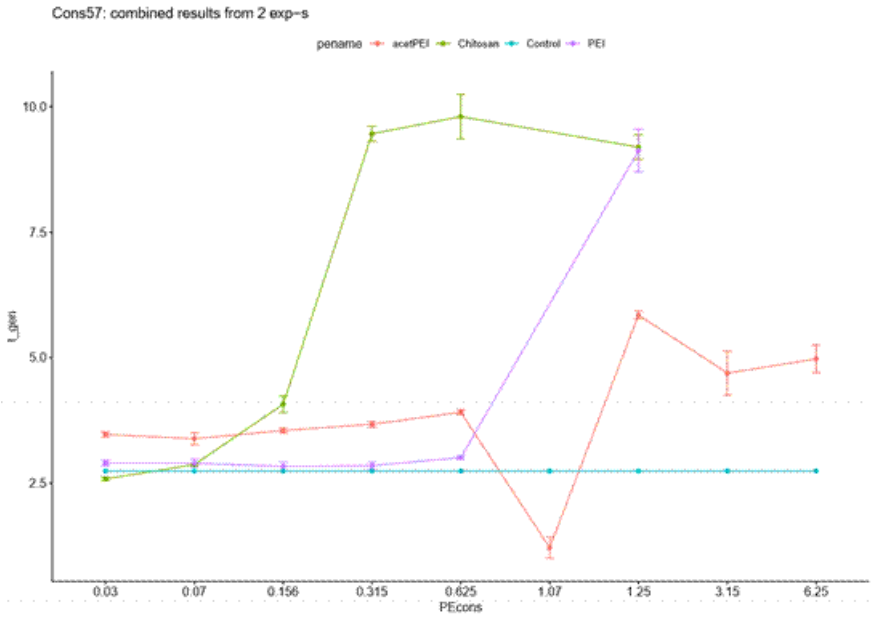

Figure 18. PE's toxicity test for the mock consortium C57: doubling time (t_gen) analysis for each concentration of each tested PE.

The selected polyelectrolytes (PEI and acetPEI) were evaluated under various application conditions to optimize bacterial surface charge modification. AcetPEI was tested at concentrations ranging from 2.5 to 12.5 mg/L, while PEI was evaluated only at 2.5 mg/L (higher concentrations were excluded due to the previously observed toxicity at 1.25 mg/L). To investigate the effect of ionic strength on PE deposition, saline solutions of two different concentrations were used: 0.9% NaCl (0.154 mol/L) and 0.009% NaCl (1.54×10^{-4} mol/L).

ELS measurements revealed that effective bacterial surface charge alteration could be achieved through two distinct mechanisms: (i) high density of primary amino groups (as with PEI treatment), or (ii) application of low ionic strength solutions, which enhance PE adsorption onto cell surfaces by compressing the electrical double layer around bacterial cells.

Given that higher amino group density potentially increases bacterial toxicity, the protocol utilizing acetPEI at 12.5 mg/L in low ionic strength solution was selected for bacterial aggregate formation. This approach provided effective surface charge modification while minimizing potential toxic effects on the consortium's viability (Figure 19).

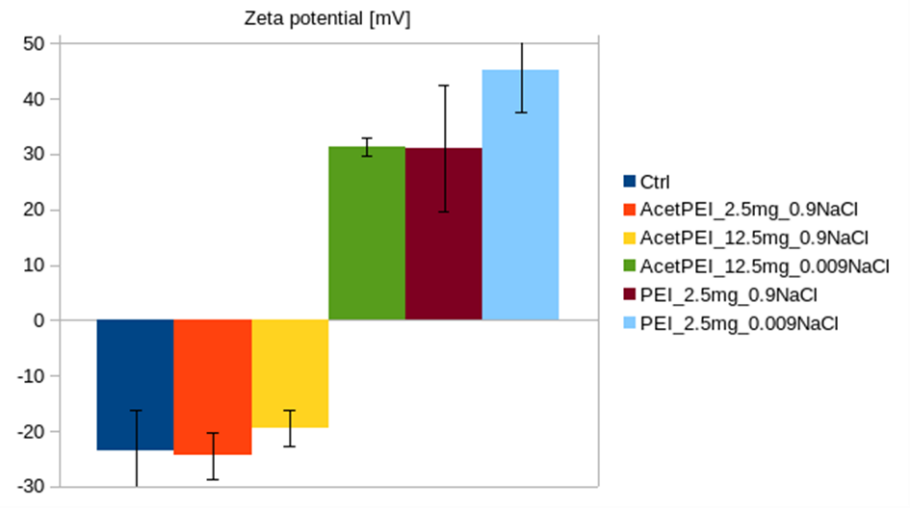

Figure 19. Surface charge of bacterial mock consortium C57 after deposition of PE's using different strategies.

The aggregates produced based on the final optimised protocol for aggregation could be observed using microscopy. It was possible to visualise the negatively charged original bacteria (in green) and the surface-modified positively charged bacteria (in red) (see Figure 20). The aggregates were also analysed by flow cytometry with the use of the same stains regarding each type of cell. The produced aggregates had a mixed stained signal (presented in yellow in the flow cytometry chart), and it was observed 38.2% of aggregate production (Figure 21).

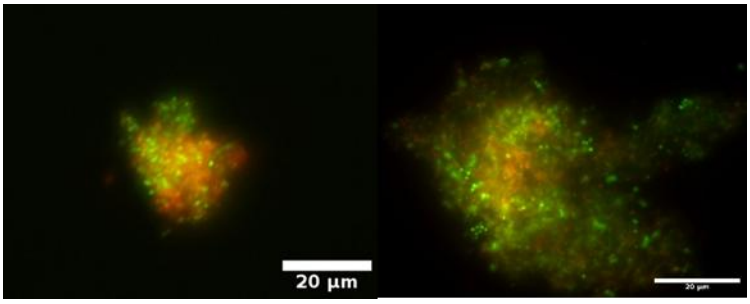

Figure 20. *Microscopic images of two of the aggregates produced with 12.5 mg/L acetPEI.*

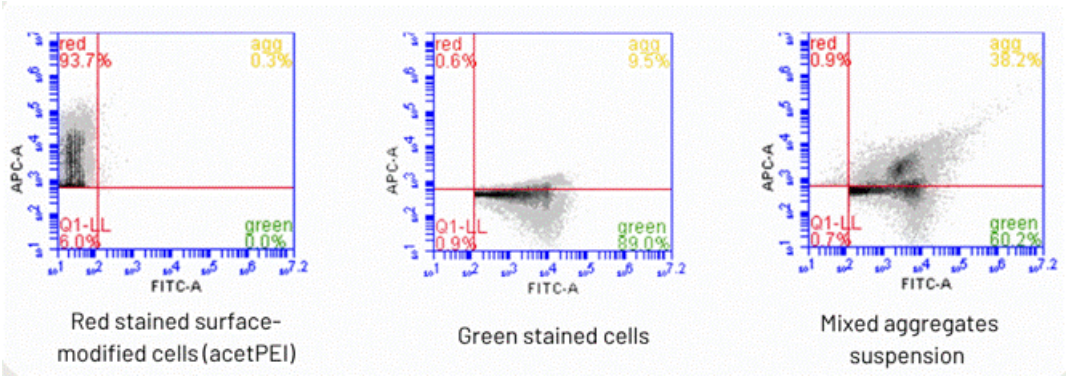

Figure 21. Flow cytometry (events/mL) of red-stained surface-modified cells (with acetPEI), green-stained cells and the mixed aggregates suspension.

Microfluidics Entrapment

To entrap the produced aggregates and potentially test the consortia for compatibility and efficiency, the Poisson distribution was calculated based on the parameters from Table 20. This analysis guided the dilution of the original aggregates solution. The calculated probability indicated an optimal dilution of 50 times the original aggregate cell suspension, to produce around 10μL of beads with just one aggregate to be further tested (the aggregates entrapped in alginate beads were observed with microscopy in Figure 22).

Table 20. Parameters used for the calculation of Poisson distribution: based on the calculation of a larger fraction of aggregates (close to 1-2 cell size events) to further direct the entrapment

Parameter	Measure
Number of events per mL	6.17E+08
Average diameter of aggregate [μm]	5.377
Volume of aggregate [μm³]	81.3989367
Average diameter of alginate bead [μm]	120
Volume of alginate bead [μm³]	904778.684

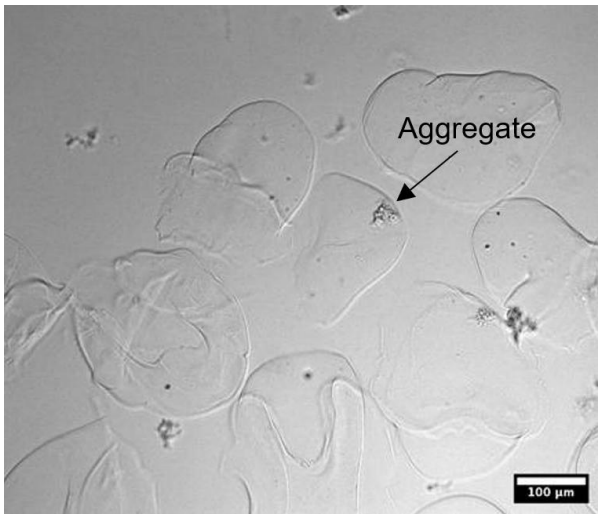

Figure 22. The aggregates produced were entrapped in**.**

iACME Consortia Candidate Selection

Growth curve analysis was performed on 88 unique aggregated consortia (representing different combinations of the 57 isolates) under each of the selective conditions described in section 3.2.5.4. Principal Component Analysis (PCA) was applied to identify clusters of candidates exhibiting similar growth characteristics, resulting in 3-4 distinct clusters per condition (Figures 23-26).

From the most promising clusters, candidates were selected using two criteria: (i) paragon candidates located closest to the centroid of each cluster, representing the typical performance profile, and (ii) outlier candidates positioned at the cluster periphery, representing extreme performance characteristics within that cluster.

A total of 12 candidates were selected from each microplate (aerobic and anaerobic) for further analysis, distributed as follows: one candidate grown under Vfx alone, one under Vfx+NaOAc, five under Vfx+Cu, and five under Vfx+Cu+NaOAc conditions. The higher number of candidates selected from the mixed conditions (Vfx+Cu and Vfx+Cu+NaOAc) reflects their relevance to subsequent experimental phases, where these combined selective pressures will be applied (Table 21).

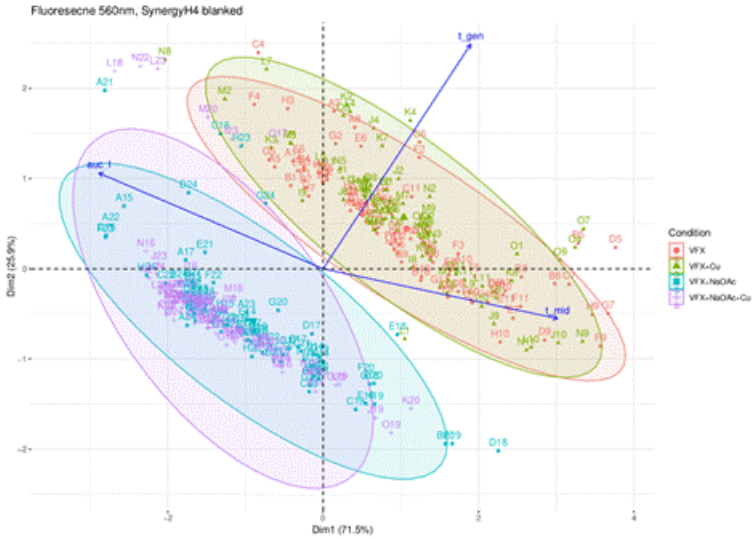

Figure 23. Overall PCA for the consortia candidates growing in aerobic conditions.

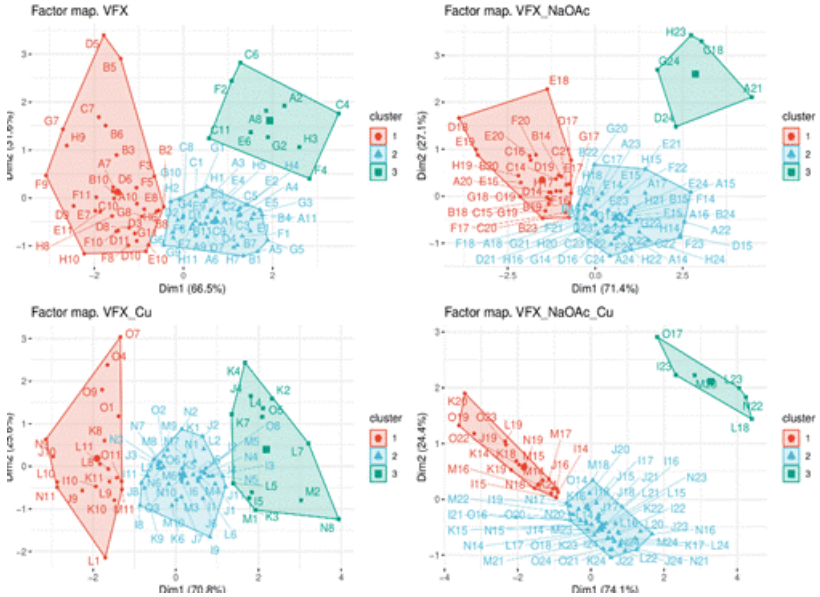

Figure 24. Factormap of clusters of aerobic consortia candidates by selected conditions (Vfx, Vfx+Cu, Vfx+NaOAc, Vfx+Cu+NaOAc).

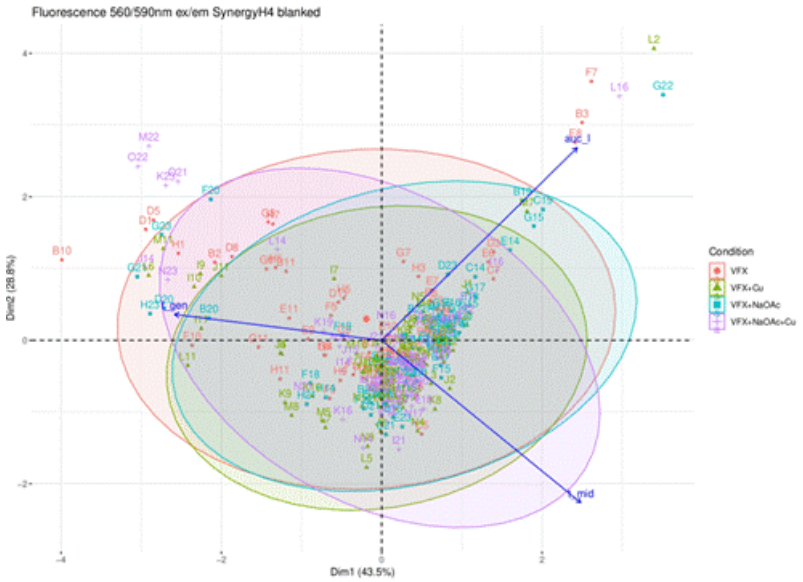

Figure 25. Overall PCA for the consortia candidates growing in anaerobic conditions.

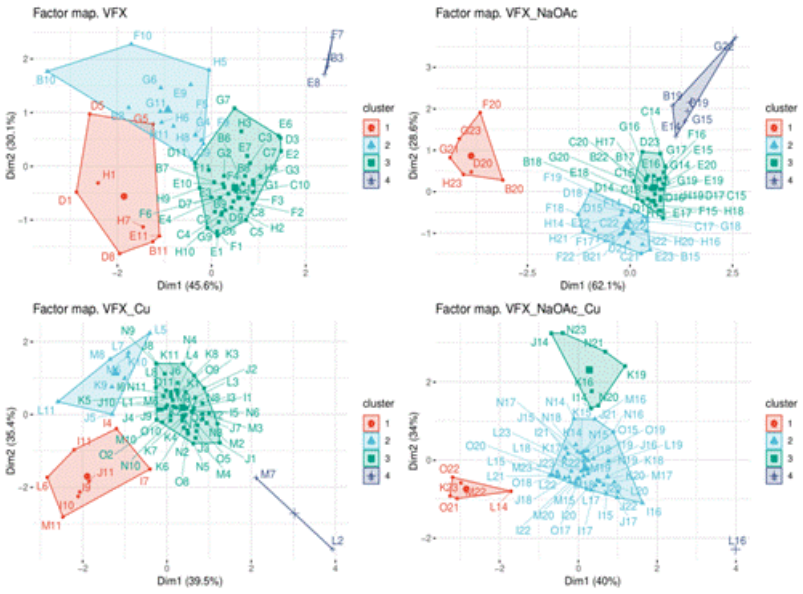

Figure 26. Factormap of clusters anaerobic consortia candidates by selected conditions (Vfx, Vfx+Cu, Vfx+NaOAc, Vfx+Cu+NaOAc).

Table 21. Summary of candidates chosen for each plate and each condition (first-second columns aerobic conditions, third-fourth columns anaerobic conditions) to explore in a first analysis.

Vfx	Vfx+NaOAc	Vfx	Vfx+NaOAc
C2 (2, paragon)	E23 (2, paragon)	B3 (4, paragon)	C19 (4, paragon)
Vfx+Cu	**Vfx+Cu+NaOAc**	**Vfx+Cu**	**Vfx+Cu+NaOAc**
O5 (2, paragon)	M20 (2, paragon)	N8 (3, paragon)	M19 (3, paragon)
M6 (3, paragon)	L15 (3, paragon)	L2 (4, paragon)	L16 (4, paragon)
N8 (2, farthest)	L18 (2, farthest)	J1 (3, farthest)	J17 (3, farthest)
I9 (3, farthest)	N21 (3, farthest)	N3 (3, farthest)	L17 (3, farthest)
J7 (3, farthest)	J23 (3, farthest)	M7 (3, farthest)	K16 (3, farthest)

Characterisation of iACME Consortia Candidates

The twelve consortia candidates selected from the aerobic plate were put to grow (since they presented the better biomass production on a larger scale). Their DNA was extracted and 16S sequencing was performed using Nanopore sequencing. The results were blasted against the 16S sequences of each bacterial isolate to analyse the presence of each isolate in the candidate consortia (and their proportion relative to the number of hits of each isolate). The results can be seen in Figure 27.

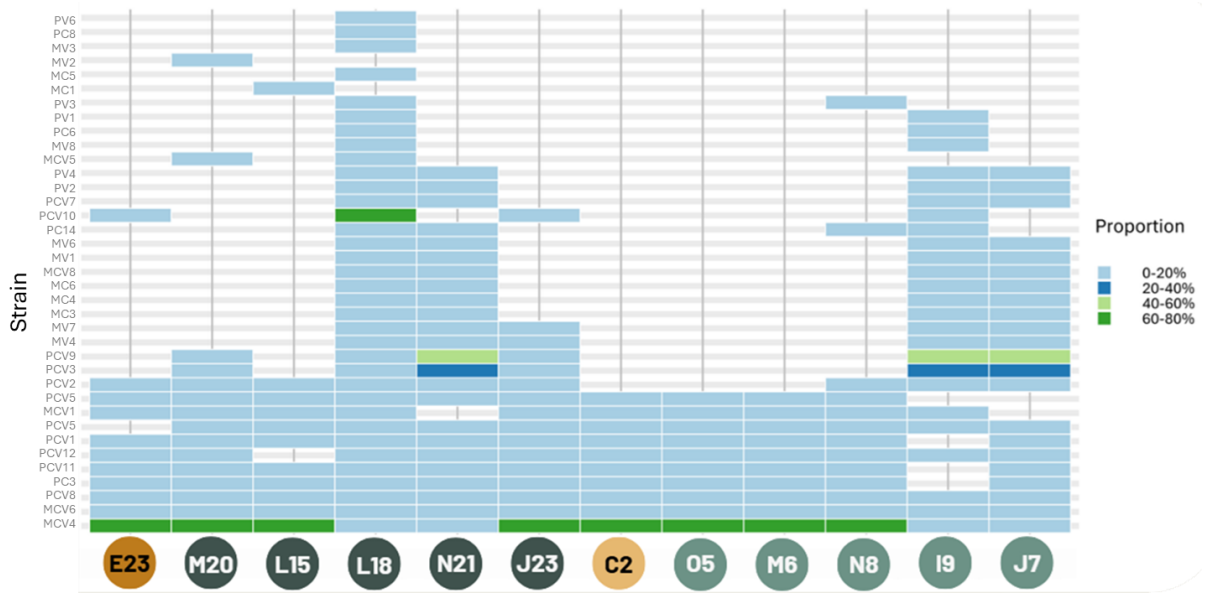

Figure 27. Analysis of the presence and proportion of each bacterial strain isolated in the selected and produced consortia via iACME C57.

3.5 Conclusions and linked activities with WP4

At site 4, from all the strains previously identified in D3.1, CIIMAR chose to focus on those isolated from the rhizosediments of *Juncus maritimus* in the Douro River estuary. These strains were obtained via conventional enrichment using Kpf, Cd, or a combination of both as selective agents.

- Out of a total of 60 strains, 37 were characterized (either one or all tests performed). Most strains exhibited resistance to the trace metals copper (Cu) and zinc (Zn), with a smaller subset showing

resistance to cadmium (Cd), chromium (Cr) and lead (Pb), despite Cd having been used as a selector contaminant during isolation. On the other hand, the minimum inhibitory concentration (MIC) for Cd, among the tested bacteria, was relatively high: two strains had MIC values of 32–64 mg/L, while five others showed MIC values of 16–32 mg/L. This discrepancy may be attributed to differences in the test conditions, as trace metal resistance was assessed on solid media, whereas MIC was determined in liquid media.

- The tested strains demonstrated ACC deaminase activity and varying biofilm production, both of which are recognised as plant growth-promoting (PGP) traits. Based on these findings, nine strains were selected for Kpf degradation evaluation: PCDK2, PCDK5, PCDK9, PCDK15, PCDK16, MCDK2, MCDK3, MCDK4 and MCDK9. These strains exhibited Kpf degradation rates ranging from 37% to 88%, with seven strains removing more than 70% of Kpf.
- Following Kpf degradation and compatibility tests, four strains: PCDK2, PCDK9, MCDK2 and MCDK3, were selected to construct a consortium. This consortium demonstrated the ability to remove approximately 84% of Kpf, with only 10% of this removal attributed to abiotic processes.

The consortium is currently being used in microcosm and mesocosm experiments within WP4 (T4.3), in conjunction with *Juncus maritimus*, to assess its full potential for microbial-assisted phytoremediation of estuarine sediments contaminated with both the target contaminants Cd and Kpf.

At site 5, Similar to site 4, from all the strains previously identified in D3.1, CIIMAR selected the 57 bacterial strains isolated from the rhizosediments of *Sporobolus maritimus* in the Lima River estuary for further study. These strains were obtained through conventional enrichment techniques with Vfx, Cu, or a combination of both as selective agents.

- The 20 bacterial strains isolated from the enriched culture containing both contaminants were primarily characterised. These strains demonstrated moderate Vfx degradation, with removal rates ranging from 0% to 48%. This suggests that, within the community context of the original enriched culture, the bacteria collectively achieved much higher pharmaceutical degradation (with nearly complete removal from solution, as reported in D3.1) compared to their performance as individual strains.
- Similar to the strains isolated from site 4, these strains generally exhibited resistance to the trace metals Cu and Zn, with only a few showings resistance to Cd, Cr, and Pb. Among the tested bacteria, five strains displayed minimum inhibitory concentrations (MICs) for Cu ranging from 64 to 128 mg/L, while another five had MICs between 32 and 64 mg/L. The average MIC for all strains was found to be between 16 and 32 mg/L. These findings indicate that the isolated strains possess a high level of resistance to the target metal, as intended.
- Regarding the PGP traits, most strains tested demonstrated biofilm production and ACC deaminase activity, and around half of them demonstrated the ability to fix nitrogen and produce siderophores. These results confirm that the isolated bacteria are well-suited for use alongside plants.
- In collaboration with JSI, CIIMAR utilised iACME tools to develop compatible and effective consortia using the 57 isolated bacterial strains with contaminant removal potential. Out of the

704 aggregate consortia combinations generated, for both aerobic and anaerobic, 88 per condition, 12 efficient consortia capable of aerobic growth were selected. The aerobic candidates were the ones that generated high biomass and by that means scalable, so their composition was further explored and selected for further working. The chosen consortia contained between 10 and 35 bacterial strains, with the *Alcaligenes* genus consistently present in all of them. Additionally, this genus was in high proportion in the consortia overall, alongside the genera *Pseudomonas* and *Hydrogenophaga*.

Currently, these consortia are being cultured and evaluated for their capacity to degrade Vfx, resist copper (Cu), and produce biofilm, an important plant growth-promoting (PGP) trait. **The top-performing consortia will then be combined and tested alongside the plant *S. maritimus* in microcosm and mesocosm laboratory experiments under WP4 (T4.3)**, designed to simulate natural estuarine conditions. The selection of the most effective plant-bacteria systems will be determined by the biosystems' ability to remove the target contaminants, Vfx and Cu, from sediments.

4 Optimization of microbes and microbial consortia from wastewater

4.1 Introduction

In the framework of Task 3.1, UBU has been working to accomplish with the objective of improving the plant-bacteria interaction to ameliorate metal removal in wastewater. The plant system consisted, as already reported in D3.1, in the macrophyte *Phragmites australis*. The polluted matrix corresponded to groundwater from Site 6 -Major non-ferrous smelter in Belgium- (D1.1). This site exhibits a pH ranging from 3.1 to 3.7 and an electrical conductivity of 4.96-5.32 mS/cm. Additionally, due to metallurgical activities and the leakage of electrolytes and acids, it is highly contaminated with metal(loid)s such as As (0.073 mg/L), Cu (207.167 mg/L), Cd (2.533 mg/L), Ni (142 mg/L), and Zn (80.33 mg/L). According to results from D1.2, the DNA content of the site is very low due to the extreme conditions described.

4.2 Methodologies

In the following sections, updates concerning methodologies and linked results derived from activities continued from month 18, when intermediate D3.1 was submitted, are reported for UBU. Thus, (i) The completion of pending PGP assays, both for epiphytic and endophytic communities isolated from control, acute, or chronic exposure conditions (protocol detailed in D3.1); (ii) The identification of the microorganisms (information complemented with D4.1); And (iii) the molecular assays regarding responses of the macrophyte *P. australis* under metal induced stress, are reported in the current document.

4.2.1 PGP traits

ACC deaminase Activity

To measure ACC deaminase activity, bacterial strains were first grown by inoculating 5 µL of each strain in 15 mL of Tryptic Soy Broth (TSB). Cultures were incubated for 24 hours at 200 rpm in a shaking water bath set at the appropriate temperature for each bacterium. Cells were then harvested by centrifugation at 8,000 × g for 10 minutes at 4°C. The supernatant was discarded, and the pellet was washed once with 5 mL of DF Salts Minimal Medium (6.0 g Na_2HPO_4, 4.0 g K_2HPO_4, 0.2 g $MgSO_4 \cdot 7H_2O$, 2.0 g glucose, 2.0 g gluconic acid, 2.0 g citric acid, 2.0 g $(NH_4)_2SO_4$, 1.0 mg $FeSO_4 \cdot 7H_2O$, 10.0 µg H_3BO_3, 11.9 µg $MnSO_4 \cdot H_2O$, 124.6 µg $ZnSO_4 \cdot 7H_2O$, 78.22 µg $CuSO_4 \cdot 5H_2O$, and 10.0 µg MoO_3), followed by another centrifugation under the same conditions following Penrose method modified by Honma and Shimomura (Ali et al., 2014; Penrose & Glick, 2003). The washed cells were resuspended in 7.5 mL of DF Salts Minimal Medium.

After resuspension in DF medium, 45 µL of 0.5 M 1-aminocyclopropane-1-carboxylic acid (ACC) was added to reach a final concentration of 3 mM, and the cultures were incubated again at the appropriate temperature for each strain for 24 hours at 200 rpm. After incubation, cells were collected by centrifugation at 8,000 × g for 10 minutes at 4°C, washed twice with 5 mL of 0.1 M Tris-HCl buffer (pH 7.6), and centrifuged again under the same conditions. The final pellet was used for the enzymatic assay.

For analysis, a standard curve was prepared using α-ketobutyrate. To each standard, 300 µL of 0.2% 2,4-dinitrophenylhydrazine dissolved in 2 M HCl was added. The mixtures were vortexed and incubated at 30°C for 30 minutes. After incubation, 2 mL of 2 M NaOH was added for color developing, and absorbance was measured at 540 nm.

For the assay, the bacterial pellet was resuspended in 1 mL of 0.1 M Tris-HCl buffer (pH 7.6) in a 1.5 mL microcentrifuge tube and centrifuged at 16,000 × g for 5 minutes. The supernatant was discarded, and the pellet was resuspended in 600 µL of 0.1 M Tris-HCl buffer (pH 8.5). Then, 30 µL of toluene was added, and the suspension was vortexed for 30 seconds to permeabilize the cells. 200 µL of the toluenized cells were then mixed with 20 µL of 0.5 M ACC, vortexed, and incubated at 30°C for 15 minutes. The reaction was stopped by adding 1 mL of 0.56 M HCl, followed by vortexing and centrifugation at 16,000 × g for 5 minutes at room temperature. Then, 1 mL of the supernatant was mixed with 800 µL of 0.56 M HCl and 300 µL of a solution of 0.2% 2,4-dinitrophenylhydrazine in 2 M HCl. The mixture was vortexed and incubated at 30°C for 30 minutes. After incubation, 2 mL of 2 M NaOH was added for color developing. Absorbance was measured at 540 nm using a spectrophotometer and compared against the standard curve to determine the amount of α-ketobutyrate produced.

To normalize the enzymatic activity by protein content, a Bradford assay was performed using the same cell extracts. This allowed the expression of ACC deaminase activity per milligram of total protein, enabling accurate comparison between samples.

Ammonia Production

Bacterial strains were tested for ammonia production using the qualitative method described by Cappuccino and Sherman (1992). In this method, 0.5 mL of Nessler's reagent was added to 10 mL of bacterial culture grown in peptone water. The mixture was allowed to react for 10 minutes at room temperature, producing a yellow to brown color indicating ammonia production, as described by Abdelwahed et al. (2022).

In a separate procedure, 0.5 mL of bacterial supernatant was mixed with 1 mL of Nessler's reagent in test tubes washed with ultrapure water. The reaction mixture was incubated at room temperature (25°C) for 10 minutes and then diluted 6x to make a final volume of 9 mL. Absorbance was measured at 450 nm. The concentration of NH_3 was calculated by comparing the absorbance with a standard curve of ammonium sulfate $(NH_4)_2SO_4$ solution in the range of 500 to 4000 µM.

Indole acetic acid Synthesis

The indole acetic acid synthesis assays were performed using the method described by Pantoja-Guerra et al. (2023). The isolates were cultured on TSA and incubated at 28°C for 48 hours. Single colonies were transferred to a 100 mL flask containing 20 mL of TSB supplemented with 500 µg/mL tryptophan and shaken at room temperature for an additional 48 hours.

After incubation, the flask contents were transferred to 50 mL Falcon tubes, centrifuged at 3,250 rpm for 15 minutes, and the supernatant was collected. A mixture was prepared by combining 200 µL of supernatant with 800 µL of Salkowski ($HClO_4$ 35% and $FeCl_3$ 0.5M 2%) indicator solution (1:4 ratio). The mixture was stirred and allowed to stand for 20 minutes to stabilize the pink color. Absorbance was

measured at 535 nm using a spectrophotometer. The IAA concentration in the supernatant was determined by comparing the absorbance values with a standard curve using known IAA concentrations.

4.2.2 Microorganisms' identification

Genomic DNA was extracted from pure cultures using the E.Z.N.A.® Bacterial DNA Kit (Omega Bio-Tek, USA), following the manufacturer's instructions. Extracted DNA samples were sent to Novogene (Beijing, China) for full-length 16S rRNA gene amplicon sequencing using the PacBio Sequel II/IIe platform. This approach allowed for high-resolution taxonomic identification, reaching species-level classification in most cases.

To identify the bacterial isolates, BLAST analyses were conducted by comparing the obtained gene sequences against the National Center for Biotechnology Information (NCBI) database, as well as other comprehensive reference databases such as SILVA and EZBioCloud.

4.2.3 Molecular analysis: Responses of *P. australis* to metal stress

In order to understand possible underlying molecular mechanisms behind the tolerance and rhizostabilization of some metal(loid)s by the macrophyte *P. australis,* a short-term tolerance experiment was designed and developed. Briefly, *P. australis* homogeneous seedlings grown *in vitro* for one-month (see D3.1 for details) were transplanted into 2.5L pots containing autoclaved tap water for acclimatization, before metal stress exposure. After 10 days of acclimatization, the tolerance experiment was initiated. Aiming to simulate the concentration of one of the key metals present in the real groundwater target of study (Site 6), plants were exposed to $CuSO_4$ at different concentrations and timings, finally reaching 48h of exposure. For this aim, tap water was replaced by the corresponding solution with different concentrations of $CuSO_4$, or water in the case of controls. After the corresponding times, aerial and root biomass were determined, and plant material was immediately frozen into liquid N_2 for further RNA extraction, cDNA synthesis, and molecular analyses.

4.3 Results on the isolation of microbes from *P. australis*-contaminated groundwater experiment (Site 6)

4.3.1 Isolation of epiphytic and endophytic bacteria from pilot experiment (updated)

Table 22 displays the update on results previously provided in D3.1 (Table 10,) where the number of epiphytic and endophytic microorganisms, including both fungi and bacteria, were reported depending on the plant treatment (control, acute, chronic).

Compared to Table 10 of D3.1, the total number of bacteria has decreased, as the identification process revealed that some of the previously isolated microorganisms turned out to be the same. This might be due to the isolation method described in D3.1, which differentiated potential bacterial strains based on morphology. As a result, if isolates appeared slightly different, we sometimes classified them separately in order to preserve as many isolates as possible.

Regarding the results, we can observe that the number of isolates from the epiphytic and endophytic communities is similar. Within these groups, the number of isolates obtained under the acute exposure

treatment was lower than in the other treatments. This could be due to the fact that in this treatment, polluted water was directly applied, and its physicochemical characteristics may have contributed to the survival of only those strains with higher tolerance to acidic environments and the presence of metals.

Table 22. Bacteria and fungi isolated from the roots of *Phragmites australis* plants exposed to metal polluted water for one month. Control Exposure refers to plants exposed to control water. Acute Exposure refers to plants directly exposed to polluted water. Chronic Exposure refers to plants progressively exposed to polluted water until metal concentrations reached real values.

Plant Treatment	Bacteria		Fungi		Total
	Epiphytic Community	Endophytic Community	Epiphytic Community	Endophytic Community	
Control Exposure	8	6	2	1	**17**
Acute Exposure	3	2	1	0	**6**
Chronic Exposure	5	6	1	0	**12**
Total	**16**	**14**	**4**	**1**	**35**

4.3.2 PGP traits

The functional characterization of epiphytic bacterial isolates from *P. australis* roots exposed to different water treatments revealed differences in the diversity of positive PGP traits (Table 23). In the control treatment, isolates showed the highest number of positive results, especially in phosphate solubilization, siderophore production and ammonia production. Three isolates (TEP-4, TEP-6, and TEP-7) demonstrated more than three PGP traits, indicating a rich and diverse functional microbiota under non-stressful conditions. In contrast, isolates from the acute exposure treatment exhibited a decline in functional diversity. Only one isolate (AEP-2) presented more than two positive traits, while the majority lacked most beneficial activities, suggesting that the sudden and severe stress limited the survival to only highly tolerant but functionally limited strains. The chronic exposure treatment showed intermediate results. The functional activity was a bit reduced compared to the control. Nevertheless, one isolate (CEP-4) showed notable multifunctionality, including IAA synthesis, ACC deaminase activity, and phosphate solubilization, possibly reflecting gradual adaptation to long-term stress.

Table 23. PGP traits of bacteria isolated from the epiphytic community of *P. australis* roots under control, acute or chronic exposure.

Treatment	Isolate	Phosphate Solubilization	Pyoverdine Production	Total Siderophore Production	ACC deaminase Activity	Ammonia Production	IAA Synthesis
Control	TEP-1	✓	X	X	✓	✓	X
	TEP-2	X	X	X	X	✓	X
	TEP-3	X	X	X	X	✓	X
	TEP-4	✓	✓	✓	X	✓	X
	TEP-5	✓	X	X	X	X	X
	TEP-6	✓	X	✓	X	✓	X
	TEP-7	✓	✓	✓	X	✓	X
	TEP-8	X	X	X	X	✓	✓
Acute Exposure	AEP-1	X	X	X	X	✓	X
	AEP-2	✓	✓	✓	X	✓	X
	AEP-3	X	X	X	X	X	X
Chronic Exposure	CEP-1	X	X	✓	X	✓	X
	CEP-2	X	X	X	X	✓	X
	CEP-3	X	X	X	X	✓	X
	CEP-4	✓	X	X	✓	✓	✓
	CEP-5	X	X	X	X	✓	X

TEP: Tap EPiphytic; AEP: Acute EPiphytic; CEP: Chronic EPiphytic.

Regarding endophytic bacterial isolates (

Table 24), it can be observed that the control group show a limited number of positive PGP traits compared with the other treatments and also with the results from the epiphytic community. Ammonia production was consistently present across all isolates, while other traits such as phosphate solubilization, siderophore production, and ACC deaminase activity appeared infrequently. Only one isolate (TEN-4) displayed multifunctionality with three positive traits, including IAA synthesis. In the acute exposure treatment, the results showed very low functional diversity, with no siderophore or IAA production detected. One isolate (AEN-1) exhibited ACC deaminase activity and ammonia production, suggesting strong selective pressure under acute stress conditions. In contrast, the chronic exposure treatment exhibited multiple functional traits. Notably, isolates CEN-2 and CEN-3 showed four or more PGP activities, including siderophore production, ACC deaminase activity, and IAA synthesis. Overall, traits such as phosphate solubilization, siderophore production, and ammonia production were consistently present across chronic isolates, indicating a stable and functionally enriched endophytic community that had adapted to contamination stress.

Table 24. PGPR traits of bacteria isolated from the endophytic community of *P. australis* roots under control, acute or chronic exposure.

Treatment	Isolate	Phosphate Solubilization	Pyoverdine Production	Total Siderophore Production	ACC deaminase Activity	Ammonia Production	IAA Synthesis
Control	TEN-1	X	X	✓	X	✓	X
	TEN-2	X	X	X	X	✓	X
	TEN-3	✓	X	X	X	✓	X
	TEN-4	✓	X	X	✓	✓	✓
	TEN-5	X	X	✓	X	✓	X
	TEN-6	X	X	X	X	✓	X
Acute Exposure	AEN-1	X	X	X	✓	✓	X
	AEN-2	X	X	X	X	✓	X
Chronic Exposure	CEN-1	✓	X	✓	X	✓	X
	CEN-2	✓	✓	✓	✓	✓	X
	CEN-3	✓	✓	✓	X	✓	✓
	CEN-4	✓	X	✓	X	✓	X
	CEN-5	✓	X	✓	✓	✓	X
	CEN-6	✓	✓	✓	X	✓	X

TEN: Tap ENdophytic; AEN: Acute ENdophytic; CEN: Chronic ENdophytic.

In summary, the functional characterization of bacterial communities, both epiphytic and endophytic, revealed notable differences in the expression of PGP traits depending on the type of water exposure. In general, control conditions supported the highest functionality, with multiple epiphytic isolates showing a broad combination of traits while acute exposure to contaminated water led to a reduction their functional potential. These isolates exhibit less PGP activity, suggesting a strong selection pressure where only the most stress-tolerant, yet functionally limited, bacteria persisted. On the other hand, chronic exposure treatment reveals similar positive PGP traits as the control or even more, particularly within the endophytic compartment. Epiphytic bacteria showed intermediate behaviour, with some retention of key functions but reduced multifunctionality compared to the control.

4.3.3 Microorganisms' identification

Table 25 compiles the information on the identification of the bacterial isolates after full-length 16S rRNA sequencing, an information not previously reported within D3.1. As it can be observed, identity details are provided reaching the genus level.

Table 25. Identification of bacterial isolates based on full-length 16S amplicon sequencing (PacBio Sequel II/IIe).

Community	Treatment	Isolate	Identity
Epiphytic Bacteria	**Control**	TEP-1	*Aeromonas sp.*
		TEP-2	*Exiguobacterium sp.*
		TEP-3	*Chryseobacterium sp.*
		TEP-4	*Pseudomonas sp.*
		TEP-5	*Paenibacillus sp.*
		TEP-6	*Pseudomonas sp.*
		TEP-7	*Flavobacterium sp.*
		TEP-8	*Pseudarthrobacter sp.*
	Acute Exposure	AEP-9	*Cellulomonas sp.*
		AEP-10	*Pseudomonas sp.*
		AEP-11	*Flavobacterium sp.*
	Chronic Exposure	CEP-12	*Flavobacterium sp.*
		CEP-13	*Pseudomonas sp.*
		CEP-14	*Pseudorhodoferax sp.*
		CEP-15	*Priestia sp.*
		CEP-16	*Cupriavidus sp.*
Endophytic Bacteria	**Control**	TEN-1	*Chryseobacterium sp.*
		TEN-2	*Stenotrophomonas sp.*
		TEN-3	*Rhizobium sp.*
		TEN-4	*Microbacterium sp.*
		TEN-5	*Brevundimonas sp.*
		TEN-6	*Microbacterium sp.*
	Acute Exposure	AEN-1	*Aminobacter sp.*
		AEN-2	*Aminobacter sp.*
	Chronic Exposure	CEN-1	*Pantoea sp.*
		CEN-2	*Pseudomonas sp.*
		CEN-3	*Pseudomonas sp.*
		CEN-4	*Ranhella sp.*
		CEN-5	*Pseudomonas sp.*
		CEN-6	*Ranhella sp.*

TEP: Tap EPiphytic; AEP: Acute EPiphytic; CEP: Chronic EPiphytic. TEN: Tap ENdophytic; AEN: Acute ENdophytic; CEN: Chronic Endophytic.

The bacterial genera identified in the epiphytic and endophytic communities have been widely documented for their tolerance to heavy metals and/or their roles as plant growth-promoting rhizobacteria (PGPR). *Pseudomonas*, *Cupriavidus*, and *Stenotrophomonas* species are frequently reported for their heavy metal resistance and bioremediation potential, primarily through mechanisms such as metal sequestration and detoxification (Fakhar et al., 2022; Sun et al., 2021; Zhang et al.,

2024). *Rhizobium*, *Paenibacillus*, and *Pantoea* are well-established PGPRs that promote plant growth via nitrogen fixation, phosphate solubilization, and phytohormone production, thereby enhancing plant tolerance to abiotic stresses, including metal toxicity (Lu et al., 2021; Mohammad et al., 2024; Purwaningsih et al., 2021).

Genera such as *Exiguobacterium* and *Aeromonas* have been isolated from contaminated environments and have demonstrated resistance to metals like cadmium and arsenic, supporting their association with metal-exposed plant microbiomes (Fakhar et al., 2022; Xiao et al., 2024). Likewise, *Flavobacterium*, *Chryseobacterium*, *Microbacterium*, and *Brevundimonas* have been reported in both contaminated and rhizospheric soils, with some species exhibiting metal tolerance and plant growth-promoting traits such as siderophore production and phosphate solubilization (Chabbi et al., 2024; Luo et al., 2024; Seo et al., 2024; Singh et al., 2013). Similar characteristics have been observed in *Pseudarthrobacter* species, which also show potential for tolerance to environmental stress and degradation of organic compounds (Li et al., 2024). Finally, *Priestia* and *Rahnella* are lesser studied but emerging genera, with increasing evidence supporting their potential roles in metal tolerance and PGPR activity, particularly in the case of *Priestia* (Xu et al., 2022).

Therefore, the detection of these genera in *P. australis* exposed to acidic, metal-contaminated water reinforces the hypothesis of a microbiota adapted to metal stress, with many taxa likely contributing to host plant tolerance and resilience through both direct and indirect mechanisms.

4.3.4. Results on molecular analysis linked to responses of *P. australis* to metal stress

In order to provide insights and advances related to gene expression behind the phytoremediation mechanisms undertaken by *P. australis* in the context of rhizostabilization, specifically for Cu, the following pipeline of work was followed with some preliminary results:

RNA extraction from shoots and roots of P. australis under Cu stress:

After the comparison of three different methods for extraction of RNA, both in roots and aerial tissues, differences in the efficiency, purity, integrity and other parameters were observed, which led to the selection of a specific method to be further implemented in the subsequent experiments (unpublished data).

Identification of reference genes for qRT-PCR analysis in P. australis under Cu stress:

Stability analyses of candidate reference genes using different algorithms have shown that: (i) There was variability within the groups analysed. (ii) Results were inconsistent when working with different tissues. (iii) Reference genes must be selected based on the tissue being analysed. (iv) The analyses suggested the use of two reference genes. These results were likewise validated by analysing two target genes, and it was observed that the expression profiles of target genes varied greatly depending on the reference gene(s) used for normalization. This underscores the need to select reference genes appropriately.

Selection and validation of candidate genes for qRT-PCR analysis in P. australis under Cu stress:

After a bibliography-based target genes search, three main gene families were identified: Heavy metal transporters (e.g., NRAMP, HMA, ZIP and VIP); oxidative stress regulators (e.g., SOD, GST, GPX,

CAT, etc.) and others (e.g., metallothionein, different responsive genes, general transporters and transcription factors). All the selected genes (unpublished data) were evaluated to select amplification systems that were specific and allowed quantification over a wide dynamic range. Twenty-three of the 35 candidate genes were selected. The expression profiles of these genes were analysed by RT-qPCR in all samples tested (at different times and copper concentrations). Pending further analysis, the following was observed: (i) An increase in the expression levels of various metal-related transporters over the course of exposure to very high copper concentrations. (ii) A change in the expression profile of several genes was observed after 24 hours of exposure to high copper concentrations. (iii) At shorter times (6 hours), high and very high copper concentrations showed a negative effect on gene expression, which was most prominent at a given concentration. (iv) Antioxidant systems such as SOD or POD showed their highest levels of overexpression under high, but not limiting, copper conditions, after 24 hours of exposure.

4.4 Conclusions and linked activities with WP4

At site 6, UBU provided some further insights into the characterization of isolated strains

- The total number of bacterial isolates was higher in the control and chronic exposure treatments compared to the acute exposure. This difference may be attributed to the lack of acclimation of bacteria to the stressful conditions posed by polluted water with metals and acidic pH during acute exposure.
- Functional analysis of PGP traits suggests that these characteristics depend more strongly on the bacterial genus rather than on the type of exposure treatment. Nevertheless, isolates from the acute exposure consistently exhibited fewer positive PGP traits than those from chronic exposure and control groups, in both epiphytic and endophytic communities. Results reveal a stable and functionally enriched endophytic community adapted to metal-driven stress.
- With these characterized isolates, WP4 related task 4.1 focuses on creating microaggregates in collaboration with JSI. Using the iACME technique, different combinations of isolates will be tested to identify consortia with optimal growth and functional potential. Following this, as part of Task 4.1, microcosm assays are being conducted where *P. australis* plants are exposed to contaminated water and inoculated with the selected consortia. This is described in D4.1 and it will allow evaluation of the consortia's effects on various phenotypic parameters such as plant height, biomass, leaf number, and metal accumulation in the various compartments. Finally, within WP4 and Task 4.1, the hybrid pilot system that integrates an optimized BES system (LEITAT) coupled with phytoremediation and assisted by PGPRs, is likewise described in D4.1.
- In regards to molecular responses in the presence of Cu, although results are preliminary and under analysis, it is suggested an important involvement of metal transporters and enzymes related to antioxidant pathways. Moreover, it seems like *P. australis* may harbour some kind of adaptative mechanism since the shorter exposure to the contaminant displayed negative effects on gene expression, whereas the triggered antioxidant defences seem to appear at longer times of exposure, independently of the concentration. Nevertheless, results on gene expression are still undergoing.

5 Synthesis and conclusions

The work developed in task T1.1 allowed the successful identification of 155 microbial isolates with potential capacities to degrade or tolerate pollutants, obtained from samples of rhizospheric soils, landfill sediments, rhizosediments, estuarine sediments, estuarine water or groundwater, as detailed in D1.2. In the present task T3.1, some of these strains were further characterized for their resistance to the metals found on the sites, their ability to promote plant growth (*e.g.*, production of growth regulators, increased nutrient collectionand to degrade organic pollutants. Final data are reported in this deliverable D3.5.

- Representatives of polluted soils, UMPL isolated bacteria and fungi from sites 2 and 10. The *Pseudomonas* sp. strain UFC_B020 from Hg-contaminated soil exhibited 20× higher mercury resistance than a strain from unpolluted soil, relying on active detoxification and efflux pathways, highlighting the role of environmental selection in microbial resistance. The rhizosphere fungus UFC_004 showed high tolerance to Cd, Pb, and Zn, improved *Salix aquatica* growth under metal stress, and harbored unique detoxification genes and metabolic pathways, confirming its bioremediation potential. Optimized microbial consortia from sites 2 and 10 were produced and are currently being evaluated in WP4 experiments.

- At site 4, 37 bacterial strains from *Juncus maritimus* rhizosediments showed resistance to Cu, Zn, and, to a lesser extent, Cd, Cr, and Pb, with several exhibiting plant growth-promoting traits. Four strains were selected to form a consortium that removed ~84% of Kpf in microcosm/mesocosm tests. At site 5, 20 bacterial strains from Sporobolus maritimus rhizosediments demonstrated moderate Vfx degradation and high resistance to Cu and Zn. PGP traits, including biofilm formation, ACC deaminase activity, nitrogen fixation, and siderophore production, were common. Twelve efficient consortia were selected, with Alcaligenes, Pseudomonas, and Hydrogenophaga dominant. These consortia are being tested with *S. maritim*us for contaminant removal in lab-scale simulations.

- At site 6, bacterial isolates from chronic exposure and control treatments were more abundant and functionally enriched than those from acute exposure. PGP traits were genus-dependent, and endophytic communities adapted to metal stress. WP4 efforts focus on forming microaggregates and optimized consortia using iACME, with Phragmites australis exposed to contaminated water to evaluate plant growth, biomass, and metal accumulation. Preliminary molecular analyses indicate the involvement of metal transporters and antioxidant enzymes in Cu response, with adaptive plant mechanisms emerging over longer exposure periods.

6 References

Abdelwahed, S., Trabelsi, E., Saadouli, I., Kouidhi, S., Masmoudi, A. S., Cherif, A., Mnif, W., & Mosbah, A. (2022). A new pioneer colorimetric micro-plate method for the estimation of ammonia production by plant growth promoting rhizobacteria (PGPR). Main Group Chemistry, 21(1), 55–68. https://doi.org/10.3233/MGC-210077

Ali, S. Z., Sandhya, V., & Rao, L. V. (2014). Isolation and characterization of drought-tolerant ACC deaminase and exopolysaccharide-producing fluorescent Pseudomonas sp. Annals of Microbiology, 64(2), 493–502. https://doi.org/10.1007/s13213-013-0680-3

Altschul, S.F., Gish, W., Miller, W., Myers, E.W., Lipman, D.J., 1990. Basic local alignment search tool. J Mol Biol 215(3), 403-410. https://doi.org/10.1016/S0022-2836(05)80360-2.

Anders, S., Pyl, P. T., & Huber, W. (2014). HTSeq—a Python framework to work with high-throughput sequencing data. Bioinformatics, 31(2), 166-169. https://doi.org/10.1093/bioinformatics/btu638

Balado, M., Souto, A., Vences, A., Careaga, V. P., Valderrama, K., Segade, Y., Rodr, J., Osorio, C. R., Jime, C., Lemos, M. L. (2015). Two Catechol Siderophores, Acinetobactin and Amonabactin, Are Simultaneously Produced by Aeromonas salmonicida subsp. salmonicida Sharing Part of the Biosynthetic Pathway. *Chem. Biol.,* 10, 2850–2860 .https://doi.org/10.1021/acschembio.5b00624

Bankevich, A., Nurk, S., Antipov, D., Gurevich, A.A., Dvorkin, M., Kulikov, A.S., Lesin, V.M., Nikolenko, S.I., Pham, S., Prjibelski, A.D., Pyshkin, A.V., Sirotkin, A.V., Vyahhi, N., Tesler, G., Alekseyev, M.A., Pevzner, P.A., 2012. SPAdes: a new genome assembly algorithm and its applications to single-cell sequencing. J Comput Biol 19(5), 455-477. https://doi.org/10.1089/cmb.2012.0021.

Bateman, A., Martin, M., Orchard, S., Magrane, M., Ahmad, S., Alpi, E., Bowler-Barnett, E. H., Britto, R., Bye-A-Jee, H., Cukura, A., Denny, P., Dogan, T., Ebenezer, T., Fan, J., Garmiri, P., Da Costa Gonzales, L. J., Hatton-Ellis, E., Hussein, A., Ignatchenko, A.,. . . Zhang, J. (2022). UniProt : the Universal Protein Knowledgebase in 2023. Nucleic Acids Research, 51(D1), D523-D531. https://doi.org/10.1093/nar/gkac1052

Becerra-Castro, C., Monterroso, C., Prieto-Fernández, A., Rodríguez- Lamas, L., Loureiro-Viñas, M., Acea, M.J., Kidd P.S. (2012). Pseudometallophytes colonising Pb/Zn mine tailings: a de- scription of the plant-microorganism-rhizosphere soil system and isolation of metal-tolerant bacteria. *J. Hazard. Mat.,* 217– 218, 350–359. doi:10.1016/j.jhazmat.2012.03.039

Boulange-Petermann, L., Herry, J.-M., & Bellon-Fontaine, M.-N. (2004). Evidence of a charge-density threshold for optimum efficiency of biocidal cationic surfaces. Microbiology, 150(9), 2901–2909. https://doi.org/10.1099/mic.0.27526-0

Braud, A. M., Hubert, M., Gaudin, P., Lebeau, T. (2015). A quick rhizobacterial selection tests for the remediation of copper contaminated soils. *J. App. Microbiol.,* 119(2), 435–445. https://doi.org/10.1111/jam.12865

Cappuccino, J. C., & Sherman, N. (1992). Ammonia production. Microbiology: a laboratory manual, 125-79.

Chaudhary, P., Xu, M., Ahamad, L., Chaudhary, A., Kumar, G., Adeleke, B. S., Verma, K. K., Hu, D.-M., Širić, I., Kumar, P., Popescu, S. M., & Abou Fayssal, S. (2023). Application of Synthetic Consortia for Improvement of Soil Fertility, Pollution Remediation, and Agricultural Productivity: A Review. *Agronomy*, *13*(3), 643. https://doi.org/10.3390/agronomy13030643

Chabbi, N., Chafiki, S., Telmoudi, M., Labbassi, S., Bouharroud, R., Tahiri, A., ... & Qessaoui, R. (2024). Plant-growth-promoting rhizobacteria improve seeds germination and growth of Argania spinosa. Plants, 13(15), 2025.

Chen, S., Zhou, Y., Chen, Y., & Gu, J. (2018). fastp : an ultra-fast all-in-one FASTQ preprocessor. Bioinformatics, 34(17), i884-i890. https://doi.org/10.1093/bioinformatics/bty560

Chen, S., 2023. Ultrafast one-pass FASTQ data preprocessing, quality control, and deduplication using fastp. Imeta 2(2), e107. https://doi.org/10.1002/imt2.107.

Cheng-Han Liu, Hans-Uwe Dahms, Chi-Ying Hsieh, Zong-Ying Lin, Tai-Yan Lin, & Xiao-Qian Huang. (2023). Bacterial Heavy Metal Resistance Related to Environmental Conditions. *Environmental Pollution*. https://doi.org/http://dx.doi.org/10.2139/ssrn.4455301

Ciadamidaro, L., Parelle, J., Tatin-Froux, F., Moyen, C., Durand, A., Zappelini, C., Morin-Crini, N., Soupe, D., Blaudez, D., & Chalot, M. (2019). Early screening of new accumulating versus non-accumulating tree species for the phytomanagement of marginal lands. *Ecological Engineering*, *130*, 147-156. https://doi.org/10.1016/j.ecoleng.2019.02.010

Ciadamidaro, L., Pfendler, S., Girardclos, O., Zappelini, C., Binet, P., Bert, V., Khasa, D., Blaudez, D., Chalot, M. (2022). Mycorrhizal inoculation effects on growth and the mycobiome of poplar on two phytomanaged sites after 7-year-short rotation coppicing. *Front. Plant Sci.*, 28, 993301. doi: 10.3389/fpls.2022.993301.

Ćirković, K., Ostojić, A., Đilas, M., Radojević, I. (2023). Assessing the impact of heavy metals and antibiotics on bacterial isolates from wastewater treatment plant. *Kragujevac J. Sci*, 45, 207–218. https://doi.org/10.5937/kgjsci2345207c

Clagnan E, Costanzo M, Visca A, Di Gregorio L, Tabacchioni S, Colantoni E, Sevi F, Sbarra F, Bindo A, Nolfi L, Magarelli RA, Trupo M, Ambrico A, Bevivino A. Culturomics- and metagenomics-based insights into the soil microbiome preservation and application for sustainable agriculture. Front Microbiol. 2024 Oct 24;15:1473666. doi: 10.3389/fmicb.2024.1473666. PMID: 39526137; PMCID: PMC11544545.

Cunha, P., Gorito, A. M., Fernandes, J. P., Mucha, A. P., Almeida, C. M. R. (2024). Saltmarsh plants role in metals retention and the potential of vegetation for metal removal in the long term. *Nat. Based Sol.*, 5, 100110. https://doi.org/10.1016/J.NBSJ.2024.100110

DeVries, A. E., Kowalski, K. P., Bickford, W. A. (2020). Growth and behavior of North American microbes on Phragmites australis leaves. *Microorganisms*, 8(5), 690.

Duarte, P., Almeida, C. M. R., Fernandes, J. P., Morais, D., Lino, M., Gomes, C. R., Carvalho, M. F., & Mucha, A. P. (2019). Bioremediation of bezafibrate and paroxetine by microorganisms from estuarine sediment and activated sludge of an associated wastewater treatment plant. *Sci. Tot. Environ.*, 655, 796–806. https://doi.org/10.1016/J.SCITOTENV.2018.11.285

Dworkin, M., Foster, J. W. (1958). Experiments with some microorganisms which utilize ethane and hydrogen '. *J. Bact.*, 75(5), 592-603.

Efremenko, E., Stepanov, N., Senko, O., Aslanli, A., Maslova, O., & Lyagin, I. (2024). Using Fungi in Artificial Microbial Consortia to Solve Bioremediation Problems. *Microorganisms*, *12*(3), 470. https://doi.org/10.3390/microorganisms12030470

Ejikeme, C., Uzoma, C. (2013). Comparative study on solubilization of tri-calcium phosphate (TCP) by phosphate solubilizing fungi (PSF) isolated from Nsukka pepper plant rhizosphere and root free soil. *J. Yeast Fung. Res*. 4, 52–57. https://doi.org/10.5897/JYFR2013.0120

Fakhar, A., Gul, B., Gurmani, A. R., Khan, S. M., Ali, S., Sultan, T., ... & Rizwan, M. (2022). Heavy metal remediation and resistance mechanism of Aeromonas, Bacillus, and Pseudomonas: A review. *Critical Reviews in Environmental Science and Technology*, *52*(11), 1868-1914.

Fernandes, J. P., Duarte, P., Almeida, C. M. R., Carvalho, M. F., Mucha, A. P. (2020a). Potential of bacterial consortia obtained from different environments for bioremediation of paroxetine and bezafibrate. *J. Environ. Chem. Eng.*, 8(4), 103881. https://doi.org/10.1016/j.jece.2020.103881

Fernandes, J.P., Almeida, C.M.R., Salgado, M.A., Carvalho, M.F., Mucha, A.P. (2021) Pharmaceutical Compounds in Aquatic Environments—Occurrence, Fate and Bioremediation Prospective. *Toxics*, 9, 257. https://doi.org/10.3390/toxics9100257

Fernandes, M. J., Paíga, P., Silva, A., Llaguno, C. P., Carvalho, M., Vázquez, F. M., Delerue-Matos, C. (2020). Antibiotics and antidepressants occurrence in surface waters and sediments collected in the north of Portugal. *Chemosphere*, 239, 124729. https://doi.org/10.1016/J.CHEMOSPHERE.2019.124729

Ferreira, M. J., Cunha, A., Figueiredo, S., Faustino, P., Patinha, C., Silva, H., Sierra-Garcia, I. N. (2021). The root microbiome of Salicornia ramosissima as a seedbank for plant-growth promoting halotolerant bacteria. *Appl. Sci.*, 11(5), 2233. https://doi.org/10.3390/app11052233

Fraga-Santiago, P., Dias, S., Silva, C., Gomes, C. R., Almeida, C.M.R. (2022). Pharmaceuticals Influence on Phragmites australis Phytoremediation Potential in Cu Contaminated Estuarine Media. *Pollutants*, 2, 42-52. https://doi.org/10.3390/POLLUTANTS2010006

Gamalero E, Glick BR. Use of plant growth-promoting bacteria to facilitate phytoremediation. AIMS Microbiol. 2024 Jun 12;10(2):415-448. doi: 10.3934/microbiol.2024021.

Ge, S. X., Son, E. W., & Yao, R. (2018). iDEP : an integrated web application for differential expression and pathway analysis of RNA-Seq data. BMC Bioinformatics, 19(1). https://doi.org/10.1186/s12859-018-2486-6

Griffiths-Jones, S., Bateman, A., Marshall, M., Khanna, A., Eddy, S.R., 2003. Rfam: an RNA family database. Nucleic Acids Res 31(1), 439-441. https://doi.org/10.1093/nar/gkg006.

Grobelak, A., Napora, A., Kacprzak, M. J. E. E. (2015). Using plant growth-promoting rhizobacteria (PGPR) to improve plant growth. *Ecol. Eng.*, 84, 22-28.

Gupta, S., Pandey, S. (2019). ACC Deaminase Producing Bacteria With Multifarious Plant Growth Promoting Traits Alleviates Salinity Stress in French Bean (Phaseolus vulgaris). *Plants*, 10, 1–17. https://doi.org/10.3389/fmicb.2019.01506

Hu, J., Fan, J., Sun, Z., Liu, S., 2020. NextPolish: a fast and efficient genome polishing tool for long-read assembly. Bioinformatics 36(7), 2253-2255. https://doi.org/10.1093/bioinformatics/btz891.

Hu, J., Wang, Z., Sun, Z., Hu, B., Ayoola, A.O., Liang, F., Li, J., Sandoval, J.R., Cooper, D.N., Ye, K., Ruan, J., Xiao, C.L., Wang, D., Wu, D.D., Wang, S., 2024. NextDenovo: an efficient error correction and accurate assembly tool for noisy long reads. Genome Biol 25(1), 107. https://doi.org/10.1186/s13059-024-03252-4.

Koren, S., Walenz, B.P., Berlin, K., Miller, J.R., Bergman, N.H., Phillippy, A.M., 2017. Canu: scalable and accurate long-read assembly via adaptive k-mer weighting and repeat separation. Genome Res 27(5), 722-736. https://doi.org/10.1101/gr.215087.116.

Lacercat Didier, L., Berthelot, C., Foulon, J., Errard, A., Martino, E., Chalot, M., & Blaudez, D. (2016). New mutualistic fungal endophytes isolated from poplar roots display high metal tolerance. *Mycorrhiza, 26*(7), 657–671. https://doi.org/10.1007/s00572-016-0699-y

Lagesen, K., Hallin, P., Rodland, E.A., Staerfeldt, H.H., Rognes, T., Ussery, D.W., 2007. RNAmmer: consistent and rapid annotation of ribosomal RNA genes. Nucleic Acids Res 35(9), 3100-3108. https://doi.org/10.1093/nar/gkm160.

Langmead, B., & Salzberg, S. L. (2012). Fast gapped-read alignment with Bowtie 2. Nature Methods, 9(4), 357-359. https://doi.org/10.1038/nmeth.1923

Lankford, I. C. E. (1994). Copyright © 1994 by Academic Press, Inc. All fights of reproduction in any form reserved. *Meth. Enzym.*, 235, 329–344.

LaVoie, S. P., & Summers, A. O. (2018). Transcriptional responses of Escherichia coli during recovery from inorganic or

organic mercury exposure. BMC Genomics, 19(1). https://doi.org/10.1186/s12864-017-4413-z

Li, H., 2018. Minimap2: pairwise alignment for nucleotide sequences. Bioinformatics 34(18), 3094-3100. https://doi.org/10.1093/bioinformatics/bty191.

Li, J., Peng, W., Yin, X., Wang, X., Liu, Z., Liu, Q., ... & Liang, R. (2024). Identification of an efficient phenanthrene-degrading Pseudarthrobacter sp. L1SW and characterization of its metabolites and catabolic pathway. Journal of Hazardous Materials, 465, 133138.

Lin, Y., Lin, H., Liu, J., Xin, F., Chen, M., Dong, W., Qian, X., & Jiang, M. (2024). Insights into constructing a stable and efficient microbial consortium system [Review]. *Chinese Journal of Chemical Engineering*. Advance online publication. https://doi.org/10.1016/j.cjche.2024.08.003

Liu C.H., Dahms H.U., Hsieh C.Y., Lin Z.Y., Lin T.Y, Huang X.Q. (2023). Bacterial Heavy Metal Resistance Related to Environmental Conditions. *Chemosphere, 347, 140539* 10.1016/j.chemosphere.2023.140539

Louden, B. C., Haarmann, D., Lynne, A. M. (2011). Use of blue agar CAS assay for siderophore detection. *J Microbiol. Biol. Educ*. 12, 51-53.

Love, M. I., Huber, W., & Anders, S. (2014). Moderated estimation of fold change and dispersion for RNA-seq data with DESeq2. Genome Biology, 15(12). https://doi.org/10.1186/s13059-014-0550-8

Lowe, T.M., Eddy, S.R., 1997. tRNAscan-SE: a program for improved detection of transfer RNA genes in genomic sequence. Nucleic Acids Res 25(5), 955-964. https://doi.org/10.1093/nar/25.5.955.

Lu, L., Chang, M., Han, X., Wang, Q., Wang, J., Yang, H., ... & Dai, S. (2021). Beneficial effects of endophytic Pantoea ananatis with ability to promote rice growth under saline stress. *Journal of Applied Microbiology*, *131*(4), 1919-1931.

Luo, H., Win, C. S., Lee, D. H., He, L., & Yu, J. M. (2024). Microbacterium azadirachtae CNUC13 enhances salt tolerance in maize by modulating osmotic and oxidative stress. *Biology*, *13*(4), 244.

Ma Y, Ankit, Tiwari J and Bauddh K (2022) Plant-Mycorrhizal Fungi Interactions in Phytoremediation of Geogenic Contaminated Soils. *Front. Microbiol*. 13:843415. doi: 10.3389/fmicb.2022.843415

Mei, S., Wang, M., Salles, J. F., & Hackl, T. (2023). Diverse rhizosphere-associated Pseudomonas genomes isolated along the marine-terrestrial transition zone of a Wadden island salt march. bioRxiv (Cold Spring Harbor Laboratory). https://doi.org/10.1101/2023.11.14.566819

Mohammad, M., Badaluddin, N. A., & Asri, E. A. (2024). Biological functions of Paenibacillus spp. for agriculture applications. *Bulgarian Journal of Agricultural Science*, *30*(5).

Nautiyal, C. S. (1999). An efficient microbiological growth medium for screening phosphate solubilizing microorganisms. *FEMS Microbiol. Let*., 170, 265-270.

Pagnani, G., Pellegrini, M., Galieni, A., D'Egidio, S., Matteucci, F., Ricci, A., Del Gallo, M. (2018). Plant growth-promoting rhizobacteria (PGPR) in Cannabis sativa 'Finola'cultivation: An alternative fertilization strategy to improve plant growth and quality characteristics. *Ind. Crops Prod*., 123, 75-83.

Pantoja-Guerra, M., Burkett-Cadena, M., Cadena, J., Dunlap, C. A., & Ramírez, C. A. (2023). Lysinibacillus spp.: an IAA-producing endospore forming-bacteria that promotes plant growth. Antonie van Leeuwenhoek, International Journal of General and Molecular Microbiology, 116(7), 615–630. https://doi.org/10.1007/s10482-023-01828-x

Paredes-páliz, K. I., Caviedes, M. A., Doukkali, B., Mateos-naranjo, E., Rodríguez-llorente, I. D., Pajuelo, E. (2016). Screening beneficial rhizobacteria from Spartina maritima for phytoremediation of metal polluted salt marshes : comparison of gram-positive and gram-negative strains. *Environ. Sci Pol. Res*., 19825–19837. https://doi.org/10.1007/s11356-016-7184-1

Patten, C. L., Glick, B. R. (2002). Role of Pseudomonas putida Indoleacetic Acid in Development of the Host Plant Root System. *Appl. Environ. Microbiol.* 68(8), 3795-801. doi: 10.1128/AEM.68.8.3795-3801.2002.

Penrose, D. M., & Glick, B. R. (2003). Technical focus Methods for isolating and characterizing ACC deaminase-containing plant growth-promoting rhizobacteria. *Physiol. Plant.* 118, 10–15. https://doi.org/10.1034/j.1399-3054.2003.00086.x

Petersen, T.N., Brunak, S., von Heijne, G., Nielsen, H., 2011. SignalP 4.0: discriminating signal peptides from transmembrane regions. Nat Methods 8(10), 785-786. https://doi.org/10.1038/nmeth.1701.

Podlipná, R., Skálová, L., Seidlová, H., Szotáková, B., Kubíček, V., Stuchlíková, L., Vokřál, I. (2013). Biotransformation of benzimidazole anthelmintics in reed (Phragmites australis) as a potential tool for their detoxification in environment. *Biores. Technol*., 144, 216-224.

Purwaningsih, S., Agustiyani, D., & Antonius, S. (2021). Diversity, activity, and effectiveness of Rhizobium bacteria as plant growth promoting rhizobacteria (PGPR) isolated from Dieng, central Java. *Iranian Journal of Microbiology*, *13*(1), 130.

Rybkin I, Gorin D, Sukhorukov G and Lapanje A (2019) Thickness of Polyelectrolyte Layers of Separately Confined Bacteria Alters Key Physiological Parameters on a Single Cell Level. Front. Bioeng. Biotechnol. 7:378. doi: 10.3389/fbioe.2019.00378

Saha L, Tiwari J, Bauddh K and Ma Y (2021) Recent Developments in Microbe–Plant-Based Bioremediation for Tackling Heavy Metal-Polluted Soils. *Front. Microbiol*. 12:731723. doi: 10.3389/fmicb.2021.731723

Salmela, L., Rivals, E., 2014. LoRDEC: accurate and efficient long read error correction. Bioinformatics 30(24), 3506-3514. https://doi.org/10.1093/bioinformatics/btu538.

Schwyn B., Neilands J.B. (1987). Universal chemical assay for the detection and determination of siderophores. *Anal. Biochem*. 160:47–56. doi:10.1016/0003-2697(87)90612-9

Seo, H., Kim, J. H., Lee, S. M., & Lee, S. W. (2024). The plant-associated Flavobacterium: a hidden helper for improving plant health. *The plant pathology journal*, *40*(3), 251.

Simao, F.A., Waterhouse, R.M., Ioannidis, P., Kriventseva, E.V., Zdobnov, E.M., 2015. BUSCO: assessing genome assembly and annotation completeness with single-copy orthologs. Bioinformatics 31(19), 3210-3212. https://doi.org/10.1093/bioinformatics/btv351.

Singh, A. V., Chandra, R., & Goel, R. (2013). Phosphate solubilization by Chryseobacterium sp. and their combined effect with N and P fertilizers on plant growth promotion. *Archives of Agronomy and Soil Science*, *59*(5), 641-651.

Sitepu, I. R., Hashidoko, Y., Santoso, E., Tahara, S. (2007). Potent phosphate-solubilizing bacteria isolated from dipterocarps grown in peat swamp forest in Central Kalimantan and their possible utilization for biorehabilitation of degraded peatland. In Proceedings of the international symposium and workshop on tropical Peatland, Yogyakarta (pp. 27-29).

Sprouffske, K., Wagner, A. Growthcurver: an R package for obtaining interpretable metrics from microbial growth curves. BMC Bioinformatics 17, 172 (2016). https://doi.org/10.1186/s12859-016-1016-7

Su, C., Xie, R., Liu, D., Liu, Y., & Liang, R. (2023). Ecological Responses of Soil Microbial Communities to Heavy Metal Stress in a Coal-Based Industrial Region in China. *Microorganisms*, *11*(6), 1392. https://doi.org/10.3390/microorganisms11061392

Sun, S. C., Chen, J. X., Wang, Y. G., Leng, F. F., Zhao, J., Chen, K., & Zhang, Q. C. (2021). Molecular mechanisms of heavy metals resistance of Stenotrophomonas rhizophila JC1 by whole genome sequencing. *Archives of Microbiology*, *203*(5), 2699-2709.

Sütterlin, S., Téllez-Castillo, C. J., Anselem, L., Yin, H., Bray, J. E., Maiden, M. C. J. (2018). Heavy metal susceptibility of Escherichia coli isolated from urine samples from Sweden, Germany, and Spain. *Antimic. Agents Chemot.,* 62. https://doi.org/10.1128/AAC.00209-18

Tarailo-Graovac, M., Chen, N., 2009. Using RepeatMasker to identify repetitive elements in genomic sequences. Curr Protoc Bioinformatics Chapter 4, 4 10 11-14 10 14. https://doi.org/10.1002/0471250953.bi0410s25.

Teste, F.P., Jones, M.D., Dickie, I.A. (2020). Dual-mycorrhizal plants: their ecology and rele- vance. *New Phytol.,* 225, 1835–1851. https://doi.org/10.1111/nph.16190.

Walker, B.J., Abeel, T., Shea, T., Priest, M., Abouelliel, A., Sakthikumar, S., Cuomo, C.A., Zeng, Q., Wortman, J., Young, S.K., Earl, A.M., 2014. Pilon: an integrated tool for comprehensive microbial variant detection and genome assembly improvement. PLoS One 9(11), e112963. https://doi.org/10.1371/journal.pone.0112963.

Xiao, M., Long, Z. E., Fu, X., & Zou, L. (2024). Versatile applications and mechanisms of genus Exiguobacterium in bioremediating heavy metals and organic pollutants: A review. International Biodeterioration & Biodegradation, 194, 105884.

Xu, S., Zhao, Y., Peng, Y., Shi, Y., Xie, X., Chai, A., ... & Li, L. (2022). Comparative genomics assisted functional characterization of Rahnella aceris ZF458 as a novel plant growth promoting rhizobacterium. *Frontiers in Microbiology*, *13*, 850084.

Yang, Y., Zhang, X., Liu, Y., Zhang, Y., & Wang, X. (2025). A fusarioid fungus forms mutualistic interactions with poplar trees that resemble ectomycorrhizal symbiosis. *IMA Fungus*, 16, e143240. https://doi.org/10.3897/imafungus.16.143240

Yang, Y.F., 2021. Emerging patterns of microbial functional traits. *Trends Microbiol*. 29, 874–882. https://doi.org/10.1016/j.tim.2021.04.004.

Zhang, Y., Zhou, Q., Gao, C., Lu, Y., Sheng, Y., Xiao, M., ... & Yu, X. (2024). Endophytic bacteria for Cd remediation in rice: Unraveling the Cd tolerance mechanisms of Cupriavidus metallidurans CML2. *Journal of Hazardous Materials*, *469*, 133846.

Zhao, Y., Hong, Y., Wang, P., Gou, Y., Zeng, R., Zhang, Q., Chen, D., & Song, Y. (2023). Assembly of Tomato Rhizobacteria from different functional groups improves seedling photosynthesis and growth. *Plants*, 12, 4000. https://doi.org/10.3390/plants12234000